

**Examination of Palladium Catalyst Structure in Regioselective Suzuki-Miyaura Cross-Coupling Reactions**

**Evans Yao Dzotsi**

**MSc by Research**

**UNIVERSITY OF YORK**

**CHEMISTRY**

**DECEMBER 2016**

## Abstract

Catalysis plays a vital role in chemical synthesis, from organic catalysis to metal catalysis. Palladium is able to affect many catalytic organic transformations, *e.g.* cross-coupling reactions, which are of great value to the synthetic chemist. While many reactions are mediated by homogeneous Pd species, there is good experimental evidence supporting a role for higher order Pd species that can operate in a quasi-heterogeneous manner. Indeed, in some cases, stabilised Pd nanoparticles mediate heterogeneous cross-coupling reactions.

This thesis examines the catalytic performance of distinct Pd catalysts in Suzuki-Miyaura Cross-Coupling reactions (SMCCs). Comparing the regioselectivity and efficacy of traditional 'homogeneous' Pd catalysts, *i.e.* Pd(PPh<sub>3</sub>)<sub>4</sub>, with heterogeneous species, *i.e.* PVP-PdNPs or phosphine-stabilised PdNPs, and 'quasi' homogeneous-heterogeneous species, *i.e.* [Pd<sub>3</sub>(PPh<sub>3</sub>)<sub>4</sub>][BF<sub>4</sub>]<sub>2</sub>, against two electrophilic substrates, namely 2,4-dibromopyridine and 2,4-dichloropyridine, allows Pd catalyst efficacy and regioselectivity to be determined in a SMCC reaction for the first time.

Many researchers have reported use of Pd(PPh<sub>3</sub>)<sub>4</sub> catalysts in cross-coupling chemistry. Until this study little has been reported on Pd catalyst screening against SMCCs, comparing homogeneous, heterogeneous and 'quasi' homo/heterogeneous Pd catalysts. In this thesis an intriguing outcome is revealed – at equivalent Pd catalyst loading and temperature [Pd<sub>3</sub>(PPh<sub>3</sub>)<sub>4</sub>][BF<sub>4</sub>]<sub>2</sub> was found to afford the C4-arylated product as the major regioisomer, whereas all other Pd catalysts afforded the C2-arylated product as the major regioisomer. The observation is juxtaposed to previous literature findings using homogeneous Pd catalysts, which favours C2-arylation. In terms of catalyst efficacy, the heterogeneous Pd catalysts were found to be less reactive of all the Pd catalysts screened.

The study confirms that there may be great value in exploiting the catalytic properties of small Pd clusters in affecting regioselectivity in cross-coupling reactions.

## List of Contents

Chapter/Section	Title	Page
	<i>Title page</i>	1
	Abstract	2
	List of Contents	3
	List of Tables	4
	List of Figures	5
	List of Schemes	6
	Acknowledgements	8
	Declaration	9
<b>Chapter 1</b>	<b>Introduction</b>	<b>10</b>
1.1	Catalysis and Green Chemistry	10
1.2	Exemplar Pd-mediated reactions	11
1.3	Pd-catalysed Suzuki-Miyaura cross-coupling (SMCC)	13
1.3.1	Background	13
1.3.2	The use of palladium catalysts in SMCC reactions	17
1.3.3	Physical methods used to test heterogeneity of reactions	25
1.4	Pd-catalyzed Heck coupling reaction	27
1.5	Negishi reactions	29
1.6	Direct arylation reactions	31
1.7	Project aim and objectives	35
<b>Chapter 2</b>	<b>Results and discussion</b>	<b>36</b>
2.1	Synthesis and characterisation of catalysts	36
2.1.1	Synthesis of quasi-homogeneous and heterogeneous catalysts (Pd Clusters (Pd <sub>3</sub> ))	36
2.2	Synthesis of PdNPs	38
2.2.1	Reactions of PdNPs	38
2.2.2	Choice of PdNPs in catalysis	39
2.2.3	Particle sizes and distribution	40
2.3	Examining the regioselectivity in Pd-catalysed SMCC reactions by alteration of Pd catalyst	45
2.3.1	Pd catalysis screening study	47
2.4	Conclusions	61
<b>Chapter 3</b>	<b>Experimental section</b>	<b>62</b>
3.1	General experimental details	62
3.2	General procedures	64
3.2.1	Synthesis of palladium catalysts	64
3.2.2	Synthesis of palladium clusters	67
3.3	Suzuki-Miyaura cross-coupling reactions – exemplar procedures	71
3.3.1	Exemplar characterisation data for SMCC products	78
	<b>Appendices (representative NMR spectra)</b>	<b>83</b>
	<b>Abbreviations</b>	<b>100</b>
	<b>References</b>	<b>102</b>

## List of Tables

**Table 1** Results of screening base and temperature for reaction of 2,4-dibromopyridine **97** with phenylboronic acid **98a**, using Pd(PPh<sub>3</sub>)<sub>4</sub> as the catalyst and THF as the solvent.

**Table 2** Results of screening solvent and reaction temperatures for the reaction of 2,4-dichloropyridine **102** with phenylboronic acid **98a**, using Pd(PPh<sub>3</sub>)<sub>4</sub> as catalyst and nBu<sub>4</sub>NOH as base.

**Table 3** Results of variations in temperature for the reaction of 2,4-dichloropyridine **102** with *p*-methoxyphenylboronic acid **98b**, using Pd(OAc)<sub>2</sub> as the catalyst, nBu<sub>4</sub>NOH as the base and THF as the solvent.

**Table 4** Results of variations in temperature for the reaction of 2,4-dichloropyridine **102** with *p*-methoxyphenylboronic acid **98b**, using, nBu<sub>4</sub>NOH as the base, THF as the solvent and Pd<sub>2</sub>(dba)<sub>3</sub>.CHCl<sub>3</sub> and Pd(PPh<sub>3</sub>)<sub>4</sub> as the catalyst.

**Table 5** Results of variations in temperature for the reaction of 2,4-dichloropyridine **102** with *p*-methoxyphenylboronic acid **98b**, using Pd<sub>3</sub>(PPh<sub>3</sub>)<sub>4</sub>[BF<sub>4</sub>]<sub>2</sub> and Pd<sub>3</sub>(PPh<sub>3</sub>)<sub>4</sub>[PF<sub>6</sub>]<sub>2</sub> as the catalyst, nBu<sub>4</sub>NOH as the base and THF as the solvent.

**Table 6** Results of variation in temperature for reaction of 2,4-dichloropyridine **102** with *p*-methoxyphenylboronic acid **98b**, using Pd<sub>3</sub>(PPh<sub>3</sub>)<sub>4</sub>[BF<sub>4</sub>]<sub>2</sub> **88**, nBu<sub>4</sub>NOH in THF.

**Table 7** Results of variation in temperature for the reaction of 2,4-dichloropyridine **102** with *p*-methoxyphenylboronic acid **98b**, using Pd/C and PdNPs as the catalysts, nBu<sub>4</sub>NOH in THF.

## List of Figures

**Figure 1** Examples of Pd-catalysed C–C bond formation reactions.

**Figure 2** Schematic representation for the role of aggregated Pd in catalysis. Reproduced with permission of The Royal Society of Chemistry.

**Figure 3** Structural features of the dialkylbiarylphosphines and the impact of structural modifications on the efficacy of catalysts.

**Figure 4** Selected examples of Buchwald ligands used in cross-coupling reactions.

**Figure 5** Buchwald ligands used in cross-coupling reactions.

**Figure 6** Bedford type Palladacyclic complexes used in SMCC reactions.

**Figure 7** An example of a N-heterocyclic carbene ligand used in SMCC reactions.

**Figure 8** Structural examples of the guanidine ligands used in cross-coupling reactions.

**Figure 9** Structure of *bis*(dicyclohexylamine)palladium(II) acetate (DAPCy).

**Figure 10** PVP **43** and BINAP **44** can both act as PdNP-stabiliser ligand systems.

**Figure 11** An example of NHC ligand used as a ligand for Heck reactions.

**Figure 12** Examples of the Buchwald ligands used in Negishi cross-coupling reactions.

**Figure 13** TEM images and particle size analysis of PPh<sub>3</sub>Pd–NPs **91**.

**Figure 14** Proposed ratio for BINAP/Pd in BINAP-PdNPs.

**Figure 15** TEM images and particle size analysis of BINAP-PdNPs **96**.

**Figure 16** TEM images and particle size analysis of PVP-PdNPs.

**Figure 17** Freshly-synthesised sample of Polyvinylpyrrolidinone-PdNPs (**46**).

**Figure 18** <sup>13</sup>C NMR chemical shifts for mono-arylated and 2,4-dibromopyridines.

## List of Schemes

**Scheme 1** Pd-catalysed aerial oxidation of ethylene **1**.

**Scheme 2** A general schematic representation of the Suzuki coupling reaction.

**Scheme 3** Simplified version of the SMCC reaction catalytic cycle.

**Scheme 4** Total synthesis of an anti-cancer agent Quindoline **7**, using SMCC reaction.

**Scheme 5** SMCC reaction using  $\text{Pd}_2(\text{dba})_3$  and ligand **9** as the catalyst system.

**Scheme 6** SMCC reactions of substituted aryl chlorides **16** and aryl boronic acids using **15**.

**Scheme 7** A SMCC reaction catalysed by a Bedford-type palladacycle.

**Scheme 8** Using N-heterocyclic carbene ligand **27** in a SMCC reaction.

**Scheme 9** Screening of the guanidine ligands in the SMCC Reaction.

**Scheme 10** An example of DAPCy-catalysed SMCC reaction.

**Scheme 11** A Pd/C-catalysed SMCC reaction of substituted aryl halides.

**Scheme 12** PdNP-catalysed SMCC reaction.

**Scheme 13** SMCC coupling of 4-iodoanisole **45** and phenylboronic acid **29**.

**Scheme 14** The general Heck synthesis of styrene mediated by Pd.

**Scheme 15** An example where DavePhos**8** was used as a ligand in a Heck reaction.

**Scheme 16** Heck reaction of 4-chlorotoluene **54** with styrene **50**.

**Scheme 17** An example of Heck reaction catalysed by Pd/C.

**Scheme 18** The use of the Negishi cross-coupling reaction in pumiliotoxin A **59** synthesis.

**Scheme 19** Examples of Negishi-coupling of substituted aryl chlorides employing the RuPhos**60** ligand.

**Scheme 20** An example of a reaction showing the use of XPhos**10** in Negishi coupling.

**Scheme 21** Oxidative addition of aryl chlorides by deprotonated (NIXANTPHOS)Pd(0).

**Scheme 22** Cation-controlled site-selective sp<sup>2</sup> C–H and sp<sup>3</sup> benzylic C–H arylation of furans.

**Scheme 23** The catalytic acetoxylation of unactivated arenes.

**Scheme 24** Sanford's acetoxylation of benzo[*h*]quinoline.

**Scheme 25** Regioselective C–H functionalisation of benzothiophene using Pd/C.

**Scheme 26** Pd/C as catalyst for regioselective C–H functionalisation of thiophene.

**Scheme 27** Synthesis of *bis*(benzonitrile)palladium(II) dichloride.

**Scheme 28** Synthesis of *trans-bis*(triphenylphosphine)palladium(II) dichloride.

**Scheme 29** Synthesis of hydroxyl-bridged palladium complex **87**.

**Scheme 30** Synthesis of trinuclear Pd cluster **88**.

**Scheme 31** Synthesis of [Pd(μ-OH)(PPh<sub>3</sub>)<sub>2</sub>]<sub>2</sub>[PF<sub>6</sub>]<sub>2</sub> **89**.

**Scheme 32** Synthesis of [Pd<sub>3</sub>(PPh<sub>3</sub>)<sub>4</sub>][PF<sub>6</sub>]<sub>2</sub> **90**.

**Scheme 33** Synthesis of PdP(Oct)<sub>3</sub> **91**.

**Scheme 34** Synthesis of TPP-PdNPs **94**.

**Scheme 35** Synthesis of BINAP-PdNPs **95**.

**Scheme 36** Synthesis of PVP-PdNPs **46**.

**Scheme 37** General SMCC reaction of 2,4-dibromopyridine (**97**) with arylboronic acids.

**Scheme 38** General SMCC reaction of 2,4-dichloropyridine (**102**) with arylboronic acids.

## **Acknowledgements**

This piece of research would not have been completed without the hand of the almighty God and the various people he placed on my path. Firstly, I want to extend my profound appreciation to my supervisor Professor Ian J. S. Fairlamb for giving me the opportunity to work in his research group and for his patience and the unquenchable desire to see me go through this process safely. I can say on authority that without his encouragement I would not have come this far. I would also like to extend my gratitude to Dr. Paul A. Clarke (IPM) for his interventions that shaped the course of this work.

I would also like to thank all members of the Fairlamb group, past and present, for their immense contribution and friendship in making this adventure worthwhile. In this regard I would like to mention some people who have been of great help, these include Josh, Anders, Ben, Allan, George 'Snr', George 'jnr', Kate, Mary and Yusuf. I like to reiterate that I have greatly appreciated the friendship and the comrade that exists in the group and I have made friends for life.

I thank the following for their technical expertise that they freely and willing put at my disposal, namely Charlotte Elkington and Naser Jasim (the Fairlamb and Perutz group), Karl Heaton (Mass spectra) and Heather Fish (NMR), Graeme McAllister (CHN) and Dr. Meg Stark (TEM) for their invaluable assistance.

I certainly cannot end this without a special mention of my girls, Akorfa and Dzifa, and my dear wife Victoria; you have been the fulcrum around which the success of this work has been hinged. Love you and thank you, I truly appreciate you.



## **Declaration**

I declare that this thesis is a presentation of original work and I am the sole author. All sources are acknowledged as reference. The work was carried out at the University of York between October 2015 and October 2016, and has not previously been presented for an award at this or any other university.

# 1. Introduction

## 1.1 Catalysis and Green Chemistry

Generally, catalysts are substances when added to a reaction medium increases the rate of formation of product of the reaction by lowering the activation energy ( $E_a$ ) that is required to convert the reactants into products. They are often regenerated at the end of the reaction and can be reused. In some cases the products of catalytic reactions can become toxic and harmful their safe disposal does pose a big challenge to the synthetic chemist.<sup>1,2,3</sup> There has been a growing need for more environmentally benign solvents and catalysts to be used in synthetic processes, due to the negative impact these chemicals are having on the environment.<sup>2</sup>

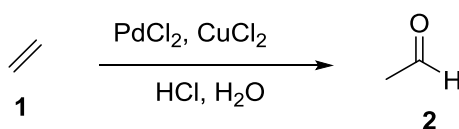
The term 'Green Chemistry' was popularised by Anastas and co, who were at the time working with the US Environmental Protection Agency (EPA). As a new field of chemistry it is developing at a very fast rate, particularly, in the last fifteen years the concept of green chemistry has gained a lot of interest from various fields, including and not limited to the synthetic chemistry.<sup>4</sup> The organic chemist is interested in designing reactions that are high yielding but uses fewer amounts of catalyst and solvent and less toxic solvent *e.g* using water as a solvent in a cross-coupling reaction.<sup>5</sup> The economic benefit of green chemistry to both the organic chemist and the environment is enormous and this has forced most synthetic chemists to embrace the concept.

More and more chemists are striving towards finding better and efficient methods of synthesis by avoiding the use of large amounts of catalysts, expensive and not readily available, to using less toxic solvents and catalysts, reducing the steps involve in synthesis and also identifying alternative metals that can be developed into efficient and environmentally friendly catalyst.<sup>2,6</sup>

Catalysts are generally classified as homogeneous and heterogeneous. Heterogeneous catalysts are known to have multiple types of active sites and are in different phase to the substrate whilst homogeneous catalysts have a single type of active site and have the same phase as substrate.<sup>3</sup> Homogeneous catalysts are generally expensive and difficult to separate from their products and hence cannot be reused. On the other hand heterogeneous catalysts have the ease of separation from their products; which meets the requirement of green chemistry.<sup>4,6</sup>

## 1.2 Exemplar Pd-mediated reactions

The role of metal-mediated catalysis and in particular the importance of palladium in organic synthesis cannot be over-emphasized; Pd has and continues to provide versatile means by which carbon-carbon (C–C) and carbon-heteroatom (C–N) bonds can be formed.<sup>2,7-9</sup> One of the earliest synthetic processes to benefit from the usefulness of Pd catalysis was the emergence of Pd-catalysed aerial oxidation of ethylene **1**, to acetaldehyde **2**, in an industrial process known as the Wacker oxidation (**Scheme 1**).<sup>10</sup> Most commercially available Pd catalysts and reagents are less sensitive to oxygen and moisture and they generally demonstrate good functional group tolerance (*e.g.* hydroxyl and carbonyl). These attributes have made Pd catalysis a very powerful method for accessing a wide range of target molecules.<sup>7,9,10</sup>



**Scheme 1** Pd-catalysed aerial oxidation of ethylene **1**<sup>10</sup>.

While Pd has been useful in chemical synthesis, the question of toxicity and sustainability has been raised over the years. In a recent review by Ananikov and co-workers, they attempted to throw more light on the toxicity of metal catalysts. In order to compare the toxicity of these metal salts, there is the need for consistency in published data, *e.g.* there should be a clear description of concentrations and composition of metal salts used in biological activity measurements studies; at the moment this is commonly not the case.<sup>1</sup>

In terms of sustainability of transition metals used in catalysis, researchers may be less inclined to the continued use of Pd in catalysis as compared with relatively less expensive transition metals such as (Fe, Ni and Cu). With the level of information currently available, it will be erroneous to say that a particular element is toxic without a holistic overview of factors such as its bioavailability, solubility, valence state, particle size and the nature of coordinated ligands, *etc.* Hence, there is the need to be cautiously optimistic in developing alternative methods for C–C bond formation using these less expensive and readily available transition metals such as (Mn, Fe, Ni and Co).<sup>1,11,12</sup> However, discovering innovative means by which Pd catalysts can be efficiently recycled and used at lower

catalyst loadings, while keeping an eye on the environment and contamination, is also widely studied area of research.<sup>2,13,14</sup>

The ability of synthetic chemists to construct C–C bonds in increasingly complex molecules has been greatly enhanced since the discovery of Pd-catalysed cross-coupling reactions in the 1960's.<sup>15</sup> These reactions have been studied extensively and various modifications have been reported within the literature. Notable among such modifications are the utilization of environmentally friendly solvent(s), *e.g.* water, the reaction of highly hindered substrates, the use of electron-rich and bulky ligands, Pd catalysts with high turnover number (TON), reactions at room temperature and the use of trifluoroborate as a substitute for the boronic acid or esters, as coupling partners.<sup>2,10,11,16</sup>

It is important to mention that the modern day C–C bond forming reactions were pioneered by luminaries such as Heck, Negishi, Stille and Suzuki, with these reactions named after them. These have found wide use in various synthetic processes, such as the synthesis of many natural products and also biologically active compounds.<sup>7,9,10</sup> The importance of the Pd-catalysed cross-coupling reactions culminated in the 2010 Nobel Prize in Chemistry being awarded to Suzuki, Heck and Negishi for their contribution to chemistry in general and Pd catalysed cross-coupling reactions in particular.<sup>9,17-20</sup>

Apart from the aforementioned eminent scientists, there are others who have also made significant contributions to the field of synthetic organic chemistry; Stille (organotin reagents),<sup>21-23</sup> Suzuki–Miyaura (organoboronic acids),<sup>24,25</sup> Sonogashira (terminal alkynes),<sup>26</sup> Kumada–Corriu (Grignard reagents),<sup>27,28</sup> Hiyama (organosilanes),<sup>29</sup> and Negishi (organozinc reagents)<sup>30</sup> reactions (**Figure 1**).

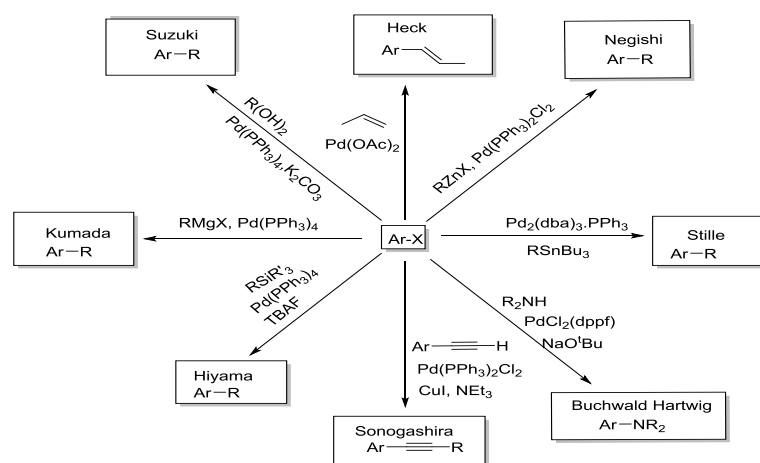
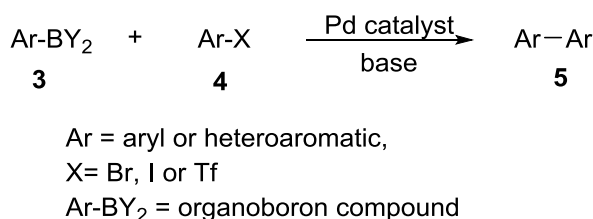


**Figure 1** Examples of Pd-catalysed C–C bond formation reactions.

## 1.3 Pd-catalysed Suzuki-Miyaura cross-coupling (SMCC)

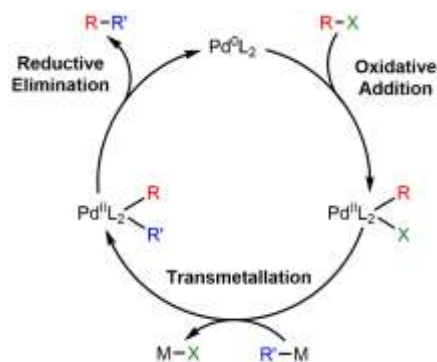
### 1.3.1 Background

In the late 1970s Suzuki and co-workers reported a Pd-catalysed cross-coupling reaction involving organoboron compounds (alkenyl boronates) **3** with alkenyl bromide **4** in the presence of a base, leading to the formation of the C–C bond (**Scheme 2**).<sup>7</sup> This reaction has since undergone various stages of modification, but still remains arguably one of the most versatile means of constructing C–C bonds known to the modern chemist.<sup>7,9</sup>



**Scheme 2** A general schematic representation of the Suzuki coupling reaction.

Since its discovery, research into the subject has been widespread and although the reaction mechanism is still not completely understood, it is believed to proceed through three main steps; oxidative addition, transmetallation and reductive elimination.<sup>2,4</sup> The oxidative addition step typically involves Pd(0) interacting with the organohalide species to form the organopalladium halide (RPdX) which is then converted to the diorganopalladium complex (R–Pd–R') through the transmetallation step and finally, the reductive elimination step which leads to the formation of the new C–C bond with regeneration of the Pd (0) species.<sup>19,25,31,32</sup> Most researchers in the field have come to agree that the mechanism may be more complicated than it is often depicted in text books (**Scheme 3**).<sup>33-36</sup> The desire to get a better and a more comprehensive understanding of the mechanism have led many groups to investigate the steps of the reaction. One of such groups was Cid and co-workers who used both experimental and computational data to suggest the long-held view (hypothesis) that transmetallation step involves multiple steps. The organoboronic acid is initially activated by the external base and then it attacks the Pd centre as an organoboronate anion.<sup>20,33,35</sup>



**Scheme 3** Simplified version of the SMCC reaction catalytic cycle.

Most suggested Pd-catalysed cross-coupling reaction mechanisms, such as above, have mainly been presumed to proceed *via* homogeneous catalysis, involving the mononuclear Pd(0) with organohalides to generate the oxidative addition product. There is however a significant amount of evidence in the literature to suggest that the mechanism may not be exclusively homogeneous.<sup>2</sup> Catalysts such as Pd(OAc)<sub>2</sub> have been shown to reduce then aggregate in solution to form a higher order Pd(0) species from which Pd species can be leached into solution, making the catalysis appear homogeneous,<sup>2,35</sup> when it may be heterogeneous or combination of the two (*i.e.* quasi-heterogeneous). The question therefore arises as to the role of these aggregated Pd species; do they act as a reservoir and leach catalytically active Pd species or do they simply come to a dead end, and do not play any active role in the catalysis? (**Figure 2**).<sup>37,38</sup> The evidence for the existence of Pd reservoirs in cross-coupling chemistry was first published by de Vries and co-workers who were able to explore this in a Mizoroki-Heck coupling reaction of bromobenzene and n-butyl acrylate in the presence of Pd(OAc)<sub>2</sub>. They observed that there was an inverse relationship between the catalyst loading and the yield of the reaction. This they attributed to the formation of Pd aggregate (Pd black) being formed at higher catalyst loading.<sup>31</sup> Additionally, although Pd(OAc)<sub>2</sub> is one of the most frequently used pre-catalysts in SMCC reactions the known impurities of the hydrate, *i.e.* Pd<sub>3</sub>(OAc)<sub>6</sub>(OH<sub>2</sub>), and nitrate, *i.e.* Pd<sub>3</sub>(OAc)<sub>5</sub>NO<sub>2</sub>, may affect the active catalyst species and hence the mechanism.<sup>38</sup>

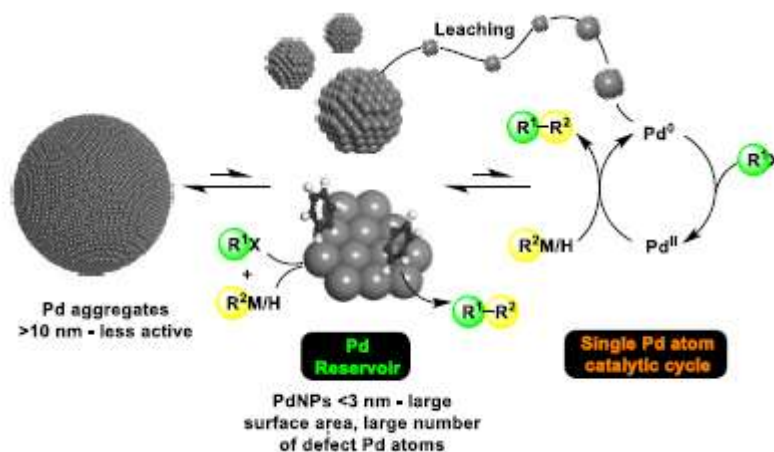
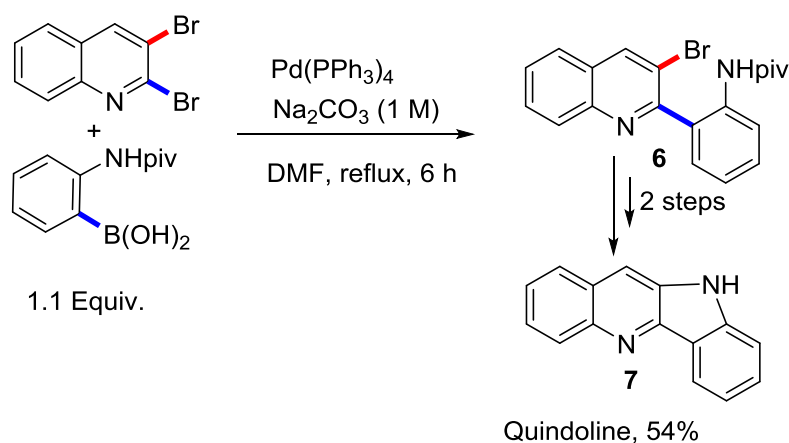


**Figure 2** Schematic representation for the role of aggregated Pd in catalysis. Reproduced with permission of The Royal Society of Chemistry.<sup>2</sup>

Jutand and co-workers have contributed immensely to the understanding of Pd catalyst leaching in SMCC reactions by investigating core shell Au–Pd nanoparticles. In one such reactions, they reported the concentration of detected leached Pd species to be below (1 ppm Pd), but this was enough to effectively perform the reaction under investigation to give 95% product after 4 h at room temperature.<sup>39</sup>

SMCC has been used extensively in total synthesis and is probably the most simple, most common, precise and efficient way of forming biaryls or substituted aromatics.<sup>7,9,11</sup> These synthetic products form the backbone of many polymers, ligands, natural products, and pharmaceutical products, making an efficient synthetic method crucial to the synthetic chemist. A good example is in the synthesis of quindoline **7**, an anticancer agent (**Scheme 4**), originally isolated from the west African plant *Cryptolepis sanguinolenta*.<sup>9</sup>



**Scheme 4** Total synthesis of an anti-cancer agent quindoline **7**, using SMCC reaction.<sup>9</sup>

Even though so many equally predictable methods of forming biaryl compounds have been established, the Suzuki-Miyaura method is still the most preferred choice of synthesising C–C bonds in aromatic and heteroaromatic systems. This is mainly due to the mild reaction condition, *e.g.* ambient temperature and aqueous medium, which pertains to the reaction and the ease of separating the products from the by-products. Also, organoboronic acids are generally readily available and do not pose that much of a hazard to the environment when compared with other organometallic reagents that are used in catalysis, although boronic acids can react with nucleobases on the ribose sugar.<sup>5,19</sup>

The solvent of choice for SMCC reactions is usually tetrahydrofuran (THF) or diethyl ether, in the presence of either a Pd(0) or Pd(II) pre-catalyst. In recent years however different green solvents such as water or co-solvents (water/organic solvent mixture) have been used as the preferred solvent of reaction.<sup>5</sup> The role played by the base additive in this reaction is vital to the transmetallation step of the catalytic cycle. The reactivity and selectivity of the reaction is highly dependent on the type of base used, as they are known to accelerate the transmetallation and the reductive elimination steps. Bases such as Ba(OH)<sub>2</sub>, K<sub>3</sub>PO<sub>4</sub>, Na<sub>2</sub>CO<sub>3</sub>, TIOH, KF, Cs<sub>2</sub>CO<sub>3</sub>, NaOH, KOH and K<sub>2</sub>CO<sub>3</sub>, have all been used in the SMCC reaction.<sup>33,35,41</sup>

In 2012, using chronoamperometry and <sup>31</sup>P-NMR spectroscopic analysis to monitor their reactions, Jutand and co-workers reported the antagonistic effect of metal carbonate bases such as Na<sub>2</sub>CO<sub>3</sub>. It was discovered that metal carbonate base was not a favourable additive for SMCC reactions, because the concentration of hydroxyl (OH<sup>-</sup>) ions produced in the aqueous medium is limited, resulting in the slowing-down of transmetallation and the reductive elimination steps. In the same report they stated that compared with the carbonate bases, nBu<sub>4</sub>NOH was a better base since it helps to accelerate the transmetallation and the reductive elimination steps.<sup>15</sup> As a result of the high concentration of the OH<sup>-</sup> ions produced in solution and the observed trend of counteranions of the anionic bases released in solution: Ti<sup>+</sup> or Ag<sup>+</sup> > nBu<sub>4</sub>N<sup>+</sup> > K<sup>+</sup> > Cs<sup>+</sup> > Na<sup>+</sup>.<sup>35</sup>



### 1.3.2 The use of palladium catalysts in SMCC reactions

The most common source of Pd catalyst in SMCCs is  $\text{Pd}(\text{PPh}_3)_4$ , and Pd(II) pre-catalysts such as  $\text{Pd}(\text{OAc})_2$  and  $\text{PdCl}_2$ , which are reduced to the catalytically active Pd(0) *insitu*.<sup>2</sup> Although phosphine ligands have been known to be effective in stabilising the Pd(0) species used in Pd-catalysed SMCC reactions of arylboronic acids, they are also known to be expensive, becoming depleted and toxic.<sup>43</sup> Therefore, the use of alternative phosphine ligands or using ligand-free catalysts have been exploited by many research groups in the field.<sup>44</sup>

In 2008, Buchwald and co-workers published their work on the development of a new family of ligands called dialkylbiarylphosphines (electron-rich and bulky phosphines) and found them to enhance the rate of both the oxidative addition and reductive elimination processes in SMCC.<sup>16,18</sup> These bulky and electron-rich phosphine ligands have contributed dramatically to the efficiency and the increase in selectivity of the SMCC reaction. Below is a detailed description of the generalised structure of these ligands (**Figure 3**).<sup>18</sup>

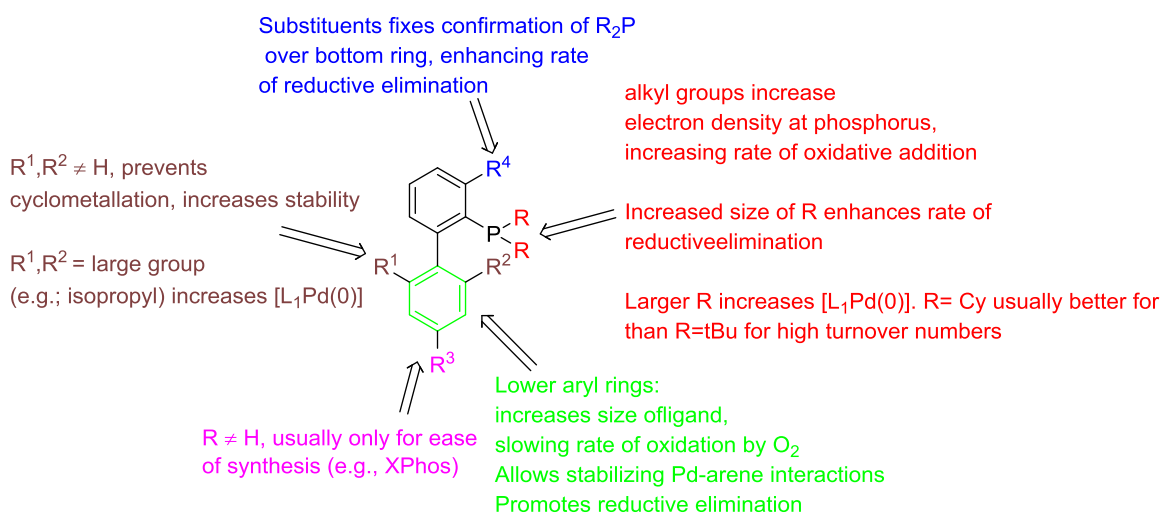


**Figure 3** Structural features of the dialkylbiarylphosphines and the impact of structural modifications on the efficacy of catalysts.<sup>18</sup>

Buchwald and co-workers went on to screen some of their developed ligands in conjunction with palladium catalysts and demonstrated that although some ligands were successful in assisting catalysis in SMCC reactions, many required higher catalyst loading to function effectively.<sup>19</sup> In their studies, they reported that the aminophosphine ligand 2-(dimethylamino)-2'-dicyclohexylphosphinobiphenyl **8** (DavePhos) (**Figure 4**) promotes the Pd-catalysed amination of aryl chlorides at room temperature. They noted that, although, the Pd catalyst supported by **8** (DavePhos) was sufficiently active in promoting this

transformation, the preparation of the ligand is cumbersome and requires four steps from readily available starting material. In all, ligand **8** was found to perform favourably with the SMCC of hindered substrates and provided for efficient reactions at low catalyst loadings.<sup>18,45</sup>

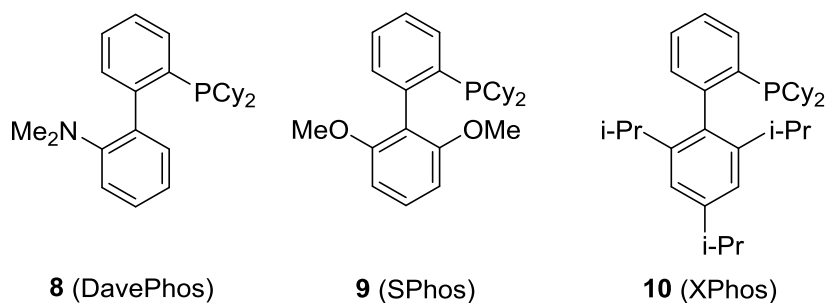
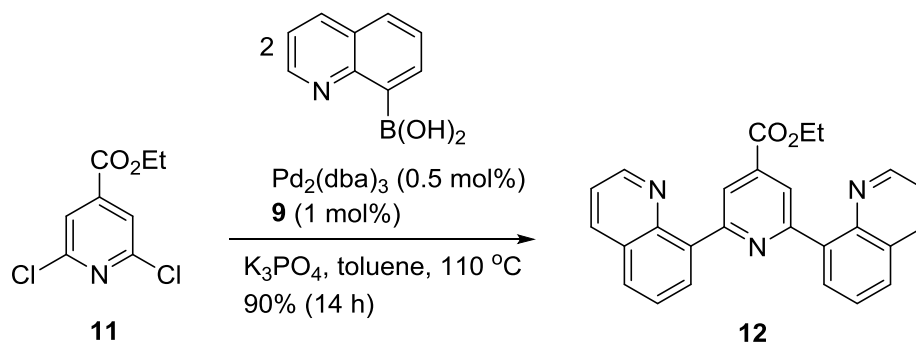


**Figure 4** Selected examples of Buchwald ligands used in cross-coupling reactions.<sup>18</sup>

In another publication, Schlosser and co-workers reported a modification to a synthetic methodology originally developed by Buchwald and co-workers. They demonstrated the efficiency of 2-(2'-6'-dimethoxybiphenyl) dicyclohexylphosphine **9** (SPhos) in a SMCC reaction of hindered substrates (**Scheme 5**).<sup>18</sup> They also reported that although ligand **9** worked very effectively with most Pd precatalysts, they recorded no conversion when they attempted to couple 2,4,6-triisopropylbromobenzene with 2,6-dimethylphenylboronic acid in the presence of 1.5 mol% of Pd<sub>2</sub>(dba)<sub>3</sub> and 6 mol% of **9** at 100 °C for 14 h. They further went on to compare the reactivity of ligands **9** and **10** and concluded that ligand **9**, being relatively more electron-rich than **10**, was generally catalytically superior to **10**, although less effective at low catalyst loading and low reaction temperature (**Figure 4**).<sup>18</sup> Electron rich ligands play an important role in catalyzing SMCC reaction because they increase electron density on the Pd centre to facilitate oxidative addition of the strong C–Cl bond.



**Scheme 5** SMCC reaction using Pd<sub>2</sub>(dba)<sub>3</sub> and ligand **9** as the catalyst system.<sup>18</sup>

In an attempt to optimise the protocol for Pd-catalysed C–O bond forming cross-coupling reactions, Buchwald and co-workers succeeded in developing a di-*tert*-butylphosphino-aminobiphenyl ligand **13** and found it to be effective for assisting the coupling of arylhalides with phenols with Pd loadings of 0.000001–0.02 mol%. They also found catalysts generated from ligands (**13** and **14**) to have comparable reactivity in some of the catalytic processes that they investigated, but with ligand **13** being catalytically more efficient for a wide variety of substrates with 0.5–1.0 mol% Pd loading<sup>45</sup> (**Figure 5**).

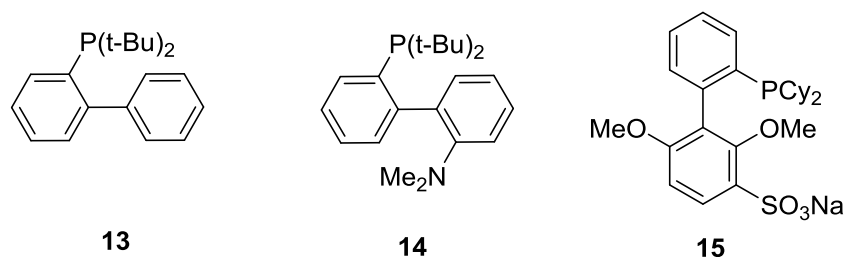
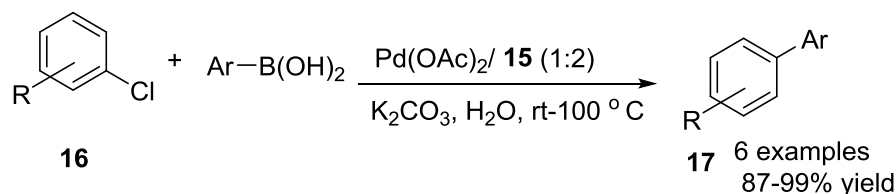


**Figure 5** Buchwald ligands used in cross-coupling reactions.<sup>18</sup>

Further modification of the Buchwald ligands led to other more suitable ligands for catalysing cross-coupling reactions, a very useful example being ligand **15** (**Figure 5**), a water soluble sulphonated derivative of SPhos **9** (**Figure 4**). Ligand **15** was found to be significantly more stable than ligand **9** and also results in a more catalytically active Pd species. Ligand **15** was used in the coupling of substituted arylchlorides **16**, affording excellent product yields (**Scheme 6**).



**Scheme 6** SMCC reactions of substituted arylchlorides **16** and arylboronic acids using **15**.<sup>18</sup>

Bedford and co-workers have also contributed to the expansion of the frontier of Pd-catalysed cross-coupling reactions by developing novel ligands.<sup>44</sup> They discovered the *ortho*-metallated Pd(II) triarylphosphite complex **19** to be an active catalyst for the SMCC reaction, given a high TON of  $1 \times 10^4$  at 110 °C, compared with the complex **18** which gave  $7.4 \times 10^4$  at 130 °C over 16 h. Furthermore, complex **19** exhibited high activity with both electronically-activated and deactivated aryl bromides. Complexes of the type **20** and **21**, *i.e.* palladacyclicphosphinites (**Figure 6**) are suitable catalysts for the coupling of

deactivated and sterically hindered aryl bromides. The advantages of the Bedford ligands compared with others are their relative low cost, ease of synthesis, air and thermal stability and typically high yields achieved at low Pd concentration.<sup>45-47</sup>

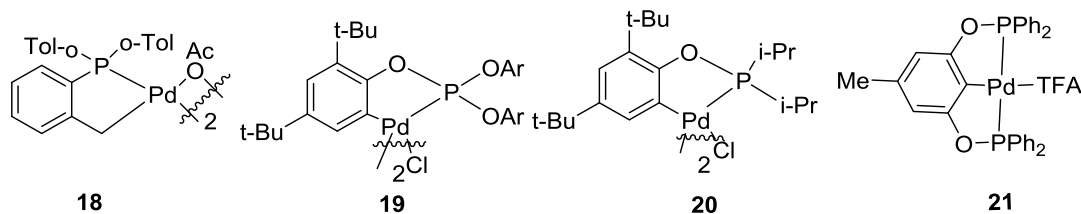
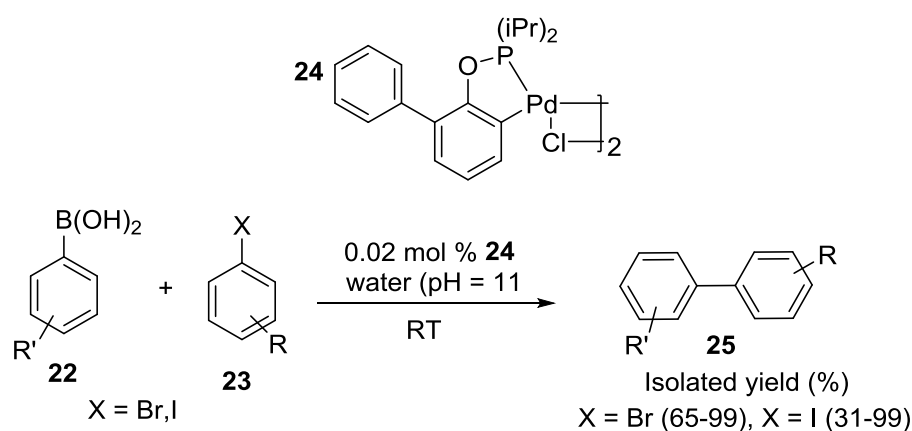


**Figure 6** Bedford type Palladacyclic complexes used in SMCC reactions.<sup>45</sup>

In 2011 Eppinger and co-workers also reported the utilization of a Bedford-inspired palladacycle ligand **24** in a SMCC reaction of bromophenol and phenylboronic acid using water as an environmentally friendly solvent (**Scheme 7**). While the catalyst was air sensitive, it exhibited high thermal and moisture stability as well as superior catalytic activity in comparison with other catalysts.<sup>45,48</sup>



**Scheme 7** A SMCC reaction catalysed by a Bedford-type palladacycle.<sup>48</sup>

Although many phosphine-based ligands have been found to be effective in catalysing a variety of cross-coupling reactions, they have the negative effect of being toxic, expensive and unrecoverable and this has limited their industrial utilization. There is therefore a need to discover phosphine, or ligand-free Pd-catalysed cross-coupling reactions.<sup>49</sup>

In order to achieve this, a lot of investment has been made towards the development and utilization of these highly-reactive non-phosphine ligands in cross-coupling reactions. One such type of ligands are *N*-heterocyclic carbenes (NHCs).<sup>46,50,51</sup> These are known to be air

sensitive, but can be generated *in situ* to aid easy handling and share similar attributes to phosphines. They have been found to be very useful in many SMCC reactions, including the coupling of sterically-hindered, unactivated aryl chlorides with sterically hindered aryl boronic acids under mild reaction conditions in high yields of di- and tri-aryl products.<sup>47,49</sup> An example of an *N*-heterocyclic carbene ligand is **26**, which is known to be the active ligand generated *in situ* from **27** (**Figure 7**). These ligands are generally effective with aryl chlorides in SMCC reactions, even though the C–Cl bonds are known to be more difficult to activate than the C–Br bonds.<sup>14</sup>

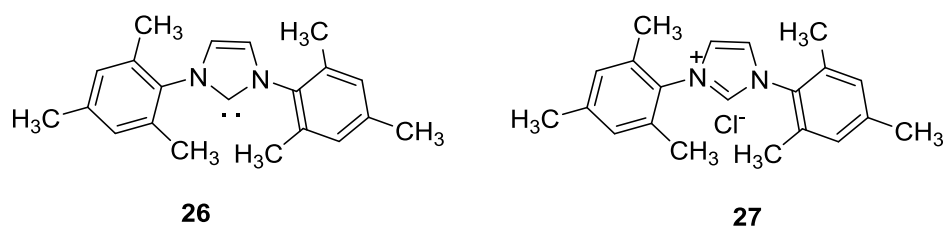
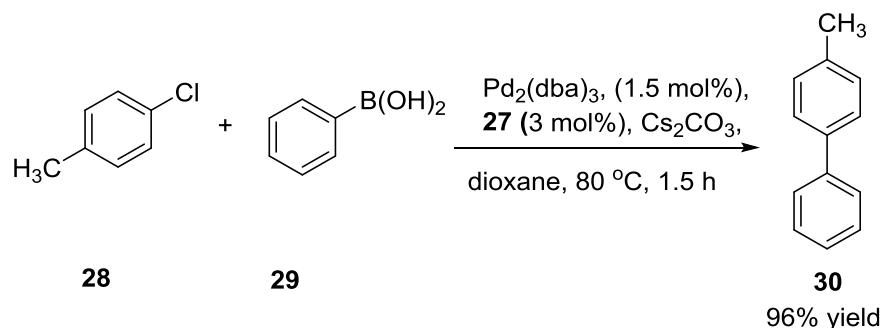


**Figure 7** An example of a *N*-heterocyclic carbene ligand used in SMCC reactions.<sup>14</sup>

$\text{Pd}_2(\text{dba})_3$  with ligand **27** was used in a SMCC reaction of 4-chloro-4-methylphenyl **28** with phenylboronic acid **29** afforded an excellent product yield of 96% (**Scheme 8**).



**Scheme 8** Using *N*-heterocyclic carbene ligand **27** in a SMCC reaction.<sup>14</sup>

Another type of phosphorus-free ligand that has been developed and is quite effective with Pd-catalysed cross-coupling reactions, are ligands containing the guanidine group (**Figure 8**). Both the tetraalkylguanidine (TAGs) and the pentaalkylguanidine (PAGs) have been found to be useful in both the Suzuki-Miyaura and the Heck cross-coupling reactions.<sup>49</sup>

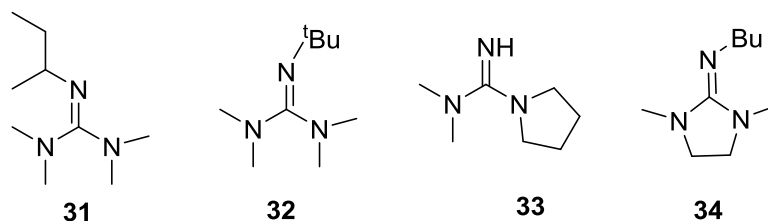
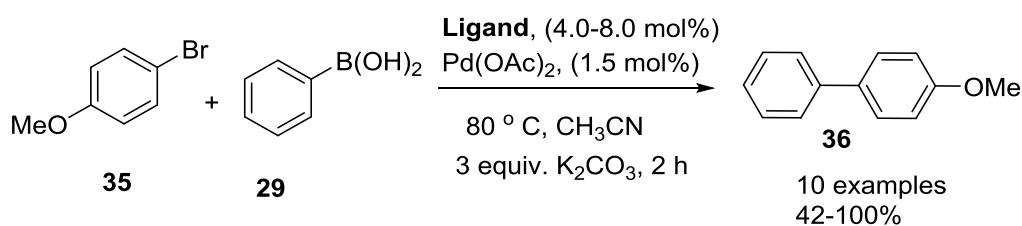


**Figure 8** Structural examples of the guanidine ligands used in cross-coupling reactions.<sup>49</sup>

The guanidine group-containing ligands were effective in assisting catalysis of SMCC reactions affording good to excellent isolated yields of the desired products (74% to quantitative) with ligand **31** and **32** giving quantitative yield of the isolated products. They however, reported a modest yield of 42% in the absence of the guanidine ligands, giving a clear indication of the vital role played by the ligand in the catalytic process (**Figure 8**).<sup>49</sup> When the Pd(OAc)<sub>2</sub> catalyst loading was increased from 1.5 mol% to 2 mol% and less reactive chlorobenzene and phenylboronic acid was reacted, a disparity in the reactivity of the catalyst, was discovered, with the bulky ligands reacting better than the less bulky ligands. Below is a bench mark reaction showing the coupling of 4-bromoanisole **35** with phenylboronic acid **29** affording moderate to excellent yields of product **36** (**Scheme 9**).<sup>49</sup>



**Scheme 9** Screening of the guanidine ligands in the SMCC Reaction.<sup>49</sup>

Finally, another phosphine-free ligand group of catalyst worth mentioning is *bis*(dicyclohexylamine) palladium(II) acetate (DAPCy) **37** developed in 2004 by Boykin and co-workers (**Figure 9**).<sup>52</sup> This catalyst was made from the reaction of Pd(OAc)<sub>2</sub> with dicyclohexylamine.

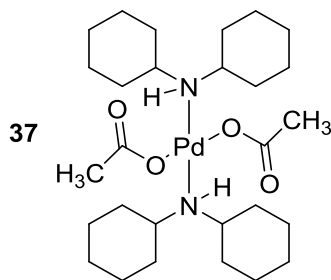
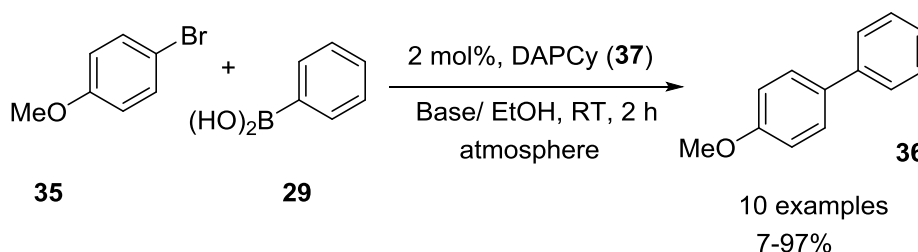


**Figure 9** Structure of *bis*(dicyclohexylamine)palladium(II) acetate (DAPCy).<sup>52</sup>

The authors went on to investigate the efficacy of this catalyst using a SMCC model reaction of aryl bromides and phenylboronic acids. They reported the reaction to be effective and affording good to excellent yields of the desired biaryl products. The catalyst also performed well at low temperatures and low catalyst loading, especially when ethanol was used as the solvent of the reaction (**Scheme 10**).<sup>50</sup>

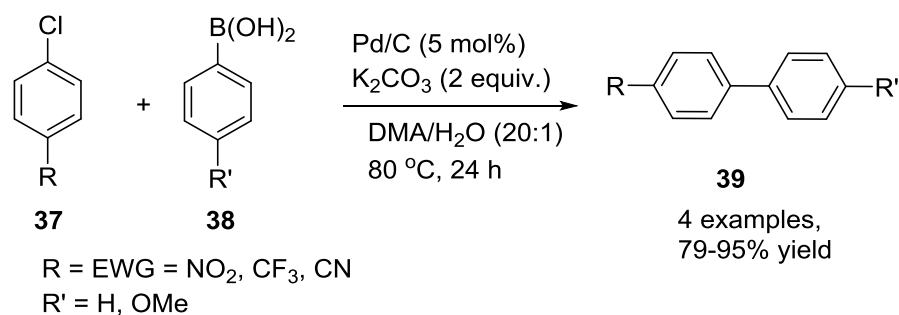


**Scheme 10** An example of DAPCy-catalysed SMCC reaction.<sup>53</sup>

They also reported that the catalytic properties were to be dependent on the type of base used, with  $\text{K}_2\text{HPO}_4$  and  $\text{LiOH}\cdot\text{H}_2\text{O}$  affording 97% and 7% yields respectively. One of the most interesting properties of this catalyst is that the reaction can be conducted under aerobic conditions, which may help to eliminate one of the side-reactions, leading to formation of homocoupled products, without affecting the yield of the desired cross-coupled product.<sup>53</sup>

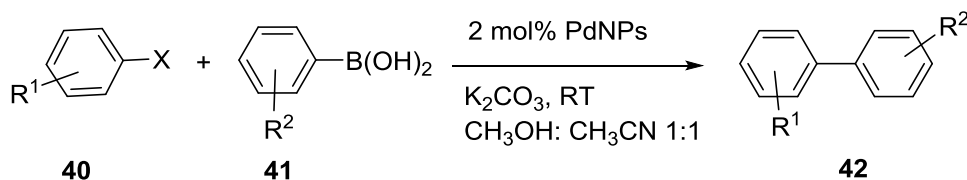
Mandali and Chand used LeBlond's methodology using Pd on carbon (Pd/C) as a catalyst for the formation of biaryls and heteroaryls *via* the SMCC reaction.<sup>54,55</sup> These catalysts are usually considered to react *via* heterogeneous catalysis and can be used in the presence or absence of a phosphine ligand in an aqueous medium. They reported that Pd/C was effective when aryl chloride substrates with electron withdrawing groups (EWGs) such as

NO<sub>2</sub>, CF<sub>3</sub>, and CN gave 79–95% **39** yields, whilst neutral and electron donating groups (EDGs) such as H and Me gave marginal yields (**Scheme 11**).<sup>53</sup>



**Scheme 11** A Pd/C-catalysed SMCC reactions of substituted arylhalides.

Unsupported Pd nanoparticles (PdNPs) have also attracted significant attention in SMCC reactions, largely due to the high surface-to-volume ratio and the high surface energy of defect atoms. This makes PdNPs worthy of development and utilization in catalytic processes such as hydrogenation, oxidation and C–C bond formation. These particles usually have distinctive size, structure and compositions ranging in sizes between 1–100 nm and are seen as a bridge between atomic and bulk metal, with unique chemical, physical and electronic properties. Below is a typical ligand-free SMCC reaction catalysed by PdNPs (**Scheme 12**).<sup>54</sup>



**Scheme 12** PdNP-catalysed SMCC reaction.

Various supports (stabilisers) such as polyvinylpyrrolidone (PVP) **43** and 2,2'-bis(diphenylphosphino)-1,1'-binaphthalene (BINAP) **44** have been used in the synthesis of PdNPs (**Figure 10**). In this regard groups of El-Sayed, Glorius, and Fairlamb *et al.*, have made significant contributions to the synthesis and investigation into the catalytic effectiveness of Pd nanoparticles in various cross-coupling reactions. El-Sayed and co-workers have also investigated the effect of particle size on catalytic activity, concluding that the reaction intermediates are adsorbed strongest to smaller nanoparticles which may then poison the reaction and result in decreased catalytic activity for smaller particles.<sup>2,56,57</sup>



Fairlamb and Lee published their findings on the investigation of the catalytic properties of PVP–PdNPs **46** in a SMCC reaction of 4-iodoanisole **45** with phenylboronic acid **29** in methanol to produce **47** heterogeneously (**Scheme 13**).<sup>2</sup> The evidence that the reactions were heterogeneous was very strong and employed a raft of physical characterisation techniques to confirm the heterogeneity of the reactions; for some examples see (**section 1.3.3**).

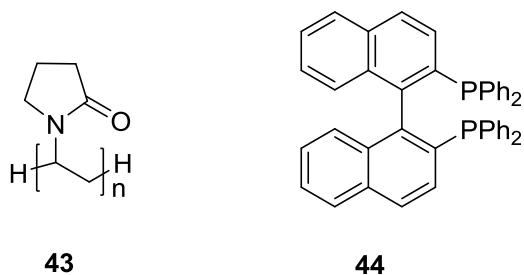
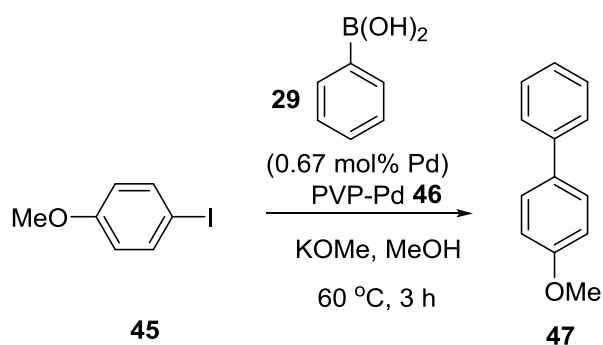


**Figure 10** PVP **43** and BINAP **44** can both act as PdNP-stabiliser ligand systems.



**Scheme 13** SMCC coupling of 4-iodoanisole **45** and phenylboronic acid **29**.<sup>2</sup>

### 1.3.3 Physical methods used to test heterogeneity of reactions

The literature is saturated with numerous information regarding the distinction between homogeneous and heterogeneous catalysis. In his recent review Finke had cited many methodologies used to distinguish between catalysis by metal nanoparticles and metal complexes when starting with metal complexes of easily reducible metals (Pd, Pt, Ru, etc.) in hydrogenation reactions.<sup>59</sup>

It should however be stated that there is no single empirical evidence available to confirm the true nature of the catalytic components of the metal species used in synthesis.<sup>2</sup>

Instead deductions from the results of several tests are used to ascertain the type of catalysis employed in a particular reaction. Techniques such as kinetic investigations, filtration test and poisoning studies have been performed to confirm whether a particular reaction was homo or heterogeneous catalysis.<sup>2,3,59</sup>

The mercury (Hg) drop test as the name implies, involves the addition of a large excess (ca. 200–500 eq.) of elemental Hg to a reaction mixture. This is added from the start of the reaction and the effectiveness of the test is enhanced with vigorous stirring to cause the high density Hg atom to be distributed effectively throughout the reaction medium.<sup>2,3</sup> The Hg amalgamation that is formed in the reaction medium poisons the reaction and hence causes the reaction to slow down or stop if there are catalytically active nanoparticles present in the reaction mixture.<sup>60</sup>

Another common method of confirming heterogeneity of a catalyst is the hot filtration test which is performed to confirm the presence of soluble leached active metal species. The test involves the reaction mixture being filtered through heated Celite (or other diatomaceous metal scavengers) at half-way point of the reaction.<sup>2,60</sup> The filtration allows the removal of large clusters and nanoparticles from the reaction medium. After the filtration, the reaction is then continued and If the reaction continue to proceed; it gives an indication of either the system is homogeneous catalysis or heterogeneous catalysis. The reaction can be monitored using TEM images of the reaction intermediates to confirm its heterogeneity.

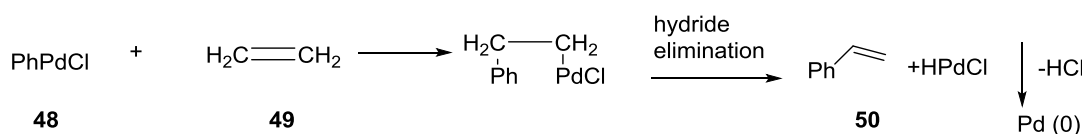
The palladium poisoning PVPy (polyvinylpyridine) test is also often employed to confirm the heterogeneity of a catalyst. This polymer binds very strongly to Pd(0) and can trap active palladium nanoparticles and stop the reaction from proceeding.<sup>60</sup> The test can be employed to confirm homogeneous catalysis, since it is known to effectively quench the reaction. The test however, has some inherent challenges in the sense that the polymer can in some cases inhibit homogenous catalytic species, preventing definitive conclusions to be drawn based on the outcome of the test alone.<sup>3</sup>

Finally, a three-phase test comprising solid-supported substrates (immobilised on a non-reactive polymer e.g. Wang resin)<sup>2</sup> can be used in place of a normal substrates to confirm the heterogeneity of a reaction. Both the reaction mixture and the solid support at the end of the reaction are analysed to confirm the presence of leaching. Active

homogeneous catalyst species are able to access the supported substrate and produce solid-supported product under normal reaction conditions.<sup>2,60</sup> These active catalysts are considered to be heterogeneous, if they are unable to interact sufficiently with the encapsulated substrate and hence provides little or no observable product.<sup>2</sup> It is a generally held opinion that inactive homogeneous particles can be formed via leaching and analytical measurements such as inductively coupled plasma mass spectrometry (ICP-MS) can be used to test for this occurrence. The process of using resins to distinguish between homogeneous and heterogeneous catalysis is however, bedeviled with a lot of complications and hence several experiments are performed to authenticate the results.

#### 1.4 Pd-catalyzed Heck coupling reaction

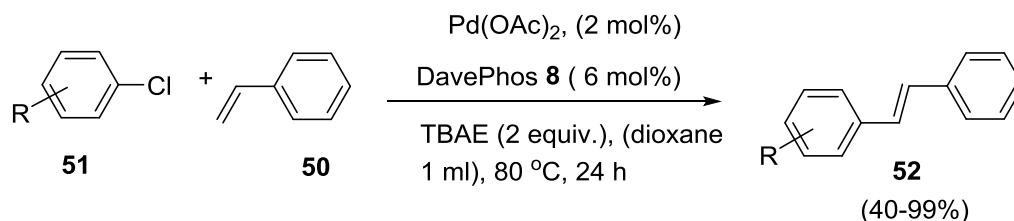
In Heck's first publication, he was able to synthesise styrene **50** from phenylpalladium chloride **48** (PhPdCl) with ethylene **49**, followed by the elimination of the Pd (**Scheme 14**).



**Scheme 14** The general Heck synthesis of styrene mediated by Pd.

The modern day Heck reaction involves aryl halides and an olefin in the presence of a Pd catalyst. It has many good attributes and this is exemplified by the countless times it has been employed in synthetic chemistry, such as ring closure reactions, the synthesis of polyenes, and fragment couplings.<sup>7,61</sup>

Zhou and co-workers reported the use of the Buchwald ligands in the Heck coupling reaction of styrene. They found out that using the same Pd catalyst and ligand, but varying the choice of base (traditional inorganic and organic bases) and temperature (60 and 80 °C) resulted in different reaction yields. At the optimum temperature of 80 °C, DavePhos **8** was found to be superior to XPhos **10** and SPhos **9** and also Pd(OAc)<sub>2</sub> superior to PdCl<sub>2</sub> and Pd<sub>2</sub>(dba)<sub>3</sub> (**Figure 4**). They then investigated the catalytic efficiency of Pd(OAc)<sub>2</sub> in the presence of DavePhos **8** in a Heck reaction using different substituted arylchlorides **51** with styrene **50** (**Scheme 15**).<sup>58,61</sup>



**Scheme 15** An example where DavePhos **8** was used as a ligand in a Heck reaction.

The development of *N*-heterocyclic carbene ligands have also contributed immensely to the usefulness of the Heck reaction, and these catalysts are found to be very effective in coupling a wide range of aryl bromides and styrene derivatives and bromides and iodides with acrylates. This mixed NHC-phosphine ligand **53** (Figure 11) have been employed in a variety of Heck reactions of styrene derivatives with EWGs or EDGs on the ring, resulting in good to excellent yields (>90%) for most of the substrates, the exception being 4-chlorostyrene **54** which afforded the product in 74% yield (Scheme 16).<sup>61</sup>

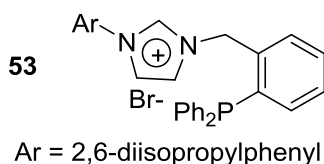
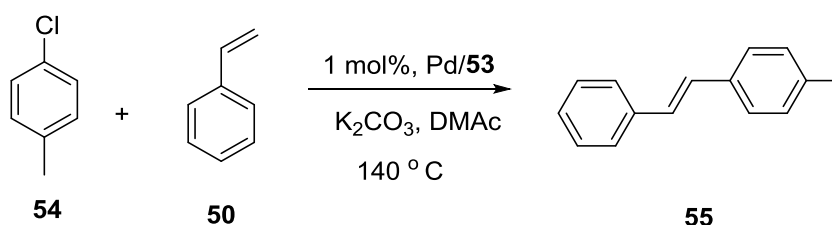
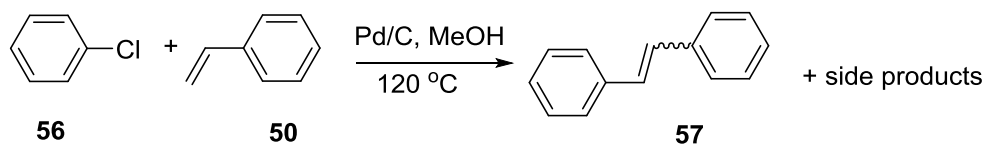


**Figure 11** An example of NHC ligand used as a ligand for Heck reactions.



**Scheme 16** Heck reaction of 4-chlorotoluene **54** with styrene **50**.

Palladium on carbon (Pd/C) has proven to be effective for Heck coupling reactions, achieving comparable reactivity and efficiency to their homogeneous counterparts. An example is the phosphine-free reaction of chlorobenzene and styrene catalysed by Pd/C in pure MeOH at 120 °C in an autoclave under pressure, affording stilbene **57** in 62% yield (82% conversion of styrene **50**). Under these conditions,  $\text{PPh}_3$  was found to be an inhibitor rather than promoter. This was confirmed in another experiment where the same reaction was performed under atmospheric pressure using alternative solvents such as ethylene glycol or ½ (v/v) of methanol/ethylene glycol mixture.<sup>62</sup>

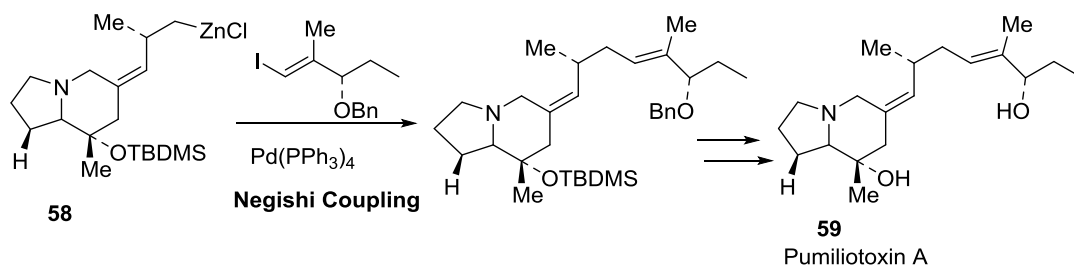


**Scheme 17** An example of Heck reaction catalysed by Pd/C.

## 1.5 Negishi reactions

Negishi reactions were discovered in the late 1970s and they are also one of the most efficient routes of constructing C–C bonds. Both the substrate scope and available catalysts have expanded over the years and this is mainly due to the relatively high functional group tolerance of zinc compounds and its applicability in total synthesis.<sup>7,63</sup> The Negishi reaction involves the use of various organozinc reagents as nucleophilic coupling partners. The most common organozinc reagents used in the Negishi transformation are diorganozinc species ( $R_2Zn$ ) and organozinc halides ( $RZnX$ ).<sup>7,64</sup> The  $RZnX$  reagent is usually prepared either by direct insertion of zinc (zinc dust) into organic halides or by transmetalation from other organometallic species, such as  $RLi$ . Although, organozinc reagents are only moderately reactive towards many organic electrophiles, they are among the most reactive nucleophiles in Pd-catalysed cross-coupling reactions.<sup>7</sup>

In recent years, there has been a renewed interest in this reaction and just like Suzuki and Heck reactions, the Negishi reaction has been used in the synthesis of mainly biaryls and heterobiaryls.<sup>7</sup> The versatility of the reaction has been well documented and appreciated by the pharmaceutical industry and others for the synthesis of natural products and agrochemicals. It is worth mentioning that although zinc compounds are generally reactive at room temperature, they can also degrade at higher temperatures. A good example of the synthetic application of the Negishi reaction is in the synthesis of pumiliotoxin A **59** in 51% yield, which is obtained after deprotection (**Scheme 18**).<sup>65</sup>



**Scheme 18** The use of the Negishi cross-coupling reaction in pumiliotoxin A **59** synthesis.

Using RuPhos **60** (Figure 12), in the presence of  $\text{Pd}_2(\text{dba})_3$ , Buchwald and co-workers reported a successful Negishi coupling reaction using tetrahydrofuran (THF) as solvent at 70 °C. The catalyst system was found to show tolerance to functional groups such as nitro, ester, alkoxy and amino substituents. Good catalyst efficiency (0.01% Pd) was found in Negishi couplings, with quantitative yields seen in some cases (Scheme 19).<sup>65</sup>

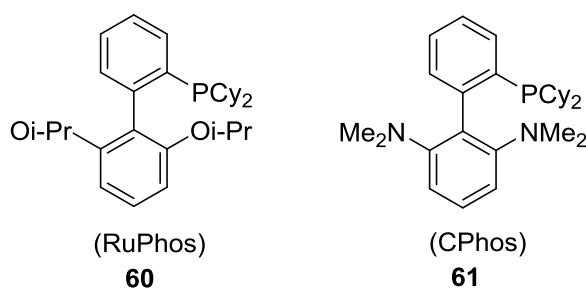
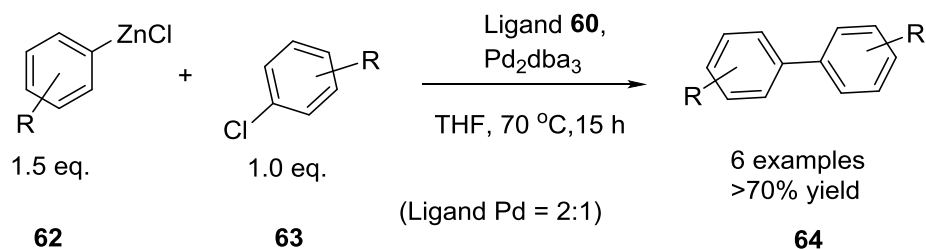


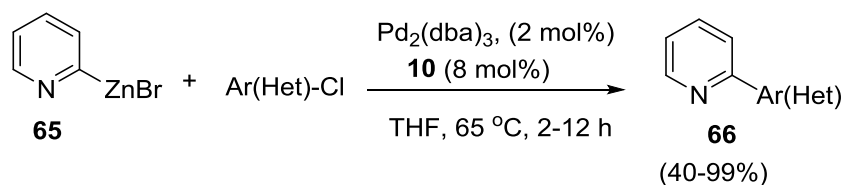
**Figure 12** Examples of the Buchwald ligands used in Negishi cross-coupling reactions.



**Scheme 19** Examples of Negishi-coupling of substituted aryl chlorides employing the RuPhos **60** ligand.

In 2010, Yin and co-workers used the Buchwald ligands in the catalysis of Negishi coupling reactions. Studying the reaction under various conditions, it was concluded that XPhos **10** (Figure 4) was a better ligand than RuPhos **60** (Figure 12).<sup>65</sup> With the optimised reaction conditions, they investigated the scope of the reaction by using several substituted aryl and heteroaryl chlorides, and commercially available 2-pyridyl- and 2-thienylzinc reagents

65. High to excellent yields of the desired products were reported from this study (Scheme 20).<sup>66</sup>



**Scheme 20** An example of a reaction showing the use of XPhos**10** in Negishi coupling.

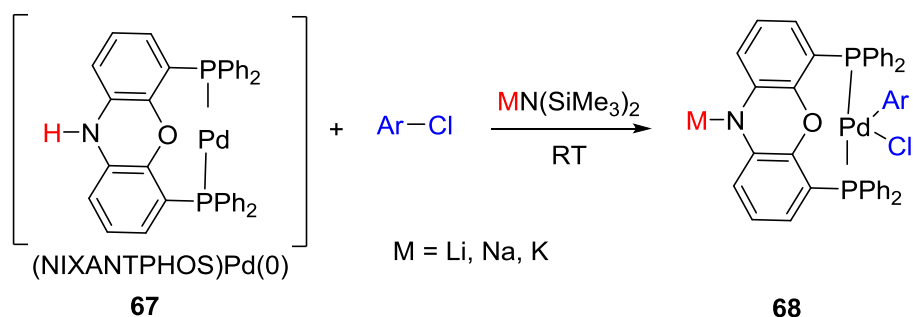
Although most developed ligand-supported Pd catalysts are unable to couple secondary alkylzinc halides with bromo- and chloroarenes, the Buchwald and Knochel groups recently reported Negishi coupling reactions under mild reaction condition, using the bulky ligand CPhos **61** (Figure 12). However, this reaction suffers from the formation of isomerised side products and hence reducing the desired yield.<sup>67,68</sup>

## 1.6 Direct arylation reactions

In recent years a new methodology termed direct arylation (DA) has emerged as a credible alternative to addressing some of the challenges posed by traditional cross-coupling reactions (*e.g.* Suzuki, Negishi, Heck, *etc.*).<sup>69</sup> The synthetic steps are reduced by omitting the pre-functionalisation step of the starting substrate and reducing the environmental impact of the reaction.<sup>2,69</sup> Just as is the case in traditional cross-coupling reactions, direct arylation reactions can be catalysed by both homogeneous and heterogeneous catalysts in the presence or absence of ligands. The reaction is continuously receiving improvements and fine tuning, to provide opportunities for the synthetic chemist. These facts are backed by the extensive research and review that is found in the literature.<sup>70,71</sup>

Although, C–H bonds are present in the vast majority of organic compounds, they are typically inert due to their relatively high bond strength. They do not show sufficient reactivity and selectivity for them to be classified as functional groups.<sup>71</sup> This notwithstanding, C–H bond activation has been exploited in recent years in the synthesis of biologically-active compounds and in this regards the pharmaceutical industry has exploited some of these reactions.<sup>70,72</sup>

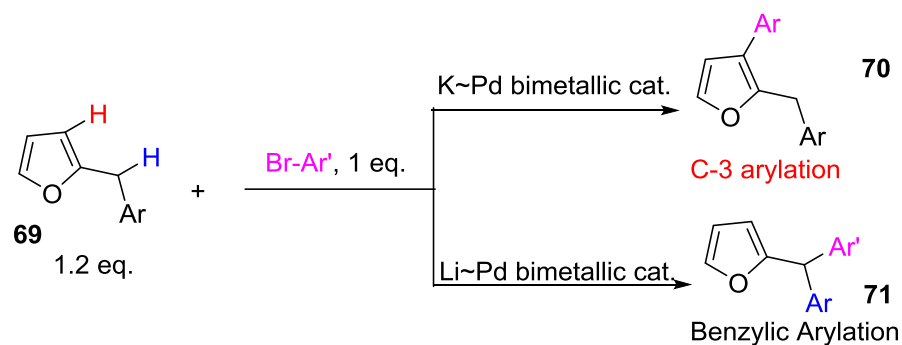
Despite the seemingly remarkable strides made in the research area of C–H bond functionalisation, there are still some challenges. For example, in a complex molecule containing two or more inequivalent C–H bonds the formation of the desired product can only be guaranteed if a particular point of reaction is selectively activated. One of such strategies being used to surmount this challenge is the installation of a directing group that will cause the catalyst to react selectively with the particular C–H bond of interest, *via* oxidative addition or other means of activation.<sup>71</sup> Walsh and co-workers have postulated the use of bimetallic catalysts to enhance catalyst selectivity beyond what was obtainable by the mononuclear catalysts.<sup>72,73</sup> They based their argument on the mode of regiochemical control from the synergistic reactivity observed in heterobimetallic Pd/M catalyst (M=Li, Na, K) based on the structure of NIXANTPHOS frame (**Scheme 21**).<sup>72</sup>



**Scheme 21** Oxidative addition of aryl chlorides by deprotonated (NIXANTPHOS)Pd(0).

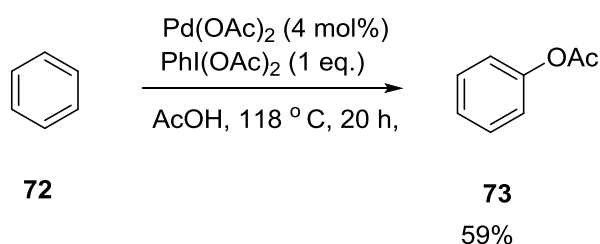
They also provided both experimental and computational data to support the observed selectivity for the above catalyst. This is supported by the cation- $\pi$  interaction showing the high selectivity generated for either C–3 or benzylic arylation products from 2-benzylfuran derivatives. This was further corroborated by the observation that the catalyst exhibited much greater reactivity in the oxidative addition of aryl chlorides than most reactive bidentate phosphine complexes of Pd, that are currently used to catalyse cross-coupling reactions. Investigating different reactions catalysed by this method, target products were obtained in moderate to excellent yields (**Scheme 22**).<sup>72</sup> Various auxiliary metals and solvents were tested and dioxane proved to be the best with 2.5 equivalents KN(SiMe<sub>3</sub>)<sub>2</sub> resulting in 55-93% assay yields (<sup>1</sup>H-NMR) of C–3 arylation.<sup>72</sup>



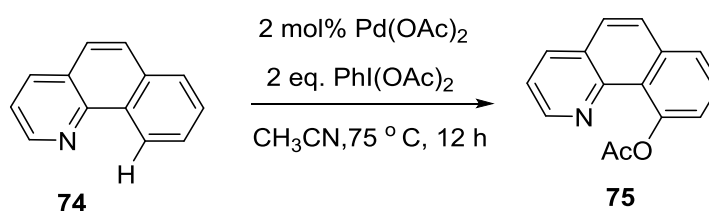


**Scheme 22** Cation-controlled site-selective  $\text{sp}^2$  C-3-H and  $\text{sp}^3$  benzylic C-H arylation of furans.

Building on Crabtree's findings (**Scheme 23**), Sanford and co-workers<sup>74,75</sup> applied the methodology to substrates containing pyridine as directing groups in order to study reaction selectivity. Using  $\text{Pd}(\text{OAc})_2$  alone, they reported C-H oxygenation of benzo[*h*]quinoline to afford a single isomer in high yields (**Scheme 24**).<sup>76</sup>



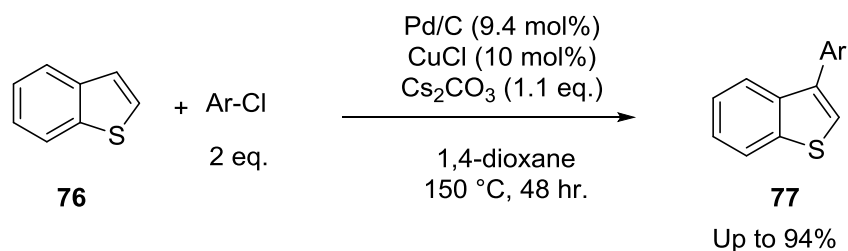
**Scheme 23** The catalytic acetoxylation of unactivated arenes.



**Scheme 24** Sanford's acetoxylation of benzo[*h*]quinoline.

While little work can be found in the literature on the regioselectivity of distinct Pd catalysts used in cross-coupling reactions, there is some remarkable evidence to suggest it is possible in some common homogeneous Pd pre-catalysts. Homogeneous and heterogeneous catalysts are known to undergo different mechanisms and the likelihood for different catalyst to show different selectivity in reaction can be traced to this. Unsupported Pd catalysts for instance, have been reported to show regioselectivity towards the C2 positions in both benzothiophenes and indoles. In this regard, both

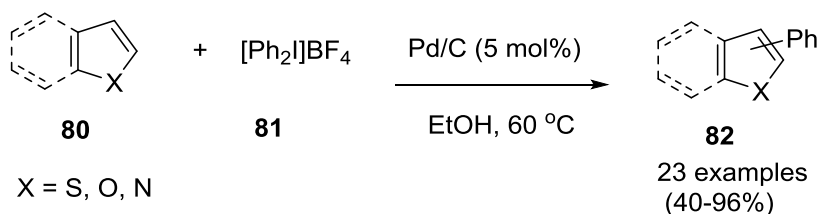
Glorius *et al.* have published their work on regioselectivity of direct C–H functionalisation of benzothiophene and indoles at the C3 positions by using heterogeneous Pd catalysts (Pd/C) (**Scheme 25**).<sup>69,77</sup>



**Scheme 25 Regioselective C–H functionalisation of benzothiophene using Pd/C.**

Also in a publication, Sames *et al.* succeeded in demonstrating the possible mechanistic attributes that allows the regioselectivity of Pd catalyst tilting towards C2 or C3 arylation of indoles.<sup>78</sup> They concluded that the regioselectivity between C2 vs C3 may be governed by factors such as steric bulk of the Pd ligands and complexation of Mg to the free NH.

Glorius and co-workers have also reported the Pd/C catalysed direct arylation of thiophenes, indoles, furans and benzofurans using iodonium salts **81** as the arylating agent, and found them to be very effective, affording regioselective products in good to excellent yields (**Scheme 26**).<sup>69</sup>



**Scheme 26 Pd/C as catalyst for regioselective C–H functionalisation of thiophene.**

In affording these yields, Glorius and co-workers observed that although Pd/C from various suppliers was reactive, those from Heraeus: 5 wt% Pd/C type K-0219, < 3% H<sub>2</sub>O showed the optimal yields. Benzofuran and 1H-indole gave corresponding C2-arylated products in 77% and 40% yields respectively. Benzo[b]thiophene on the other hand also gave the desired products with complete selectivity in 67-94% yield depending on kind of substituents attached to the benzene ring or to the thiophene ring.<sup>69</sup>

However, there is no evidence in the literature to suggest that the thiophene poisons the Pd catalysts.

## 1.6 Project aim and objectives

**Aim:** To assess the effect of  $\text{Pd}(\text{PPh}_3)_4$  ( $\text{Pd}_1$ ), palladium clusters ( $\text{Pd}_3$ ) and PdNPs, stabilised by suitable ligands, in catalytic SMCC reactions, with a particular emphasis on the regioselectivity and catalytic performance.

### Objectives:

- 1) Examine the regioselectivity in the arylation of 2,4-dihalopyridines as electrophilic substrates for Suzuki-Miyaura cross-coupling reactions (SMCCs).
- 2) Develop suitable NMR assays, enabling quantification of catalytic performance to be discerned.
- 3) Examine  $\text{Pd}(\text{PPh}_3)_4$ ,  $[\text{Pd}_3(\text{PPh}_3)_4]^{2+}$  cluster and  $\text{PPh}_3$ -stabilised PdNPs as catalysts in suitable SMCCs.

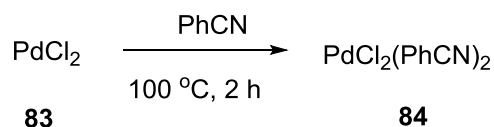
## 2. Results and Discussion

### 2.1 Synthesis and characterisation of catalysts

#### 2.1.1 Synthesis of quasi-homogeneous and heterogeneous catalysts (Pd Clusters (Pd<sub>3</sub>))

The palladium (trinuclear) clusters [Pd<sub>3</sub>(PPh<sub>3</sub>)<sub>4</sub>][BF<sub>4</sub>]<sub>2</sub> **88** was synthesised using standard protocols found in the literature.<sup>79</sup> Whilst [Pd<sub>3</sub>(PPh<sub>3</sub>)<sub>4</sub>][PF<sub>6</sub>]<sub>2</sub> **90** was synthesised based on the modification of the literature employed in the synthesis of **88**. These involved four main steps from the starting material of PdCl<sub>2</sub> **83** to the precursors **84**, **86**, **87** and **89** and the final trinuclear species **88** and **90** with the third step carried out under nitrogen (using standard Schlenk technique) and the other three steps under air (open vessel). Caution!: during the synthetic step between the transformation of the hydroxyl-bridge intermediate *i.e.* [Pd(μ-OH)(PPh<sub>3</sub>)<sub>2</sub>]<sub>2</sub>[BF<sub>4</sub>]<sub>2</sub> **87** and [Pd(μ-OH)(PPh<sub>3</sub>)<sub>2</sub>]<sub>2</sub>[PF<sub>6</sub>]<sub>2</sub> **89** and the trinuclear Pd species [Pd<sub>3</sub>(PPh<sub>3</sub>)<sub>4</sub>][BF<sub>4</sub>]<sub>2</sub> **88** and [Pd<sub>3</sub>(PPh<sub>3</sub>)<sub>4</sub>][PF<sub>6</sub>]<sub>2</sub> **90** it is very important to note that the resultant crystals in solution should not be kept longer than necessary (*ca* 45 min) since the crystals starts turning into Pd black NPs, when they are not decanted fast, washed and dried quickly enough.

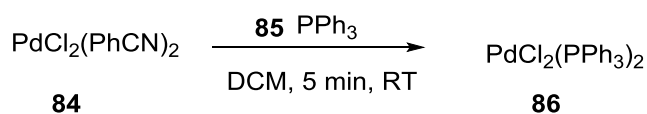
#### 2.1.2 Synthesis of PdCl<sub>2</sub>(PhCN)<sub>2</sub> **84**



**Scheme 27** Synthesis of *bis*(benzonitrile)palladium(II) dichloride.

Bis(benzonitrile)palladium(II) dichloride was synthesised by a modification of the standard protocol (100 °C rather than 110 °C, as reported),<sup>80</sup> affording a product yield of **84** of 80%. The compound was characterised by <sup>1</sup>H NMR and used without any further purification. See characterisation data on page 67.

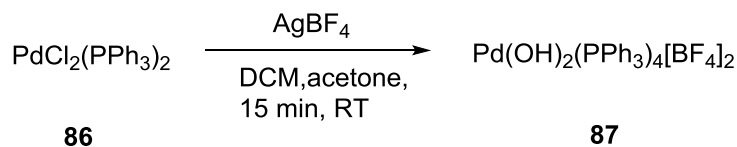
#### 2.1.3 Synthesis of *trans*-PdCl<sub>2</sub>(PPh<sub>3</sub>)<sub>2</sub> **86**



**Scheme 28** Synthesis of *trans*-*bis*(triphenylphosphine)palladium(II) dichloride.

Reacting  $\text{PdCl}_2(\text{PhCN})_2$  **84** in the presence of  $\text{PPh}_3$  **85** afforded *trans*-*bis*(triphenylphosphine)palladium(II) dichloride **86** in 85% yield. This compound was characterised by  $^1\text{H}$ NMR and  $^{31}\text{P}$  NMR, and used in the next process without any further purification. See characterisation data on page 68.

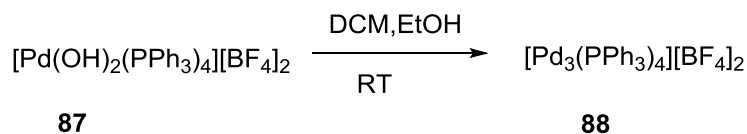
#### 2.1.4 Synthesis of $[\text{Pd}(\mu\text{-OH})(\text{PPh}_3)_2]_2[\text{BF}_4]_2$ **87**



**Scheme 29** Synthesis of hydroxyl-bridged palladium complex **87**.

$[\text{Pd}(\mu\text{-OH})(\text{PPh}_3)_2]_2[\text{BF}_4]_2$  **87** was synthesised<sup>81</sup> in a mixture of DCM/acetone by treatment with  $\text{AgBF}_4$ , forming a pale white powdery compound (64 %). It was then characterised by both  $^1\text{H}$ NMR and  $^{31}\text{P}$  NMR and used without any further purification, and finally used in the synthesis of the trinuclear Pd complex. See characterisation data on page 68.

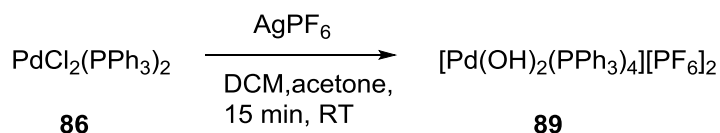
#### 2.1.5 Synthesis of $[\text{Pd}_3(\text{PPh}_3)_4][\text{BF}_4]_2$ **88**



**Scheme 30** Synthesis of trinuclear Pd cluster **88**.

Addition of a few drops of DCM and EtOH to **87** led to the formation of the desired Pd cluster  $[\text{Pd}_3(\text{PPh}_3)_4][\text{BF}_4]_2$  **88** in 46% yield as red crystals, shown to be 98 % pure by  $^1\text{H}$ NMR spectroscopic analysis. The literature does not state how long this process should take, our observation however is that the intermediate **87** should lead to the formation of **88** in about 30 minutes and any time beyond that is critical to the kind of crystals that will be isolated (the red crystals start to form Pd black). See characterisation data on page 69.

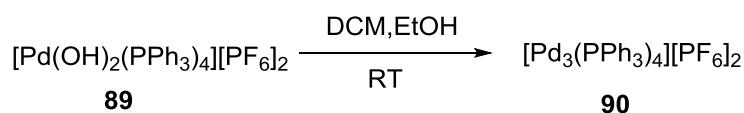
### 2.1.6 Synthesis of $[\text{Pd}(\mu\text{-OH})(\text{PPh}_3)_2]_2[\text{PF}_6]_2$ **89**



**Scheme 31** Synthesis of  $[\text{Pd}(\mu\text{-OH})(\text{PPh}_3)_2]_2[\text{PF}_6]_2$  **89**.

The Pd hydroxo-bridged intermediate **89**, which is the  $\text{PF}_6$  analogue of **87**, was synthesised as for **87**, in 55% yield (**Scheme 29**). It was then characterised by  $^1\text{H}$ NMR and  $^{31}\text{P}$  NMR and used without any further purification, and finally used in the synthesis of the trinuclear Pd complex. See characterisation data on page 70.

### 2.1.7 Synthesis of $[\text{Pd}_3(\text{PPh}_3)_4][\text{PF}_6]_2$ **90**



**Scheme 32** Synthesis of  $[\text{Pd}_3(\text{PPh}_3)_4][\text{PF}_6]_2$  **90**.

This Pd trinuclear species **90**  $[\text{Pd}_3(\text{PPh}_3)_4][\text{PF}_6]_2$  was synthesised in the same way as for **88** (**Scheme 30**). Addition of several drops of DCM and EtOH led to the formation of  $[\text{Pd}_3(\text{PPh}_3)_4][\text{PF}_6]_2$  **90** in 42% yield. The purity of was found to be 97%, based on  $^1\text{H}$ NMR spectroscopic analysis. See characterisation data on page 71.

## 2.2 Synthesis of PdNPs

### 2.2.1 Reactions of PdNPs

Pd-catalysed reactions are divided mainly into homogeneous (same phase as the reactant) and heterogeneous (different phase to the reactant). It is widely documented that homogeneous Pd catalysts are difficult to separate and recover after each use, whilst on the other hand heterogeneous Pd catalysts are more readily-separated and recovered after each use. Heterogeneous catalysts are known to be effective in catalysis because, of their large surface area to volume ratio. As the demand for the use of Pd as a catalyst increases, so is the alternative ways of utilising it. In recent years there has been a surge in the use of palladium nanoparticles in the construction of C–C bonds and to this effort

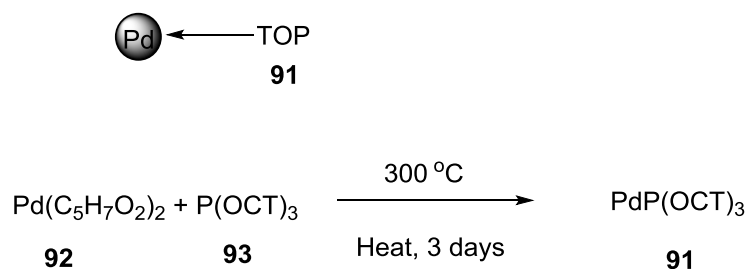
many researchers have gradually found better methods in the preparation of these catalysts.

Groups including, Fairlamb and co-workers, have synthesised many monodisperse PdNPs with sizes ranging between 2-4 nm and have found them to be useful in catalysing many cross-coupling reactions.<sup>34,83</sup> A good example is PVP–PdNPs **46** which has been found to be effective in catalysing not only traditional cross-coupling reactions but also C–H functionalisation reactions. These catalysts are known to work best at relatively high temperatures (>60 °C) and using polar solvents *e.g.* (MeOH). Polymers and surfactants are known to play critical roles such as acting as stabilisers in the synthesis of PdNPs. A very good example is the amine-containing ligands and this is very much demonstrated in the synthesis of PVP–Pd NPs **46**.<sup>2,34,83</sup> The common method of preparing metal stabilised NPs is the reduction of the metal ion in the presence of a stabilising polymer (ligand). Most PdNPs are prepared by reducing palladium (II) acetylacetonate, Pd(acac)<sub>2</sub>, palladium(II) chloride, PdCl<sub>2</sub>, and Pd(OAc)<sub>2</sub>, in the presence of stabilising agents such as polyvinylpyrrolidone (PVP) **43**. It usually results in formation of monodisperse PdNPs with small sizes (2-5 nm), but the sizes of these nanoparticles can then be increased over time by using the stepwise seed-mediated growth method, and Ostwald ripening.<sup>34,84</sup>

### 2.2.2 Choice of PdNPs in catalysis

The effectiveness of the commercially available heterogeneous catalyst (Pd/C) in various synthetic processes, particularly in cross-coupling reactions has been reported in the literature. However the question has always been asked about its morphology and particle sizes.<sup>2</sup> In order to have an idea of the size and morphology of the more defined nanoparticles used, we decided to synthesise triphenylphosphine PdNPs (TPP–PdNPs) and (±)-2,2'-bis(diphenylphosphino)-1,1'-binaphthyl (BINAP–PdNPs) using standard protocols found in the literature *via* a TOP–Pd NPs ligand exchange reaction. We were confronted by some challenges (see synthesis of trioctylphosphine) and as time was of essence, we decided to settle on the synthesis of PVP–PdNPs nanoparticles since the synthesis was fairly easy and their authentication and characterisation was also well-known (it has been previously synthesised and used by members of the group).

## Synthesis of trioctylphosphine stabilised TOP-Pd NPs 91



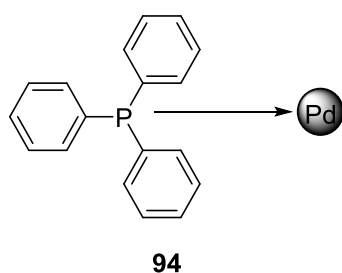
**Scheme 33** Synthesis of PdP(Oct)<sub>3</sub> **91**.

The synthesis of the trioctylphosphine-stabilised PdNPs **91** (TOP–Pd) proved more difficult than anticipated; the nanoparticles appeared unstable. Removal of the excess of methanol was difficult, as sublimation was noted. Therefore, in order to get the required amount of **91** (TOP–Pd) needed to do the ligand exchange reaction with **85** (PPh<sub>3</sub>) and **44** (BINAP), the procedure was repeated several times to get enough synthetic material.

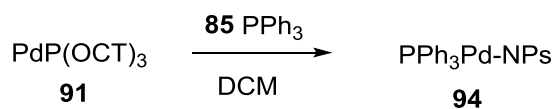
### 2.2.3 Particle sizes and distribution

It is a never-ending quandary deciding on the sampling size in any statistical analysis. In order to make precise inferences on the particle size distribution of the synthesised nanoparticles, a sampling pool of 200,162 and 105 particles were selected for the catalysts **94**, **95** and **46** (PPh<sub>3</sub>–PdNPs, BINAP–PdNPs and PVP–PdNPs) respectively. It was important to use freshly synthesised PVP–Pd NPs **46**, since it is known that the catalytic stability and reactivity decreases when stored at ambient temperature for long periods of time (>30) months (documented within our group). There is also a colour change from black (glassy) to greyish (loose metallic), hence rendering them ineffective when used in catalysis.<sup>84</sup>

#### 2.2.3.1 Synthesis of triphenylphosphine palladium nanoparticles (TPP–PdNPs) 94

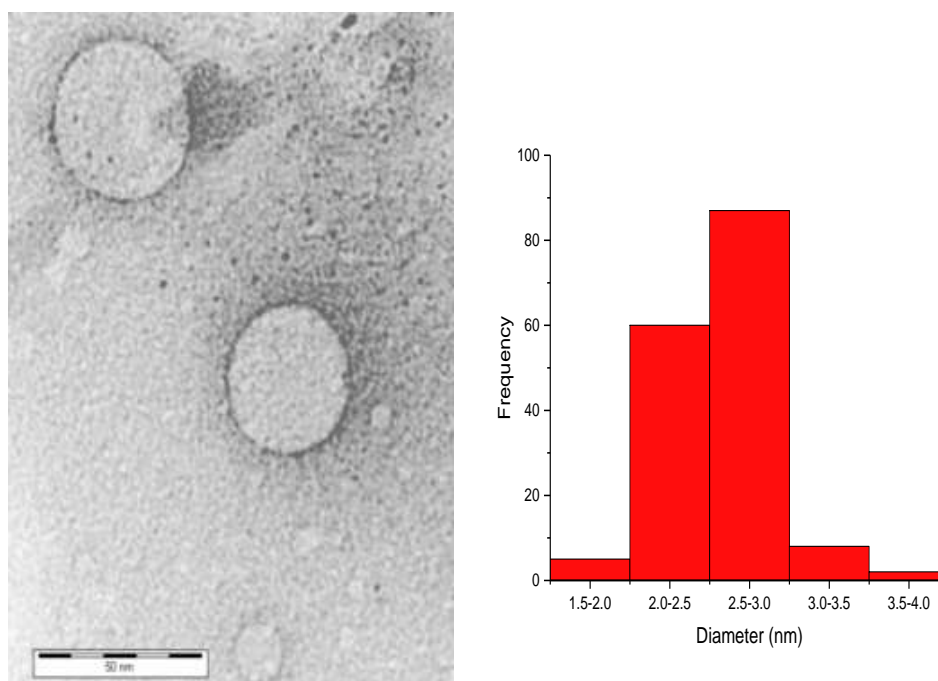






**Scheme 34** Synthesis of TPP-PdNPs **94**.

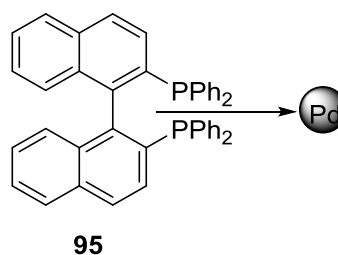
Analysis of the TPP-PdNPs was performed by TEM, in order to ensure the size distribution data reflected the true nature of the synthesised nanoparticles, several images were recorded and the best ones (visual inspection and identification of well developed spherical particle spots) selected for the subsequent statistical analysis. This was synthesised using TOP-PdNPs **91** in a ligand exchange reaction in the presence of TPP dissolved in DCM, stirred at room temperature overnight. A typical image is shown in **(Figure 13)**, with spherical shapes and average diameter ranging between 1.5-3.5 nm.



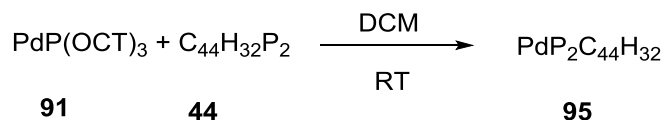
n =162, mean = 2.92 nm, std. dev. = 0.870, median = 2.9

**Figure 13** TEM images and particle size analysis of PPh<sub>3</sub>Pd–NPs **91**.

### 2.2.3.2 Synthesis of BINAP–PdNPs **95**



BINAP-PdNPs were synthesised using TOP-PdNPs **91** in a ligand exchange reaction yielding **95** (391.7 mg) black solid (**Scheme 35**). Analysis of the BINAP-PdNPs was performed by TEM, in order to ensure that the size distribution data reflected the true nature of the synthesised nanoparticles; several images were recorded and the best ones selected for the subsequent statistical analysis.



**Scheme 35** Synthesis of BINAP-PdNPs **95**.

TEM shows particles with an average diameter ranging between 5-7 nm (**Figure 14**). The elemental analysis calculated for **96** shown below (C, 56.11; H, 3.42; P, 6.58; Pd, 33.89) found (C, 56.69; H, 3.74, rest 39.56). Considering all the evidence, and within the limit of experimental error, the a ratio of BINAP:Pd is 1:3. Using this ratio, the percentage yield of the BINAP-PdNPs calculated was greater than 100%, suggesting that TOP ligand may also be present.

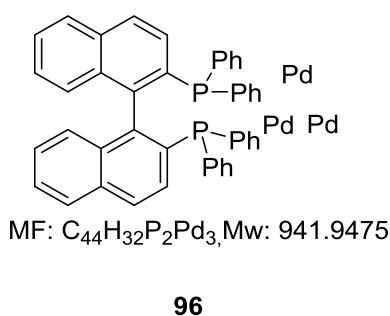
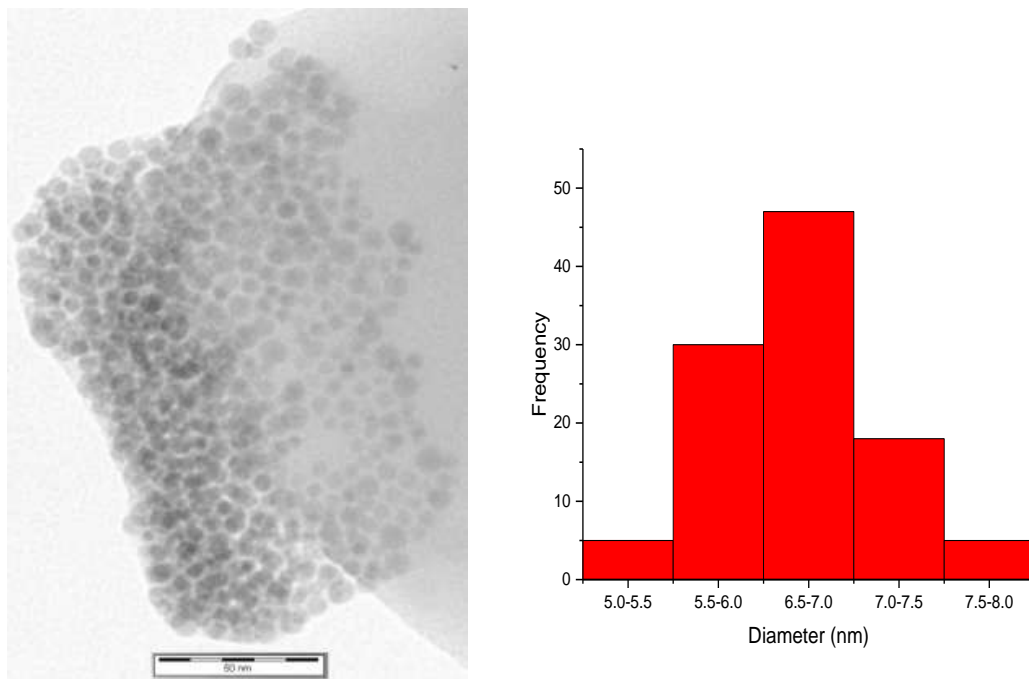


**Figure 14** Proposed ratio for BINAP/Pd in BINAP-PdNPs.

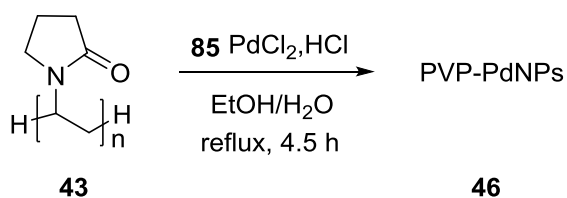


n =105 mean = 6.67 nm, std. dev = 2.108, median= 6.67

**Figure 15** TEM images and particle size analysis of BINAP-PdNPs **96**.

### 2.2.3.3 Synthesis of PVP-PdNPs **46**

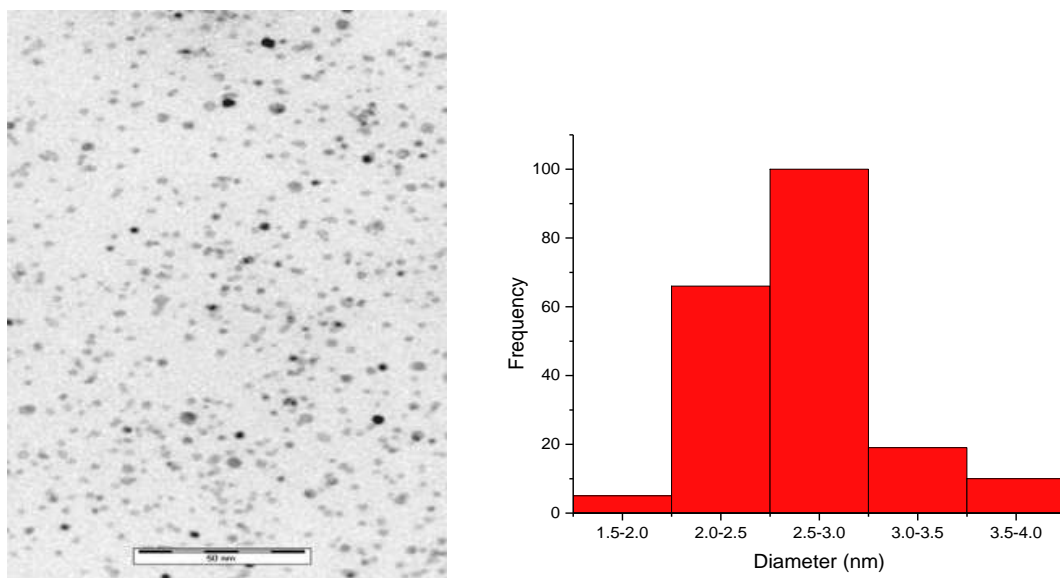
Analysis of the PVP polymer-stabilised nanoparticles (8 wt % Pd) was performed by TEM at the Biology Department and in order to ensure that the size distribution data reflected the true nature of the synthesised nanoparticles, several images were recorded and the best ones selected for the subsequent statistical analysis. The PVP-PdNPs **46** were synthesised by the reduction of PdCl<sub>2</sub> **85** in aqueous acid in the presence of a (poly)vinylpyrrolidinone (PVP) **45**. The synthesis afforded quantitative amount of regularly+-shaped (monodisperse) Pd nanoparticles, having diameters typically in the range of 2-5 nm in a one pot reaction (**Scheme 36**).



**Scheme 36** Synthesis of PVP-PdNPs **46**.

The IR (solid-state ATR) agrees with the catalysts previously synthesised and reported in the group.<sup>85</sup> A typical TEM image is shown in this shows particle distribution and sizes ranging

between 2-5 nm (**Figure 16**). The catalyst, although soluble in ethanol, appeared non-ionisable by both LIFDI-MS and ESI-MS; also found to be insoluble in acetonitrile. No further authentication and characterisation was done and we had to rely on previous knowledge from the group; former members<sup>85</sup> have synthesised and applied this catalyst in various cross-coupling reactions, apart from the fact that it is fairly easy to synthesis on a large scale in a one-pot reaction.



n = 200, mean = 2.5 nm, std. dev. = 0.988, median= 2.5,

**Figure 16** TEM images and particle size analysis of PVP-PdNPs.

### 2.3 Examining the regioselectivity in Pd-catalysed SMCC reactions by alteration of Pd catalyst

Cid and co-workers<sup>87</sup> reported on the regioselectivity of homogeneous catalysts in SMCC reactions. Further information on regioselective cross-coupling catalysis is however surprisingly limited. Concerning the regioselectivity observed using 2,4-dibromopyridine **97** in a Pd-catalysed SMCC reaction, there are two choices for the position of functionalisation (arylation), either at C2 or C4. The regioselectivity observed was attributed to the chemical/electrophilicity differences between the two carbon centres (C2 and C4), an indication of which derives from the <sup>13</sup>CNMR data for the two carbon centres (142.5 and 133.9 ppm respectively). The difference in chemical shift might account for the regioselectivity exhibited for the C2 position, quite generally (**Figure 16**). The authors also observed that the diarylated product was not formed as a result of a simultaneous double arylation of the two positions (C2 and C4), but rather it is formed from the monocoupled product(s) **97a** and **97b**.<sup>87</sup> Similar regioselectivity was seen for 2,4-dichloropyridine **102** using an Fe catalyst.<sup>88</sup>

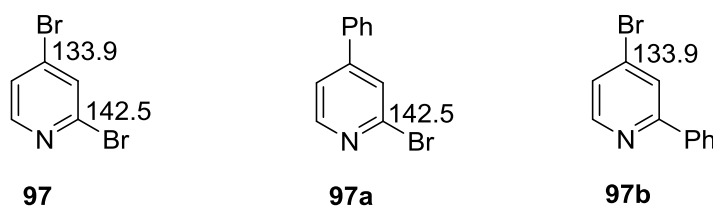
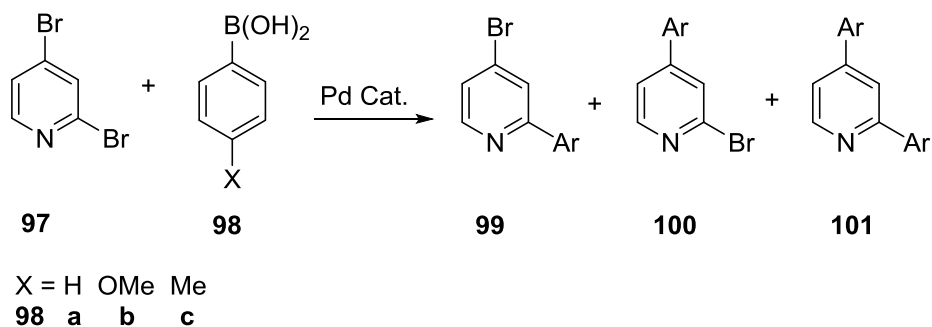
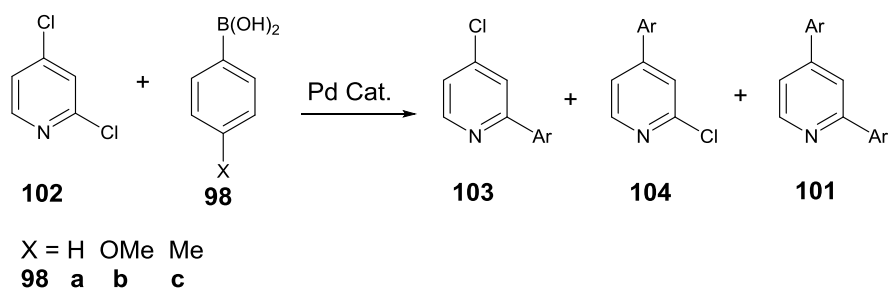


**Figure 17** <sup>13</sup>C NMR chemical shifts for mono-arylated and 2,4-dibromopyridines.

It was decided to address the regioselectivity outcome of several Pd catalysts, with a focus on catalysts containing PPh<sub>3</sub> ligands—arguably the most widely employed ligand in transition metal catalysis. This was particularly important to conduct given that no previous study had examined the effect of the Pd catalyst structure on SMCC regioselectivity. A benchmark SMCC reaction was identified employing 2,4-dibromopyridine **97** as the model electrophilic substrate. Work by Cid and co-workers suggested that the arylation regioselectivity could be influenced by changes in Pd catalyst structure (comparing Pd(OAc)<sub>2</sub> versus Pd(PPh<sub>3</sub>)<sub>4</sub>), from the brief results on this variable reported (**Scheme 37**).<sup>87</sup>



**Scheme 37** General SMCC reaction of 2,4-dibromopyridine(**97**) with arylboronic acids.



**Scheme 38** General SMCC reaction of 2,4-dichloropyridine(**102**) with arylboronic acids.

To achieve this aim, a series of experiments were devised where different bases and reaction temperatures were altered to enable optimal conditions to be identified, thereby allowing the interrogation of efficacy and regioselectivity of the Pd catalysts to be fully discerned. The nucleophilic coupling partner, *p*-methoxyphenylboronic acid **98b**, was identified as an optimal partner for SMCC. THF was identified as the best solvent, with temperatures ranging from 40-70 °C (oil bath temperature) and tetrabutylammonium hydroxide (nBu<sub>4</sub>NOH) as the base. With the optimised reaction conditions available, commercial Pd catalysts, and those made within the laboratory, were examined against the SMCC reaction to ascertain the regioselectivity and the efficacy of each Pd catalyst.

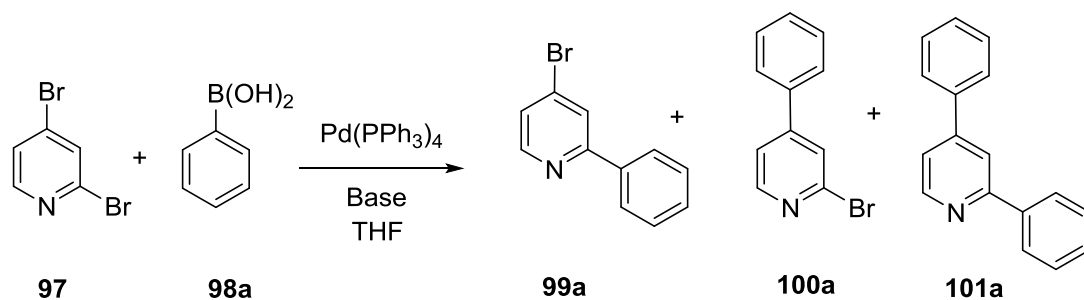
During the study it became apparent that the 2,4-dibromopyridine **97** substrate was contaminated (from the supplier, having a low carbon/hydrogen content, confirmed by elemental analysis). This led to 2,4-dichloropyridine **102** also being examined within this study. The optimised reaction conditions employed for this research appear to favour some Pd catalysts, whilst disfavouring others in terms of regioselectivity and yield.

### 2.3.1 Pd catalysis screening study

The principal aim of the study was to investigate the regioselectivity and efficiency of different Pd catalyst types used in the SMCC reaction of 2,4-dibromopyridine **97** or 2,4-dichloropyridine **102** with phenylboronic acid **98a** or *p*-methoxyphenylboronic acid **98b**. The regioselectivity is given as the ratio of three possible products, the mono-arylated regioisomers **99**, **100**, **103** and **104**, and the diarylated product **101**. Traditionally classified homogeneous Pd catalysts were selected, *e.g.* Pd(PPh<sub>3</sub>)<sub>4</sub> and Pd(OAc)<sub>2</sub>, and well-defined heterogeneous Pd catalysts, *e.g.* Pd/C and PVP–Pd **46**, and ‘quasi’ homogeneous and heterogeneous catalysts, *e.g.* [Pd<sub>3</sub>(PPh<sub>3</sub>)<sub>4</sub>][BF<sub>4</sub>]<sub>2</sub> **88** and [Pd<sub>3</sub>(PPh<sub>3</sub>)<sub>4</sub>][PF<sub>6</sub>]<sub>2</sub> **90**. The cross-coupling products were identified by <sup>1</sup>H NMR experiments and also comparing the data with published literature data.<sup>87,88</sup> The results are collated in the tables of data below. All of the Pd catalysts examined were treated as mono-palladium atoms/species and their catalytic loading calculated accordingly. The Pd catalysts contain PPh<sub>3</sub> ligands, except in the case of the Pd nanoparticles, which were used in stabilised form (with a polymer).

To begin the study, it was necessary to synthesise the Pd catalysts using standard literature procedures. These Pd catalysts and the selected commercially available Pd catalysts were then screened in a SMCC reaction of 2,4-dibromopyridine **97** and 2,4-dichloropyridine **102**. It is important to note that apart from the different catalysts used in these studies, there was an attempt at varying some parameters such as solvent, base and temperature, to investigate the effects of these conditions on the effectiveness of these catalysts in a SMCC reaction. Some examples of these reactions are highlighted below.

**Table 1** Results of screening base and temperature for reaction of 2,4-dibromopyridine **97** with phenylboronic acid **98a**, using Pd(PPh<sub>3</sub>)<sub>4</sub> as the catalyst and THF as the solvent.



Entry	Base	Temp. / °C	Time / h	Product yield / %			Lab book reference
				<b>99a</b>	<b>100a</b>	<b>101a</b>	
1	nBu <sub>4</sub> NOH	50	6	58	8	4	EYD-1-34
2	nBu <sub>4</sub> NOH	25	6	40	11	4	EYD-1-33
3	Me <sub>4</sub> NOH	50	24	28	0	72	EYD-1-31
4	Na <sub>2</sub> CO <sub>3</sub>	50	24	80	13	7	EYD-1-32

All reactions conducted with **97** (472 mg, 2 mmol, 1 eq.), Pd(PPh<sub>3</sub>)<sub>4</sub> (116 mg, 0.10 mmol, 5 mol%), **98a** (292 mg, 2.4 mmol, 1.2 eq.), dry THF solvent (2.5-5 ml) and (2.5-5 ml) of bases at 25 °C and 50 °C for 6-24 h. All percentage conversion as determined by <sup>1</sup>H NMR spectroscopic analysis of the crude reaction mixture following filtration through celite plug using DCM as eluent.

When Pd(PPh<sub>3</sub>)<sub>4</sub> was used (5 mol% catalyst loading) at (50 °C), it was found that sodium carbonate (Na<sub>2</sub>CO<sub>3</sub>) and tetramethylammonium hydroxide (Me<sub>4</sub>NOH) exhibited similar activity, affording complete substrate conversion (**97**) after 24 h; differences in the regioselectivity for the reaction were noted. For example, using Na<sub>2</sub>CO<sub>3</sub>, the C2 regioisomer **99a** was the dominant product (80%), with the C4 regioisomer **100a** (13%) and diarylated product **101a** (7%) formed as minor products. Use of Me<sub>4</sub>NOH showed a significant difference in regioselectivity, with the C2 arylated product **99a** formed in (28%) and diarylated product **101a** formed as the major product (72%) (**Table 1**, entries 4 and 3). Interestingly, the C4 regioisomer **100a** was not observed under these reaction



conditions. The C2 regioisomer is presumed to be the kinetically-favoured product of the reaction and it is formed first and sometimes with the C4 arylated product. If the duration of the reaction was increased to 24 h it leads to the gradual consumption of the C2 and C4 regioisomeric mono-arylated products leading to the formation of the diarylated product **101a** of the SMCC reactions (presumably at different rates, with C2-Br most likely being more reactive than C4-Br).

The screening of Pd(PPh<sub>3</sub>)<sub>4</sub> (5 mol%) using tetrabutylammonium hydroxide (nBu<sub>4</sub>NOH) in THF at 50 °C and 25 °C showed (70%) and (55%) overall conversion after 6 h respectively (**Table 1**, entries 1 and 2). In general, with respect to the duration of reaction, nBu<sub>4</sub>NOH afforded higher product conversion than Me<sub>4</sub>NOH and Na<sub>2</sub>CO<sub>3</sub>, but with similar regioselectivity. This reaction gave an indication of the catalysis being dependent on temperature, as expected, it is however premature to definitively conclude on the best base to be used in this reaction, by examination of the data above alone.

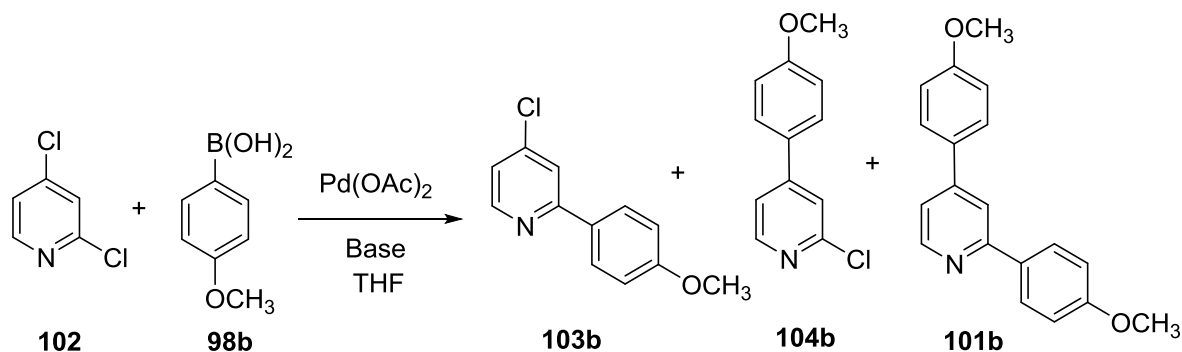
The initial option of base was going to be TIOH, as was employed by Cid and co-workers in their published work on regioselectivity of 2,4-dibromopyridine **97**.<sup>87</sup> It was decided not to use TIOH because of its acute toxicity and also to be in tune with the current movement towards using environmentally benign reagents. Our choice of nBu<sub>4</sub>NOH as a base was not an accidental one; it was influenced mainly by the work of Jutand and co-workers.<sup>35</sup> They demonstrated the effectiveness of nBu<sub>4</sub>NOH (although less effective as compared with TIOH, but far more effective than Na<sub>2</sub>CO<sub>3</sub>) acting as a base to increase the rate of the transmetallation step of the SMCC reaction, which is the likely rate-determining step in the reaction of 2,4-dibromopyridine **97**.<sup>35</sup> Hence, nBu<sub>4</sub>NOH was selected as the base for the screening of the selected Pd catalysts.



The screening of Pd(OAc)<sub>2</sub> in the presence of phenylboronic acid **98a** (5 mol%), at 60 °C showed differences in regioselectivity affording C2 arylated product **103a** (67%), C4 arylated product **104a** (0%) and diarylated product **101a** (33%) after 4 h (**Table 2**, entry 1). In order to determine whether the solvent had any effect on catalysis, some of these catalysts were screened against two different solvents. Generally, the reactions mediated by Pd(PPh<sub>3</sub>)<sub>4</sub> in the presence of phenylboronic acid **98a** and 2,4-dichloropyridine **102** in THF afforded moderate to quantitative conversion (69% and 100%) after 4 h (**Table 2**, entry 3 and 6), whilst the same reaction in ethylene glycol (ETG) afforded moderate conversions (45% and 38%) respectively (**Table 2**, entry 4 and 5). Interestingly, at higher temperature the selectivity of the reaction appears to be skewed towards the C2 arylated product **103a** with none of the C4 **104a** and the diarylated product **101a** being formed (**Table 2**, entries 2 and 3). The two solvents exhibited similar regioselectivity in their catalysis, with ETG affording both the C2 arylated product **103a** in (38%) and C4 arylated product **104a** (7%). On the other hand, the reaction carried out in THF afforded the C2 arylated **103a** (53%) and C4 arylated product **104a** (47%) (**Table 2**, entries 4 and 6). At 80 °C and 60 °C respectively, the reactions in ETG showed the same regioselectivity (**103a** and **104a**) arylated products with the reaction at 60 °C offering a higher % conversion (45%) and at 80 °C, (38%) after 5 h respectively (**Table 2**, entries 5 and 4).

Based on the above observations it can be ascertained that the reaction solvent appears to influence the reactivity of the Pd catalyst *i.e.* the percentage conversion decreased with increasing temperature, with THF favouring the catalysis more than ETG. The similarity in efficacy and regioselectivity of these Pd catalysts were expected since they are both intrinsically similar, generating 'PdL<sub>n</sub>' type catalyst species, where L = PPh<sub>3</sub>.

**Table 3** Results of variations in temperature for the reaction of 2,4-dichloropyridine **102** with *p*-methoxyphenylboronic acid **98b**, using Pd(OAc)<sub>2</sub> as the catalyst, nBu<sub>4</sub>NOH as the base and THF as the solvent.



Entry	Temp. / °C	Time / h	Product conversion / %			Lab book reference
			<b>103b</b>	<b>104b</b>	<b>101b</b>	
1	70	4	62	11	1	EYD-1-68
2	70	24	67	11	3	EYD-1-68
3	60	4	44	17	0	EYD-1-45
4	50	4	21	11	0	EYD-1-51
5	40	4	29	6	0	EYD-1-53
6	40	24	93	0	7	EYD-2-113

- All reactions conducted with **102** (110 μl, 1 mmol, 1 eq.), Pd(OAc)<sub>2</sub> (2.71 mg, 0.01 mmol, 1 mol% eq.), PPh<sub>3</sub> (2.86 mg, 0.01 mmol, 1 mmol%), **98b** (182.80 mg, 1.2 mmol, 1.2 eq.), dry THF (2.5 mL) and nBu<sub>4</sub>NOH (2.5 mL) at 70 °C for 4-24 h.
- 102** (215 μl, 2 mmol, 1 eq.), Pd(OAc)<sub>2</sub> (4.63 mg, 0.02 mmol, 1 mol% eq.), PPh<sub>3</sub> (5.50 mg, 0.02 mmol, 1 mmol%), **98b** (364.60 mg, 2.4 mmol, 1.2 eq.), dry THF (2.5 mL) and nBu<sub>4</sub>NOH (5 mL) at 70 °C for 4 h.
- 102** (650 μl, 6 mmol, 1 eq.), Pd(OAc)<sub>2</sub> (13.5 mg, 0.06 mmol, 1 mol% eq.), PPh<sub>3</sub> (31.5 mg, 0.12 mmol, 2 mol%), **98b** (1.095 mg, 7.2 mmol, 1.2 eq.), dry THF (2.5 mL) and nBu<sub>4</sub>NOH (5 mL) at 70 °C for 24 h. All percentage conversion as determined

by  $^1\text{H}$  NMR spectroscopic analysis of the crude reaction mixture following Celite<sup>TM</sup> filtration plug using DCM as eluent.

When the reaction was carried out at 70 °C using Pd(OAc)<sub>2</sub> (1 mol% Pd loading) it afforded (74%) and (81%) conversion of **102**, after 4 and 24 h respectively (**Table 3**, entries 1 and 2). It was observed that there was a decrease in percentage conversion and regioselectivity of **102** as the temperature was reduced from 70 °C to 40 °C (**Table 3**, entry 1-5). It is worth noting that the reaction percentage conversion of **102** increased with an increase in ligand loading (2 mol%) affording (100%) conversion with the C2 regioisomer **103b** being the major isomer (93%), C4 regioisomer **104b**, (0%) and the diarylated product **101b** (7%) respectively (**Table 3**, entry 6).

**Table 4** Results of variations in temperature for the reaction of 2,4-dichloropyridine **102** with *p*-methoxyphenylboronic acid **98b**, using, nBu<sub>4</sub>NOH as the base, THF as the solvent and Pd<sub>2</sub>(dba)<sub>3</sub>.CHCl<sub>3</sub> and Pd(PPh<sub>3</sub>)<sub>4</sub> as the catalyst.

Entry	Pd catalyst	Pd catalyst / mol%	Temp. / °C	Time / h	Product conversion / %			Lab book reference
					103b	104b	101b	
1	Pd <sub>2</sub> (dba) <sub>3</sub> .CHCl <sub>3</sub>	5	40	4	6	3	0	EYD-1-65
2	Pd <sub>2</sub> (dba) <sub>3</sub> .CHCl <sub>3</sub>	5	70	4	96	0	4	EYD-1-62
3	Pd <sub>2</sub> (dba) <sub>3</sub> .CHCl <sub>3</sub>	1	40	24	21	9	0	EYD-1-66
4	Pd <sub>2</sub> (dba) <sub>3</sub> .CHCl <sub>3</sub>	1	70	4	70	2	0	EYD-1-63
5	Pd(PPh <sub>3</sub> ) <sub>4</sub>	1	40	4	89	0	11	EYD-1-52
6	Pd(PPh <sub>3</sub> ) <sub>4</sub>	5	60	4	100	0	0	EYD-1-56

- a. **102** (110 μl, 1 mmol, 1 eq.), Pd<sub>2</sub>(dba)<sub>3</sub>.CHCl<sub>3</sub> (25.53 mg, 0.025 mmol, 5 mol % eq.), PPh<sub>3</sub> (13.13 mg, 0.05 mmol, 5 mol %), **98b** (182.68 mg, 1.2 mmol, 1.2 eq.), dry THF (2.5 mL) and nBu<sub>4</sub>NOH (1.0 M, 2.5 mL) at 40 °C for 4 h.

- b. **102** (110  $\mu$ l, 1 mmol, 1 eq.), Pd<sub>2</sub>(dba)<sub>3</sub>.CHCl<sub>3</sub> (5.10 mg, 0.005 mmol, 1 mol% eq.), PPh<sub>3</sub> (2.62 mg, 0.01 mmol, 1 mmol%), **98b** (182.80 mg, 1.2 mmol, 1.2 eq.), dry THF (2.5 mL) and nBu<sub>4</sub>NOH (2.5 mL) at 70 °C for 4 h.
- c. **102** (215  $\mu$ l, 2 mmol, 1 eq.), Pd(PPh<sub>3</sub>)<sub>4</sub> (23.04 mg, 0.02 mmol, 1 mol% eq.), **98b** (365 mg, 2.4 mmol, 1.2 eq.), dry THF (5 mL) and nBu<sub>4</sub>NOH (1.0M, 5 mL) at 40 C for 4 h.
- d. **102** (215  $\mu$ l, 2 mmol, 1 eq.), Pd(PPh<sub>3</sub>)<sub>4</sub> (115 mg, 0.10 mmol, 5 mol% eq.), **98b** (365 mg, 2.4 mmol, 1.2 eq.), dry THF (5 mL) and nBu<sub>4</sub>NOH (5 mL) at 60 °C for 4 h. All percentage conversion as determined by <sup>1</sup>H NMR spectroscopic analysis of the crude reaction mixture following Celite™ filtration plug using DCM as eluent.

The screening of Pd<sub>2</sub>(dba)<sub>3</sub>.CHCl<sub>3</sub> at 40 °C using (5 mol% Pd loading) afforded a 9% conversion, whilst the same reaction at 70 °C afforded a (100%) conversion of **102** after 4 h respectively (**Table 4**, entry 1 and 2). The use of this Pd catalyst also provided evidence of similarity in regioselectivity, with all the reactions affording the C2 regioisomer **103b** as the major product. The reaction at 70 °C (5 mol% Pd loading) however afforded both the C2 arylated and the diarylated products (**103b** and **101b**), unlike the other reactions which afforded the C2 and C4 arylated products only (**103b** and **104b**) (**Table 4**, entries 1-6).

The reaction of Pd(PPh<sub>3</sub>)<sub>4</sub> at 60 °C (5 mol% Pd loading) afforded exclusively the C2 arylated regioisomer **103b** (100%) (**Table 4**, entry 6) whilst the same catalyst at 40 °C (1 mol% Pd loading), afforded C2 arylated product 103b (89%), C4 arylated product 104b (0%) and diarylated product **101b** (11%) after 4 h (**Table 4**, entry 5).

Even after 24 h the conversion of **102** due to Pd<sub>2</sub>(dba)<sub>3</sub>.CHCl<sub>3</sub> catalyst was 30% (**Table 4**, entry 3) suggesting that at 40 °C Pd<sub>2</sub>(dba)<sub>3</sub>.CHCl<sub>3</sub> was comparatively not as effective in playing an active role in the catalysis of SMCC reactions of **102**, as compared with Pd(OAc)<sub>2</sub>. The results and observation from the screening of these catalyst, *e.g.* Pd(OAc)<sub>2</sub> and Pd<sub>2</sub>(dba)<sub>3</sub>.CHCl<sub>3</sub>, demonstrates the temperature dependency of this catalysts and their reactions. Whilst that of Pd(PPh<sub>3</sub>)<sub>4</sub> appears not to be affected by changes in temperature.

**Table 5** Results of variations in temperature for the reaction of 2,4-dichloropyridine **102** with *p*-methoxyphenylboronic acid **98b**, using [Pd<sub>3</sub>(PPh<sub>3</sub>)<sub>4</sub>][BF<sub>4</sub>]<sub>2</sub> and [Pd<sub>3</sub>(PPh<sub>3</sub>)<sub>4</sub>][PF<sub>6</sub>]<sub>2</sub> as the catalyst, nBu<sub>4</sub>NOH as the base and THF as the solvent.

Entry	Pd catalysts	Temp. / °C	Time / h	Product conversion / %			Lab book reference
				103b	104b	101b	
1	[Pd <sub>3</sub> (PPh <sub>3</sub> ) <sub>4</sub> ][BF <sub>4</sub> ] <sub>2</sub>	70	24	87	7	2	EYD-2-110
2	[Pd <sub>3</sub> (PPh <sub>3</sub> ) <sub>4</sub> ][BF <sub>4</sub> ] <sub>2</sub>	40	24	15	52	28	EYD-2-126
3	[Pd <sub>3</sub> (PPh <sub>3</sub> ) <sub>4</sub> ][PF <sub>6</sub> ] <sub>2</sub>	70	4	70	0	30	EYD-2-130
4	[Pd <sub>3</sub> (PPh <sub>3</sub> ) <sub>4</sub> ][PF <sub>6</sub> ] <sub>2</sub>	40	4	40	3	0	EYD-2-149

- a. All reactions conducted with **102** (215 μl, 2 mmol, 1 eq.), [Pd<sub>3</sub>(PPh<sub>3</sub>)<sub>4</sub>][BF<sub>4</sub>]<sub>2</sub> (10.5 mg, 1 mmol, 1 mol% eq.), **98b** (365 mg, 2.4 mmol, 1.2 eq.), solvent dry THF (5 mL) and nBu<sub>4</sub>NOH (5 mL) at 40 °C and 70 °C for 4-24 h.
- b. **102** (110 μl, 1 mmol, 1 eq.), [Pd<sub>3</sub>(PPh<sub>3</sub>)<sub>4</sub>][PF<sub>6</sub>]<sub>2</sub> (5.5 mg, 3.3 μmol, 1 mol% eq.), **98b** (185 mg, 1.2 mmol, 1.2 eq.), solvent dry THF (2.5 mL) and nBu<sub>4</sub>NOH (2.5 mL) at 70 °C for 4 h. All percentage conversion as determined by <sup>1</sup>H NMR spectroscopic analysis of the crude reaction mixture following Celite™ filtration using DCM as solvent.

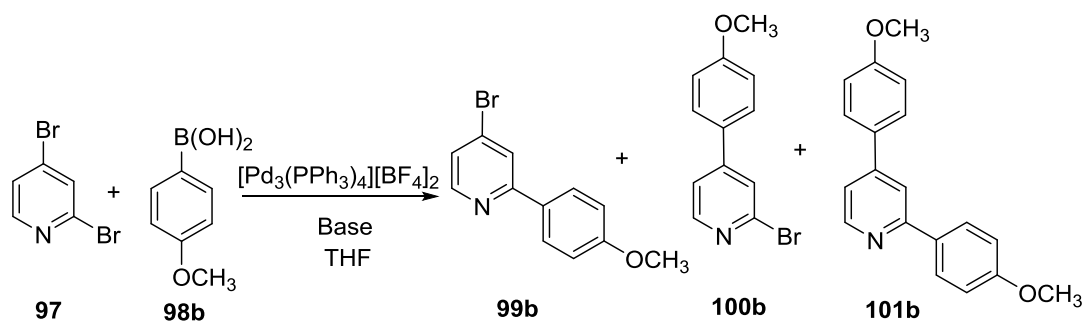
The trinuclear palladium catalyst [Pd<sub>3</sub>(PPh<sub>3</sub>)<sub>4</sub>][BF<sub>4</sub>]<sub>2</sub> **88** (1 mol% Pd loading) reacted with 2,4-dichloropyridine **102** in the presence of *p*-methoxyphenylboronic acid **98b** at 70 °C and 40 °C for 24 h affording (96%) and (95%) overall conversions respectively (**Table 5**, entry 1 and 2). Interestingly, the reaction at 40 °C offered a different regioselectivity compared with the same reaction at 70 °C (**Table 5**, entry 1 and 2). This regioselectivity was replicated when 2,4-dibromopyridine **97** was used affording 85% conversion after 24 h (**Table 6**, entry 2). The regioselectivity observed in this reaction was in contrast to what we have observed and has been corroborated in the literature. The C4 regioisomer **104b** was formed as the major product which contradicts the literature. This reaction afforded the C4 arylated product **104b** as the major product (52%) and (59%) for 2,4-

dichloropyridine **102** and 2,4-dibromopyridine **97** respectively. To the best of our knowledge this is the first time such regioselectivity has been observed in this type of catalysis. With this observation,  $[\text{Pd}_3(\text{PPh}_3)_4][\text{PF}_6]_2$  **90** was anticipated to exhibit the same regioselectivity as  $\text{Pd}_3(\text{PPh}_3)_4[\text{BF}_4]_2$  **88** at 40 °C, since both Pd catalysts have the same backbone and only differ in the presence of tetrafluoroborate anion (the  $\text{BF}_4^-$  anion) in  $[\text{Pd}_3(\text{PPh}_3)_4][\text{BF}_4]_2$  **88** and hexafluorophosphate anion (the  $\text{PF}_6^-$  anion) in  $[\text{Pd}_3(\text{PPh}_3)_4][\text{PF}_6]_2$  **90**. To our surprise this unique selectivity was not observed when  $[\text{Pd}_3(\text{PPh}_3)_4][\text{PF}_6]_2$  **90** was screened at 40 °C. However, at 70 °C and with the same catalyst loading of (1 mol% Pd)  $[\text{Pd}_3(\text{PPh}_3)_4][\text{PF}_6]_2$  **90** afforded quantitative conversion of the substrate **102** after 4 h (**Table 5**, entry 3), however at 40 °C,  $[\text{Pd}_3(\text{PPh}_3)_4][\text{BF}_4]_2$  **88** was superior in catalytic activity (selectivity and percentage yield). Differences in size of the anions could have been a factor in the regioselectivity observed at 40 °C when **88** was used as catalyst. The ( $\text{BF}_4^-$ ) anion has a tetrahedral geometry whilst ( $\text{PF}_6^-$ ) has an octahedral geometry and as such the bulkiness of ( $\text{PF}_6^-$ ) leading to steric hindrance is higher than in ( $\text{BF}_4^-$ ) which is a comparatively smaller in size. Hence ( $\text{BF}_4^-$ ) will form a stronger bond interaction between  $[\text{Pd}_3(\text{PPh}_3)_4]^{2+}$  backbone than in the case of ( $\text{PF}_6^-$ ). Hence at this temperature the geometry of the catalyst **88** will have been maintained leading to the formation of the observed regioisomer. It should be noted that the reactions were also compared at different temperatures and it is at 40 °C, that we see the contrast between the two catalysts and hence we can postulate that the temperature may have an influence on the selectivity of the catalysts.

We also believe that the acids liberated in the reaction medium could be responsible for the differences in regioselectivity observed in the catalysis. It should be noted that these reactions although performed at different time intervals were monitored by NMR spectroscopy and hence it was observed that the C2 and or the C4 arylated products were being converted to the bis-arylated products and there was no observed inter-conversion between the C2 and the C4.

**Table 6** Results of variation in temperature for reaction of 2,4-dichloropyridine **97** with *p*-methoxyphenylboronic acid **98b**, using  $[\text{Pd}_3(\text{PPh}_3)_4][\text{BF}_4]_2$  **88**,  $n\text{Bu}_4\text{NOH}$  in THF.





Entry	Temp. / °C	Time / h	Product conversion / %			Lab book reference
			<b>99b</b>	<b>100b</b>	<b>101b</b>	
1	40	4	9	27	7	EYD-2-118
2	40	24	15	59	11	EYD-2-118

All reactions conducted with **102** (474 mg, 2 mmol, 1 eq.),  $[Pd_3(PPh_3)_4][BF_4]_2$  (10.5 mg, 1 mmol, 1 mol%), **98b** (365 mg, 2.4 mmol, 1.2 eq.), solvent dry THF (5 mL) and  $nBu_4NOH$  (5 mL) at 40 °C for 4-24 h. Percentage conversion as determined by  $^1H$  NMR spectroscopic analysis of the crude reaction mixture following Celite<sup>TM</sup> filtration plug using DCM as solvent.

**Table 7** Results of variation in temperature for the reaction of 2,4-dichloropyridine **102** with *p*-methoxyphenylboronic acid **98b**, using Pd/C and PdNPs as the catalysts, nBu<sub>4</sub>NOH in THF.

Entry	Pd catalyst / mol%	Temp. / °C	Time / h	Product conversion / %			Lab book reference
				103b	104b	101b	
1	Pd/C	60	6	4	0	0	EYD-1-59
2	Pd/C	70	4	23	0	0	EYD-1-60
3	Pd/C	40	24	3	4	0	EYD-1-58
4	BINAP–Pd	70	6	10	1	0	EYD-2-148
5	BINAP–Pd	40	3	trace	0	0	EYD-2-133
6	BINAP–Pd	40	3	trace	0	0	EYD-2-139
7	BINAP–Pd	40	3	trace	0	0	EYD-2-136
8	PVP–Pd	40	3	0	0	0	EYD-2-137
9	PVP–Pd	40	3	0	0	0	EYD-2-138
10	PPh <sub>3</sub> –Pd	40	3	trace	0	0	EYD-2-151

- a. All reactions conducted with **102** (110 µl, 1 mmol, 1 eq.), Pd/C (106.89 mg, 0.05 mmol, 5 mol%), PPh<sub>3</sub> (13.23 mg, 0.05 mmol, 5 mol %), **98b** (182.4 mg, 1.2 mmol, 1.2 eq.), solvent dry THF (2.5 mL) and nBu<sub>4</sub>NOH (2.5 mL) at 60 °C and 70 °C for 6 & 4 h.
- b. **102** (215 µl, 2 mmol, 1 eq.), Pd/C (42.84 mg, 0.02 mmol, 1 mol%), PPh<sub>3</sub> (5.49 mg, 0.02 mmol, 1 mol %) **98b** (365.13 mg, 2.4 mmol, 1.2 eq.), solvent dry THF (5 mL) and nBu<sub>4</sub>NOH (5 mL) at 40 °C for 24 h.
- c. **102** (215 µl, 2 mmol, 1 eq.), BINAP–Pd (6.3 mg, 0.02 mmol, 1 mol%), PPh<sub>3</sub> (5.7 mg, 0.02 mmol, 1 mol%) **98b** (365 mg, 2.4 mmol, 1.2 eq.), solvent dry THF (5 mL) and nBu<sub>4</sub>NOH (5 mL) at 40 °C for 24 h.

- d. **102** (215  $\mu$ l, 2 mmol, 1 eq.), BINAP–Pd (6.3 mg, 0.02 mmol, 1 mol%), **98b** (365 mg, 2.4 mmol, 1.2 eq.), solvent dry THF (5 mL) and Bu<sub>4</sub>NOH (5 mL) at 40 °C for 3 h.
- e. **102** (215  $\mu$ l, 2 mmol, 1 eq.), BINAP–Pd (6.3 mg, 0.02 mmol, 1 mol%), **98b** (365 mg, 2.4 mmol, 1.2 eq.), solvent dry THF (5 mL) and nBu<sub>4</sub>NOH (5 mL) at 40 °C for 3 h.
- f. **102** (215  $\mu$ l, 2 mmol, 1 eq.), PVP–Pd (133 mg, 0.1 mmol, 5 mol%), **98b** (365 mg, 2.4 mmol, 1.2 eq.), solvent dry THF (5 mL) and nBu<sub>4</sub>NOH (5 mL) at 40 °C for 3 h.
- g. **102** (215  $\mu$ l, 2 mmol, 1 eq.), PVP–Pd (133 mg, 0.1 mmol, 5 mol%), **98b** (365 mg, 2.4 mmol, 1.2 eq.), solvent dry THF (5 mL) and nBu<sub>4</sub>NOH (5 mL) at 40 °C for 3 h.
- h. **102** (215  $\mu$ l, 2 mmol, 1 eq.), PPh<sub>3</sub>–Pd (42.6 mg, 0.02 mmol, 5 mol%), **98b** (365 mg, 2.4 mmol, 1.2 eq.), solvent dry THF (5 mL) and nBu<sub>4</sub>NOH (5 mL) at 40 °C for 3 h. All percentage conversion as determined by <sup>1</sup>H NMR spectroscopic analysis of the crude reaction following Celite™ filtration plug using DCM as solvent.

The screening of the heterogeneous Pd catalysts with 2,4-dichloropyridine **102** in the presence of *p*-methoxyphenylboronic acid **98b** offered little or no conversions at all, especially when the PdNPs were used in the catalysis. An example of the heterogeneous catalysts, palladium supported on activated carbon containing 5% by weight palladium Pd/C (Sigma Aldrich, catalogue number 205680; no information was given about the Pd particle size on the carbon support within the product specification sheet) was tested and found to be the most reactive compared with the nanoparticles **97** and **46** (TPP–Pd, BINAP–Pd and PVP–Pd) respectively. In general, the reaction mediated by the Pd/C catalyst seem to depend on temperature and catalyst loading, with the reaction at (70 °C and 60 °C) and (5 mol% Pd loading) affording (23%) and (4%) exclusively of the C2 regioisomer **103b** after 4 and 6 h respectively (**Table 7** entry 2 and 1). However, when the reaction was conducted using (1 mol% Pd catalyst loading) at 40 °C an overall conversion of only (7%) after 24 h was afforded (**Table 1**, entry 3).

With regards to the Pd nanoparticle-mediated reactions there was little difference in percentage conversion between the presence and absence of PPh<sub>3</sub> ligands, though, the catalysis appears to be temperature dependent, which was expected. Screening BINAP–Pd **95** (a Pd to BINAP ratio of 3:1) at 70 °C, (1 mol% Pd loading) afforded (11%) overall conversion of **102** and with the following selectivity **103b** C2 regioisomer (10%) and the **104b** C4 arylated product (1%), after 6 h respectively (**Table 7**, entry 4). All the Pd NPs

screened at 40 °C performed woefully, affording trace conversion to no conversion at all (**Table7**, entries 5-10). When PVP–Pd **46** (8 wt% Pd) was screened at 40 °C and at (1 mol% and 5 mol% Pd catalyst loading) respectively, there no observed conversion of **102**.

## 2.4 Conclusions

It was found that the structure of the Pd catalyst dramatically affects the regioselectivity of SMCC reactions of 2,4-dihalopyridines. The heterogeneous Pd catalysts used in this study were found to be less reactive as catalysts than  $\text{Pd}(\text{PPh}_3)_4$ ,  $\text{Pd}(\text{OAc})_2/\text{PPh}_3$  or the  $\text{Pd}_3$  cluster catalysts. With the exception of  $[\text{Pd}_3(\text{PPh}_3)_4][\text{BF}_4]_2$ , all other Pd catalysts screened gave outcomes that are generally in agreement with the literature,<sup>87,88</sup> e.g. the major arylated regioisomer being the C2 arylated products, with the C4 and diarylated products differing in terms of both yield and regioisomeric ratio. This is due to the differences in electronic environment of the two carbon-halogen (X) bonds – the C2-X bond being weaker than the C4-X bond, making for a more facile oxidative addition step with Pd(0) – the first committed step in a cross-coupling catalytic cycle.<sup>2</sup>

An unprecedented observation was made with  $[\text{Pd}_3(\text{PPh}_3)_4][\text{BF}_4]_2$ , at 1 mol% Pd catalyst loading, in a reaction conducted at 40 °C (mild conditions) in the presence of  $n\text{Bu}_4\text{NOH}$  as base and THF as solvent. The major regioisomer was found to be the C4 arylated product as opposed to the C2 regioisomer. The difference imparted by  $[\text{Pd}_3(\text{PPh}_3)_4][\text{BF}_4]_2$  could be explained by its stability in solution as a  $\text{Pd}_3$  cluster, the bulky nature/structure of which could change the regioselectivity of the reaction. As a relatively low reaction temperature was used, the  $\text{Pd}_3$  cluster may remain intact in solution. Further studies could focus on examining whether the  $\text{Pd}_3$  cluster is present under the working SMCC reaction conditions. Intriguingly, in terms of regioselectivity, the  $[\text{Pd}_3(\text{PPh}_3)_4][\text{PF}_6]_2$  catalyst did not behave the same as for  $[\text{Pd}_3(\text{PPh}_3)_4][\text{BF}_4]_2$ . This suggests that the  $\text{PF}_6^-$  anion may cause the  $\text{Pd}_3$  cluster to be less stable under the same reaction conditions as opposed to when  $\text{BF}_4^-$  anion is present.  $[\text{Pd}_3(\text{PPh}_3)_4][\text{PF}_6]_2$  may deliver mononuclear  $\text{Pd}(\text{PPh}_3)_n$  species into solution, thus mirroring the behavior of  $\text{Pd}(\text{PPh}_3)_4$  whereas  $[\text{Pd}_3(\text{PPh}_3)_4][\text{BF}_4]_2$  behaves as a cluster. There would be further value in altering the non-coordinating anion (X) further in the  $[\text{Pd}_3(\text{PPh}_3)_4][\text{X}]_2$  to assess the full impact of this observation.

Overall, the study has confirmed that there could be great value in exploiting the catalytic properties of small Pd clusters in affecting regioselectivity in cross-coupling reactions, but that subtle effects associated with the supporting anion may be critical. It should be noted that in order to make conclusive deductions on the effect of these catalysts, the reactions would have to be done at the same time intervals and the reaction profile monitored.

### 3. Experimental section

#### 3.1 General experimental details

**Solvents and reagents:** Reagents and solvents were purchased from commercial sources such as Sigma-Aldrich, Alfa Aesar, Fluorochem, Fisher Scientific or Across Organic and were used as received unless otherwise stated. Dry THF was obtained from a Pure Solv MD-7 solvent system and stored under nitrogen. The THF was machine dried and sonicated under bubbling nitrogen and was dispensed under bubbling nitrogen. Petrol refers to the fraction of petroleum ether which has a boiling point range of 40/60 °C. Aqueous Na<sub>2</sub>CO<sub>3</sub> (2 M) solution was freshly prepared each time and degassed with sonication under bubbling nitrogen before use. Tetrabutylammonium hydroxide (1.0 M) was obtained from Fluorochem and each time it was warmed to 40 °C in a water bath to aid solubility, and degassed under sonication and bubbling with nitrogen prior to use. All air sensitive reactions, unless otherwise noted, were performed in inert atmosphere (typically nitrogen or argon) using standard Schlenk line techniques, using thoroughly-dried glassware in a hot oven (120 °C). Thin layer chromatography (TLC) was carried out using Merck 5554 aluminium backed silica plates and spots were visualized using UV-light (270 and 365 cm<sup>-1</sup> respectively). All synthesised products, unless otherwise stated, were isolated using flash column chromatography using either Merck 60 or Fluorochem 60 Å silica gel (particle size 40–63 µm) and solvent systems are reported in the text. Retardation factor (*R<sub>f</sub>*) values from TLC analysis are quoted to two decimal places.

**Nuclear Magnetic Resonance spectroscopy:** Unless otherwise stated, <sup>1</sup>H, <sup>13</sup>C and <sup>31</sup>P NMR spectra were recorded on a JEOL ECS400 or JEOL ECX400 spectrometer at 298K. Chemical shifts are reported in parts per million (ppm) using deuterated chloroform (CDCl<sub>3</sub>), deuterated methylene chloride (CD<sub>2</sub>Cl<sub>2</sub>), and deuterated benzene (C<sub>6</sub>D<sub>6</sub>) as solvents. Coupling constants (J values) are reported in Hertz (Hz) and quoted to the nearest (± 0.5) and the spectra were processed using MestReNova (version 8.1) software. Multiplicities are described as singlet (s), doublet (d), triplet (t), quartet (q), quintet (quin), sextet (sext), multiplet (m). Documentary evidence of the products is given in **Appendix 1**.

Unless otherwise stated, Proton (<sup>1</sup>H), Carbon-13 (<sup>13</sup>C) and Phosphorus-31 (<sup>31</sup>P) spectra were recorded at 400, 101 and 162 MHz respectively. Chemical shifts are internally referenced to residual signals of deuterated solvents (CDCl<sub>3</sub>:δ<sub>H</sub> = 7.26 ppm, δ<sub>C</sub> = 77.16

ppm; CD<sub>2</sub>Cl<sub>2</sub>:  $\delta_{\text{H}} = 5.32$  ppm,  $\delta_{\text{C}} = 54.00$  ppm and C<sub>6</sub>D<sub>6</sub>:  $\delta_{\text{H}} = 7.16$  ppm,  $\delta_{\text{C}} = 128.39$  ppm) respectively. Chemical shifts ( $\delta$ ) values are quoted for (<sup>1</sup>H) and (<sup>13</sup>C) to 2 decimal places and (<sup>31</sup>P), chemical shifts are externally referenced to H<sub>3</sub>PO<sub>4</sub> and given to one decimal place.

**Mass Spectroscopy:** Mass spectrometry was performed using a Bruker DaltronicsmicrOTOF spectrometer using electron spray ionisation (ESI) and in some cases liquid induction field desorption ionisation (LIFDI) using a Waters GCT premier mass spectrometer. Mass to charge ratios ( $m/z$ ) are reported in Daltons. High resolution mass spectra (HRMS) are reported, with less than 5 ppm error, typically as pseudo-molecular ions, *e.g.* [MH]<sup>+</sup> or [MNa]<sup>+</sup>.

**Transmission Electron Microscopy:** Transmission electron microscopy was performed using the Department of Biology Technology Facility (with the expertise of Dr. Meg Stark), University of York using an FEI Technai 12 G2BioTWIN microscope operating at 120 kV, and images were captured using an SIS Megaview III camera. Samples were prepared by suspending *ca.* 1 mg of material in a reagent grade ethanol with vigorous shaking. A pipette drop of the solution was placed on to a TEM grid and the solvent was allowed to evaporate. The grids used were 200 mesh copper grids with a Formvar/carbon support film. The resulting images were enlarged (to A4 size) and with a measuring ruler, the diameter of each nanoparticles spot was manually measured and rounded to the nearest whole number. Statistical analyses were performed and histograms created using the Origin-Pro 2016 program (Data Analysis and Graphing Software-OriginLab).

**Elemental Analysis:** Elemental (CHN) analysis was performed at the Department of Chemistry, University of York, using Exeter Analytical CE-440 Elemental Analyser. All values were recorded as percentages to two decimal places.

**Infrared Spectroscopy:** Infrared spectra were obtained using a Bruker ALPHA-Platinum FTIR Spectrometer with a platinum-diamond ATR (attenuated total reflection) sampling module.

**Melting Point:** Melting point data was obtained using a digital Stuart SMP3 melting point apparatus and values are recorded to the nearest whole number.

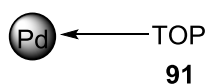
**Reaction monitoring by  $^1\text{H}$  NMR spectroscopy:** For reactions monitored by  $^1\text{H}$ NMR spectroscopic analysis, aliquots (100  $\mu\text{l}$ ) were removed from the reaction mixture and transferred into sample vials. Each sample was diluted with DCM (2 mL), and then filtered through a Celite plug in a glass pipette (1 cm). Each  $^1\text{H}$  NMR sample was run using dimethyl sulfone ( $\text{Me}_2\text{SO}_2$ , 0.6 mL) in  $\text{CDCl}_3$  external standard solution.

The reaction progress was calculated by  $^1\text{H}$  NMR spectroscopic analysis, by taking the ratios of the proton integrals corresponding to the diagnostic protons (C6) of products C2 arylated (**99** and **103**), C4 arylated (**100** and **104**) and di-arylated, (**101**) and starting materials (**97** and **102**). Conversions are reported to the nearest percentage. The ratios of the products were quantified against the amount of external standard present.

## 3.2 General Procedures

### 3.2.1 Synthesis of palladium catalysts

#### Trioctylphosphine stabilised palladium nanoparticles<sup>86</sup>

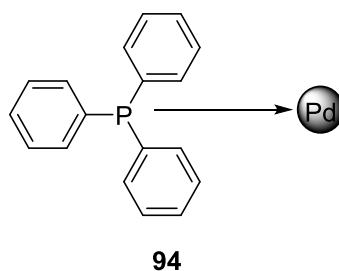


In an oven-dried round bottomed flask, equipped with a magnetic stirrer bead, was added  $\text{Pd}(\text{OAc})_2$  (100 mg, 0.33 mmol) dissolved in trioctylphosphine (7mL, 16 mmol). The reaction mixture was covered with aluminium foil and heated to 300  $^\circ\text{C}$  for 3 days, using a graphite bath. The solution was allowed to cool to room temperature and methanol (15 mL) was added. After stirring for 5 minutes the mixture was centrifuged (*ca* 400 rpm) for 10 minutes. The black precipitate isolated was washed with methanol (5 x 10 mL) and dried *in vacuo* to afford a black precipitate **91** (66.9 mg, 103%). The over 100% yield recorded maybe due to our inability to dry the sample completely and at the time of use it was still sticky to touch. No characterisation was done on the precipitate before it was used in the ligand exchange reaction to synthesize the other Pd stabilised NPs.

*Lab reference book number: EYD-1-77*



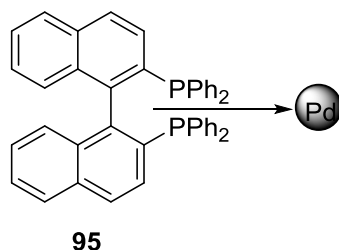
## Triphenylphosphine-PdNPs



In a round bottomed flask, TOPPdNPs **91** (105 mg, 0.168 mmol) was dissolved in DCM (3 mL) and PPh<sub>3</sub> **85** (107 mg, 0.41 mmol) was added and stirred at room temperature overnight. Methanol (4 mL) was added to the resulting black solution, centrifuged for 10 minutes and the particles retrieved and washed with methanol (5 x 10 mL). The nanoparticles were then dried *in vacuo* affording a black solid **94** (56 mg). Transmission electron microscopy images show the presence of palladium nanoparticles with spherical shapes and average diameter ranging between 1.5-3.5 nm.

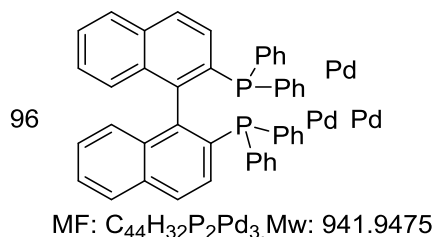
Lab reference book number: EYD-2-116

## (±)-2,2'-bis(diphenylphosphino)-1,1'-binaphthyl-PdNPs<sup>86</sup>



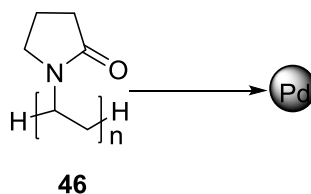
TOPPdNPs **91** (300 mg, 0.48 mmol) were dissolved in dichloromethane (3 mL) and (±)-2,2'-bis(diphenylphosphino)-1,1'-binaphthyl **44** (200 mg, 0.32mmol) was added and stirred at room temperature overnight. Methanol (10 mL) was added to the resulting black precipitate and the solution centrifuged for 10 min. The black precipitate was retrieved and washed with methanol (5 x 10 mL).The solvents were removed *in vacuo* and finally dried under high vacuum (~0.1 mmHg) to afford black particulate matter **95** (391.7 mg 130%).Transmission electron microscopy images show particles with an average diameter ranging between 5-7 nm, which is consistent with the literature. Elemental analysis C, 56.11; H, 3.42; P, 6.58; Pd, 33.89 found C, 56.69; H, 3.74, rest 39.56; ESI-MS m/z: 623.2050 [C<sub>44</sub>H<sub>33</sub>P<sub>2</sub>]<sup>+</sup>.i.e. [95+H]<sup>+</sup> (C<sub>44</sub>H<sub>32</sub>P<sub>2</sub> requires 623.2052). No Pd-BINAP species were detected by ESI-MS. Considering all the evidence as above, and within the limit of

experimental error, we are proposing the structure below as the most plausible structural formula of our BINAP **44** stabilised Pd nanoparticles species; a ratio of 1 ligand to 3 Pd atoms.



Lab reference book number: EYD-1-82

### Polyvinylpyrrolidinone-PdNPs(**46**)



To a 2.5 L 3-necked round bottom flask fitted with a mechanical stirrer and a reflux condenser was added PdCl<sub>2</sub> **85** (255 mg, 1.44 mmol, 1 eq.), HCl (0.2 M, 14.4 mL) and deionised water (706 mL). The reaction mixture was stirred at room temperature for 1 h to give an orange solution. Polyvinylpyrrolidinone (PVP) **45** (3.2 g, 28.3 mmol, 14 eq.), deionised water (672 mL) and EtOH (1000 mL) were added and the reaction heated to reflux with stirring for 4.5 h. The mixture was allowed to cool to room temperature and the solvent removed under reduce pressure and in *vacuo* to give a brittle, glassy black solid. The black glassy solid was scraped from the round bottom flask and crushed with a pestle and mortar to afford a crystalline solid **46** (3.2 g).

Transmission electron microscopy (TEM) images show the presence of nanoparticles, with average diameter ranging between 1.5-3.5 nm. The particles were non-ionisable by both LIFID and ESI and also insoluble in acetonitrile. IR (solid-state ATR, cm<sup>-1</sup>): 2953 (w, br) 1645 (s) 1421 (s) 1285 (s), this is in accordance with the literature data, presented Reay a former member of the group.<sup>85</sup>

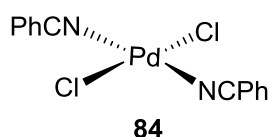
Lab book reference number: EYD-2-122



**Fig 17** Freshly-synthesised sample of Polyvinylpyrrolidinone-PdNPs (**46**)

#### 4.2.2 Synthesis of Palladium Clusters

##### Preparation of $\text{PdCl}_2(\text{PhCN})_2$ (**84**)<sup>80</sup>

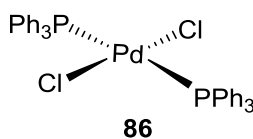


The synthetic procedure by Szlyket *al.*, was adapted.<sup>80</sup> In an oven-dried Schlenk tube (251.8 mg, 1.42 mmol) of **83**  $\text{PdCl}_2$  was dissolved in benzonitrile (10 mL, 0.1 mmol) and heated to 100 °C for 2 hours. The resulting dark orange solution was filtered hot; n-hexane (50 mL) was added to the filtrate at room temperature with the yellow compound **84**  $\text{PdCl}_2(\text{PhCN})_2$  precipitating out. It was then filtered under suction and washed with n-hexane (40 mL) and dried in air and in *vacuo* to afford **84** (436.7 mg, 80.2 %).

<sup>1</sup>H NMR (400 MHz,  $\text{C}_6\text{D}_6$ ): 6.98-6.94 (m, 4H, NCCCHCH) 6.82-6.76 (m, 2H, NCCCHCHCH), 6.66-6.60 (m, 4H, NCCCH): <sup>13</sup>C 131.73 (NCCCHCH), 131.68 (NCCCHCHCH), 128.53 NCCCH), 112.74 (NCC), 100.03 (NC).

*Lab reference book number: EYD-1-74*

##### Preparation of *trans*- $\text{PdCl}_2(\text{PPh}_3)_2$ (**86**)<sup>81</sup>



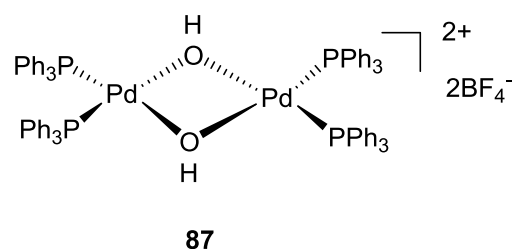
The synthetic procedure by Brumbaugh *et al.*, was adapted.<sup>81</sup>  $\text{PPh}_3$  **85** (287 mg, 1.2 mmol) was dissolved in an oven-dried Schlenk tube under nitrogen in deoxygenated DCM (1.5

mL) and cannula transferred into a second Schlenk tube containing PdCl<sub>2</sub>(PhCN)<sub>2</sub> **84** (200 mg, 0.52 mmol) dissolved in deoxygenated DCM under nitrogen. The mixture stirred at RT for 5 minutes, after 1 minute the yellow product had crashed out of the solution and diethyl ether (3 mL) was added to encourage precipitation. The solution was then filtered under suction and washed with (10 mL) of diethyl ether, dried in air and in vacuo to afford a bright yellow compound **86** (375.4 mg, 85%).

<sup>1</sup>H NMR (400 MHz, C<sub>6</sub>D<sub>6</sub>, δ): 7.93 (m, 12H, PCCH), 7.02 (m, 18H, PCCHCHCH): <sup>13</sup>C NMR (101 MHz, C<sub>6</sub>D<sub>6</sub>, δ): 135.4 (t, J<sub>CP</sub> = 6 Hz, PCCH), 130.3 (d, J<sub>CP</sub> = 25, PC), 128.1 (s, PCCHCHCH), 127.6 (s, PCCHCH); <sup>31</sup>P NMR (161 MHz, C<sub>6</sub>D<sub>6</sub>, δ): 24.41 (s).

Lab reference book number: EYD-1-94

### Preparation of [Pd(μ-OH)(PPh<sub>3</sub>)<sub>2</sub>]<sub>2</sub>[BF<sub>4</sub>]<sub>2</sub> **87**

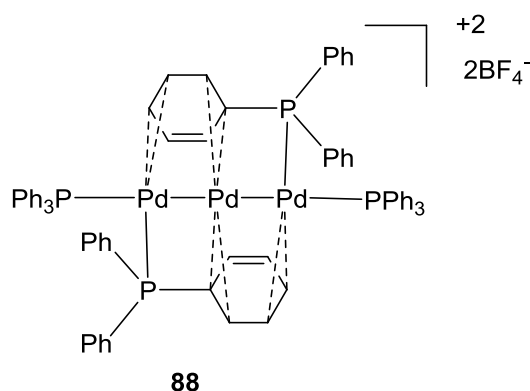


The synthetic procedure by Bushnell, *et al.*, was adopted.<sup>82</sup> In an oven-dried Schlenk tube was AgBF<sub>4</sub> (83.5 mg, 0.43 mmol), dissolved in acetone (6 mL). In a second Schlenk tube PdCl<sub>2</sub>(PPh<sub>3</sub>)<sub>2</sub> **86** (152 mg, 0.22 mmol) was dissolved in a mixture of DCM (8 mL) and acetone (4 mL). The solution was then transferred dropwise in the first Schlenk tube and stirred at RT for 15 minutes. White AgCl precipitated out of the solution and this was removed by Celite™ filtration, diethyl ether (45 mL) was added to the filtrate and refrigerated overnight. The creamy/orange powder was filtered under suction and washed with cold diethyl ether and dried in air and in *vacuo* to afford **87** (103.10 mg, 64%).

<sup>1</sup>H NMR (400 MHz, CD<sub>2</sub>Cl<sub>2</sub>, δ): 7.50 (t, J = 7.7, 12H PCCHCHCH), 7.35 (d.d 11.5, 7.6, 24H, PCCH), 7.25 (t = 7.6, 24H, PCCHCH) <sup>13</sup>C NMR (101 MHz, CD<sub>2</sub>Cl<sub>2</sub>, δ): 135 (PCCH), 133 (PCCHCHCH), 132 (PCCHCH), 130 (PC), <sup>31</sup>P NMR (162 MHz, CD<sub>2</sub>Cl<sub>2</sub>, δ): 37.98 (s).

Lab reference book number: EYD-1-83

## Preparation of $[\text{Pd}_3(\text{PPh}_3)_4[\text{BF}_4]_2]$ (**88**)<sup>79</sup>

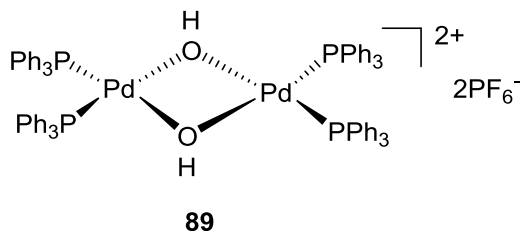


The synthetic procedure by Kannan, *et al.*, was adopted.<sup>79</sup> To a round bottomed flask was added  $[\text{Pd}(\mu\text{-OH})(\text{PPh}_3)_2]_2[\text{BF}_4]_2$  **87** (81.6 mg, 55.7  $\mu\text{mol}$ ) and few drops of DCM, followed by drops of EtOH until the solution turned brick red. The volume of the solution was reduced to about 2/3 the initial volume and then cooled in an ice bath and the solvent decanted. The resulting red solid was washed with cold EtOH and traces of solvent removed under *vacuo* to afford reddish solids **88** (26.4 mg, 46%). The molecular ion was not observed when the LIFID mass spectrum was recorded, but both the  $^{13}\text{C}$ -NMR and the  $^1\text{H}$ -NMR appear to support the structure.

$^1\text{H}$  NMR (400 MHz,  $\text{CD}_2\text{Cl}_2$ ,  $\delta$ ): 7.48-7.18 (m, 50 H), 6.96 (br, s, 2H, PCCHCHCH), 5.93 (t, J = 8.0, 6.3, 1.5 Hz, 4H, PCCHCH of PPh-Pd), 4.76 (t, 4H, PCCH of PPh-Pd):  $^{31}\text{P}$  NMR (162 MHz,  $\text{CD}_2\text{Cl}_2$ ): 43.43  $^{13}\text{C}$  NMR (101 MHz,  $\text{CD}_2\text{Cl}_2$ ,  $\delta$ ): 135 (t,  $J_{\text{CP}} = 6.8$  PCCH of  $\text{PPh}_2$ ), 134 (t,  $J_{\text{CP}} = 6.4$ , PCCH of  $\text{PPh}_3$ ), 133 (s, PCCHCHCH of  $\text{PPh}_2$ ), 131 (s, PCCHCHCH of  $\text{PPh}_3$ ), 129 (m, PCCHCH of both  $\text{PPh}_2$  and  $\text{PPh}_3$ ), 117 (t,  $J_{\text{CP}} = 4$ , PC of both  $\text{PPh}_2$  and  $\text{PPh}_3$ ), 100 (t,  $J_{\text{CP}} = 4$ , PCCHCH of PPh-Pd).

*Lab reference book number: EYD-1-91*

### Preparation of $[\text{Pd}(\mu\text{-OH})(\text{PPh}_3)_2]_2[\text{PF}_6]_2$ (**89**)

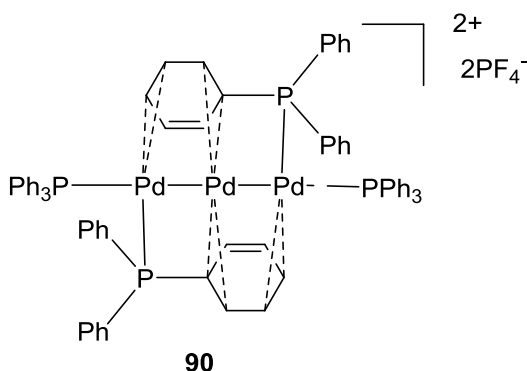


In Schlenk tube equipped with a magnetic stirrer was  $\text{PdCl}_2(\text{PPh}_3)_2$  **86** (500 mg, 0.712 mmol) dissolved in a mixture of DCM (20 mL) and acetone (10 mL). In a second Schlenk tube was  $\text{AgPF}_6$  (376 mg, 1.495 mmol), dissolved in acetone (15 mL) and transferred dropwise into the first Schlenk tube and stirred at RT for 15 minutes. White  $\text{AgCl}$  precipitated out of the solution and this was removed by filtration through Celite™. Diethyl ether (160 mL) was added to the filtrate and refrigerated overnight. The creamy/orange powder was filtered under suction and washed with cold diethyl ether and dried in air and in *vacuo* to afford an off white powdery compound **89** (287.2 mg, 55%).

$^1\text{H}$  NMR (400 MHz,  $\text{CD}_2\text{Cl}_2$ ,  $\delta$ ): 7.58 – 7.50 (m, 12H, PCCHCHCH), 7.46 – 7.38 (m, 24H, PCCH), 7.33 (td,  $J = 7.8, 3.1$  Hz, 24H, PCCHCH);  $^{19}\text{F}$  NMR (376 MHz,  $\text{CD}_2\text{Cl}_2$ ,  $\delta$ ): (d -73.1, 1JPF 714.4Hz)

Lab reference book number: EYD-2-106

### Preparation of $[\text{Pd}_3(\text{PPh}_3)_4][\text{PF}_6]_2$ (**90**)



To a round bottomed flask was added  $[\text{Pd}(\mu\text{-OH})(\text{PPh}_3)_2]_2[\text{PF}_6]_2$  **89** (50 mg, 33.95  $\mu\text{mol}$ ) and few drops of DCM followed by drops of EtOH until the solution turned brick red. The volume of the solution was reduced to about 2/3 the initial volume and then cooled in an ice bath and decanted. The resulting red solid was washed with cold EtOH and traces of

solvent removed under *vacuo* to afford **90** as a red solid (14.6 mg, 42%), the molecular ion was not observed when the LIFID mass spectra was recorded.

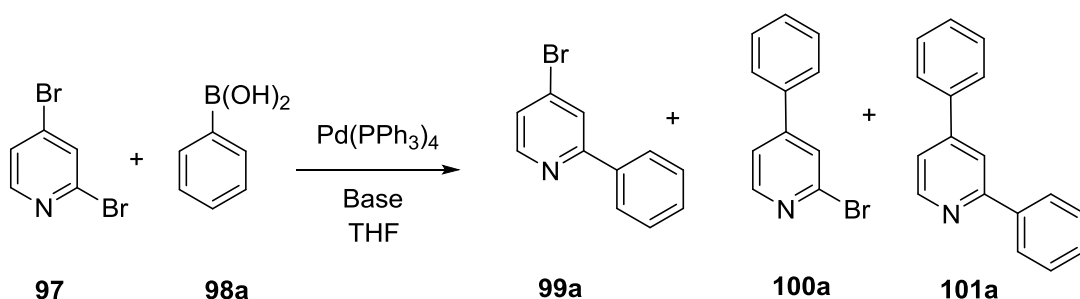
$^1\text{H}$  NMR (400 MHz,  $\text{CD}_2\text{Cl}_2$ ,  $\delta$ ): 7.51-7.19 (m, 50H), 7.00 (br. s, 2H), 5.91 (ddd,  $J = 8.0, 6.2, 1.5\text{Hz}$ , 4H), 4.76 (dd,  $J = 9.0, 7.4\text{Hz}$ , 4H);  $^{13}\text{C}$  NMR (101 MHz,  $\text{CD}_2\text{Cl}_2$ ,  $\delta$ ): 134 (t,  $J_{\text{CP}} = 6.8$ , PCCH of  $\text{PPh}_2$ ), 133 (t,  $J_{\text{CP}} = 6.3$ , PCCH of  $\text{PPh}_3$ ), 132 (s, PCCHCHCH of  $\text{PPh}_2$ ), 130 (s, PCCHCHCH of  $\text{PPh}_3$ ), 107 (m, PCCHCH of both  $\text{PPh}_2$  and  $\text{PPh}_3$ ), 105 (d,  $J_{\text{CP}} = 61$ , PCCH of both  $\text{PPh}_2$  and  $\text{PPh}_3$ ), 104 (t,  $J_{\text{CP}} = 4$ , PCCHCH of  $\text{PPh-Pd}$ ), 100 (t,  $J_{\text{CP}} = 4$ , PCCH of  $\text{PPh-Pd}$ ).

Lab reference book number: EYD-1-86

### 3.3 Suzuki-Miyaura cross-coupling reactions – exemplar procedures

Unless otherwise stated, all the experiments in this section were modelled on the work done by Cid *et al.*,<sup>87</sup> All throughout this section, laboratory notebook reference numbers are given to each of the experimental procedures quoted. For experiment references for specific data; see the relevant NMR spectra in **Appendix**.

#### Exemplar SMCC reaction

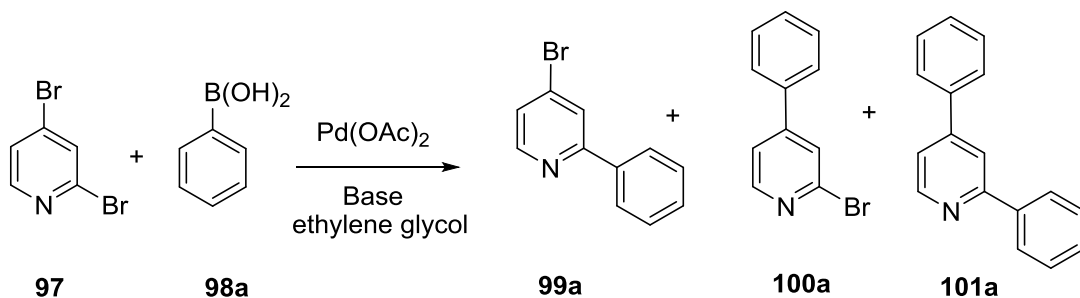


To an oven-dried Schlenk tube  $\text{Pd}(\text{PPh}_3)_4$  (116 mg, 0.10 mmol, 5 mol %) and phenylboronic acid **98a** (292 mg, 2.4 mmol, 1.2 eq.) was added in dry THF (3 mL). The tube was evacuated three times and back filled with nitrogen. In another oven-dried Schlenk tube under nitrogen was added 2,4-dibromopyridine **97** (472 mg, 2 mmol, 1 eq.) and then dry THF (2 mL). The solution was transferred dropwise into the first Schlenk tube, by cannula transfer. Thoroughly-degassed tetrabutylammonium hydroxide (1.0 M, 5 mL) was added and the reaction mixture stirred at 50 °C for 6 hours. The  $^1\text{H}$  NMR spectrum of the crude material showed the presence of C2 arylated product **99a**, C4 arylated product **100a**, and the diarylated product **101a**, in a ratio of 58%, 8% and 4%

respectively. The crude product was purified by flash column chromatography ( $\text{SiO}_2$ , 85:15, hexane/EtOAc) to afford the major product **99a** as yellow oil (0.46 mg). The other regioisomers could not be recovered from the column chromatographic process.

*Lab reference book number: EYD-1-34-4*

#### Exemplar SMCC reaction using different solvent and base

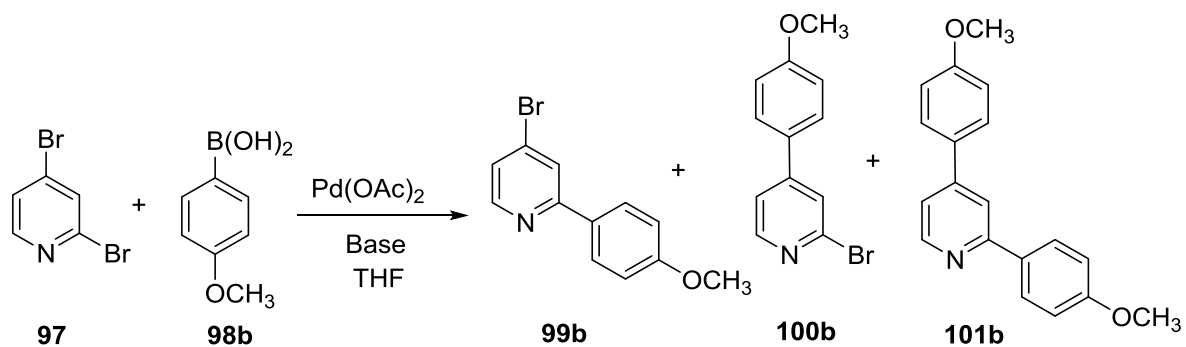


To an oven-dried Schlenk tube was added 2,4-dibromopyridine **97** (1.0 g, 4.2 mmol, 1.0 eq.), phenylboronic acid **98a** (1.543 g, 12.6 mmol, 3 eq.),  $\text{Pd}(\text{OAc})_2$  (4.8 g, 0.021 mmol, 0.5 mol %) and  $\text{K}_3\text{PO}_4$  (2 eq.). The tube was evacuated three times and back filled with nitrogen. A previous degassed ethylene glycol (25 mL) under nitrogen and sonication was cannula transferred into the Schlenk tube containing the reaction mixture. The reaction was heated in an oil bath to 80 °C for 150 min, allowed to cool to room temperature, water (30 mL) and saturated brine solution (30 mL) was added and the product extracted using DCM (4 x 10 mL). The DCM layer was dried over  $\text{MgSO}_4$ , filtered and the solvent removed on a rotary evaporator. The crude product a dark yellow viscous oil was purified using flash column, ( $\text{SiO}_2$ , 90:10, pet ether /diethyl ether) to afford the diarylated product as a pale yellow liquid which solidified after a few days **101a** (0.2781 g, 29%). The low yield reported here is due mainly to the lost of sample as it was being transferred from the round bottomed flasks to the sample vial for storage. It is worth noting that at the earlier stage of the research, our focus was on the synthesis of the three possible regioisomers (**99a**, **100a** and **101a**) to serve as standard in monitoring the reaction kinetics by Gas Chromatography (GC) and hence the reaction condition was skewed towards the formation of the diarylated product by using excess boronic acid.

*Lab reference book number: EYD-1-25-3*



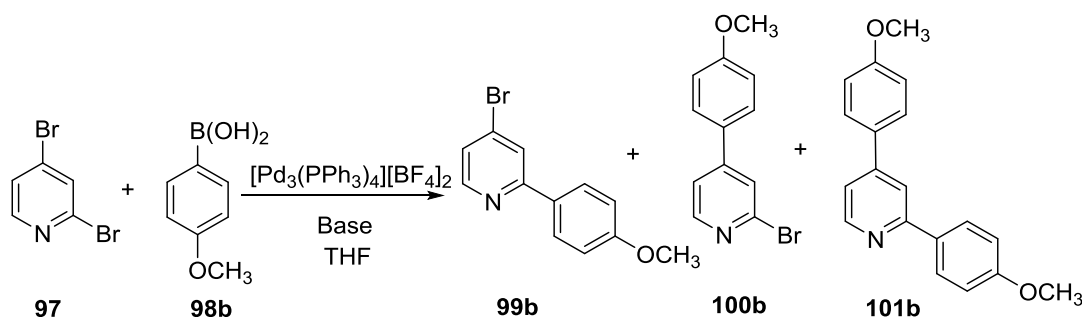
**Exemplar SMCC reaction using Pd(OAc)<sub>2</sub> as the catalyst with different arylboronic acid, *p*-methoxyphenylboronic acid **98b****



To an oven-dried Schlenk tube was added 2,4-dibromopyridine **97** (1.0 g, 4.22 mmol, 1.0 eq.), *p*-methoxyphenylboronic acid **98b** (1.92 g, 12.6 mmol, 3 eq.), Pd(OAc)<sub>2</sub> (4.44 mg, 0.021 mmol, 0.5 mol%) and K<sub>3</sub>PO<sub>4</sub> (1.785 g, 8.4 mmol, 2 eq.). The tube was evacuated and back filled three times with nitrogen. A degassed ethylene glycol (25 mL) was cannula transferred into the Schlenk tube containing the reaction mixture. The reaction was heated in an oil bath at 80 °C for 150 min; allowed to cool to room temperature, water (30 mL) and saturated brine (30 mL) was then added and extracted with DCM (4 x 40 mL). The DCM (organic layer) was dried over MgSO<sub>4</sub>, filtered and the solvent removed under vacuum. The crude product was purified by flash column chromatography to afford the diarylated product an off white solid **101b** (0.63 g, 52%). It is worth noting that at the earlier stages of the research, our focus was on the synthesis of the three possible regioisomers (**99b**, **100b**, and **101b**) to serve as standard in monitoring the reaction kinetics on a GC and hence the reaction conditions were biased towards the formation of the diarylated product by using excess boronic acid.

*Lab book reference number: EYD-1-24-5*

**Exemplar SMCC reaction using  $[\text{Pd}_3(\text{PPh}_3)_4][\text{BF}_4]_2$  as the catalyst with different arylboronic acid, *p*-methoxyphenylboronic acid **98b****



To an oven-dried Schlenk tube equipped with a magnetic stirrer and a thermocouple thermometer was added  $[\text{Pd}_3(\text{PPh}_3)_4][\text{BF}_4]_2$  **88** (10.5 mg, 6.67  $\mu\text{mol}$ , 1 mol %) and *p*-methoxyphenylboronic acid **98b** (365 mg, 2.4 mmol, 1.2 eq.) in dry THF (3 mL). The tube was evacuated three times and back filled with nitrogen. In another oven-dried Schlenk tube under nitrogen was added 2,4-dibromopyridine **97** (474 mg, 2 mmol, 1 eq.) and then dry THF (2 mL). The diluted substrate, the catalyst-boronic acid mixture and thoroughly-degassed tetrabutylammonium hydroxide (1.0 M, 5 mL) were placed in an oil bath to attain a steady temperature of (37.5°C). The substrate and the base were quickly added to the catalyst-boronic acid mixture and the reaction monitored by NMR for 24 h. The  $^1\text{H}$  NMR spectrum of the crude material showed the presence of **99b**, **100b** and **101b** in a ratio of 15%, 59% and 11%. The crude residue was purified by flash column chromatography ( $\text{SiO}_2$ , 4:1, hexane/EtOAc) to afford the major product, the C4 arylated product **100b** as white solid (45.8 mg, 56%) and the C2 arylated product **99b** also as a white solid (13 mg, 16%). The diarylated product **101b** could not be recovered from the chromatographic process.

*Lab reference number: EYD-2-118-3*

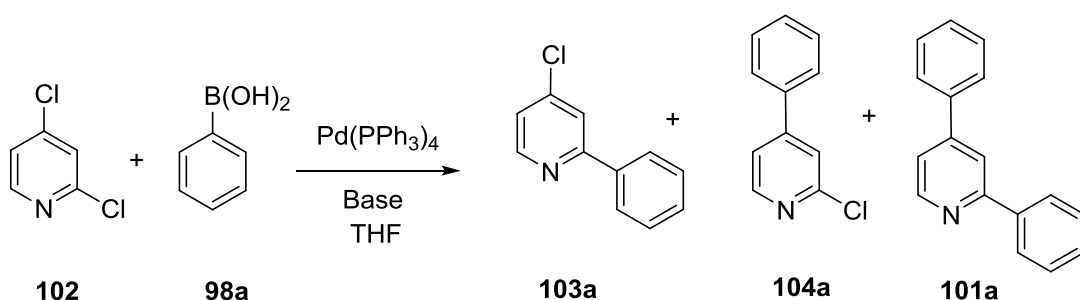
*Lab reference number: EYD-2-118-2*

### Single SMCC reaction using Pd(PPh<sub>3</sub>)<sub>4</sub> as the catalyst with *p*-methylphenylboronic acid **98b**

To an oven-dried Schlenk tube was added Pd(PPh<sub>3</sub>)<sub>4</sub> (118.7 mg, 0.1 mmol, 5 mol%) and 4-tolylboronic acid **98c** (327 mg, 2.4 mmol, 1.2 eq.) in dry THF (3 mL). The tube was evacuated three times and back filled with nitrogen. In another oven-dried Schlenk tube under nitrogen was added 2,4-dibromopyridine **97** (478 mg, 2 mmol, 1 eq.) and then dry THF (1.6 mL). The solution was transferred dropwise into the first Schlenk tube, by cannula transfer. Freshly prepared and thoroughly-degassed 2 M aqueous sodium hydroxide solution (5 mL) was added and the reaction mixture stirred at 25 °C in an oil bath for 5 h. The process of isolating the C2 arylated product **99c**, a light yellow solid (282.2 mg) involved combining two or more crude products and purifying by flash chromatography (SiO<sub>2</sub>, 92: 8, hexane/EtOAc).

Lab reference book number: EYD-1-22-4

### Exemplar SMCC reaction using Pd(PPh<sub>3</sub>)<sub>4</sub> as the catalyst, employing 2,4-dichloropyridine and phenylboronic acid **98a** as substrates

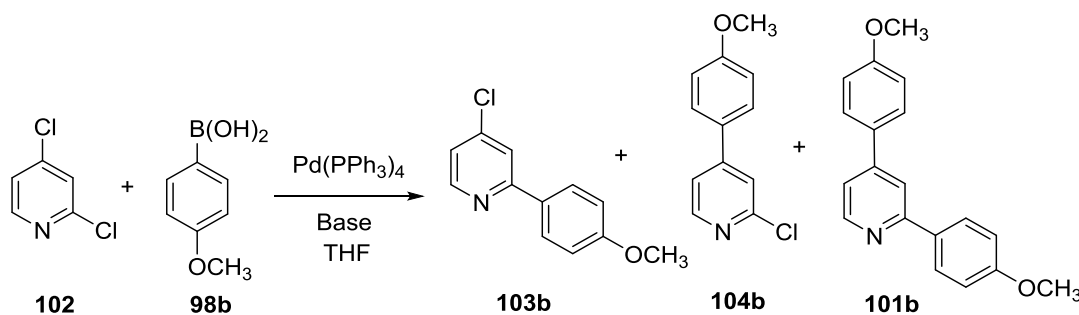


To an oven-dried Schlenk tube was added Pd(PPh<sub>3</sub>)<sub>4</sub> (37.64 mg, 0.033 mmol, 5 mol%), phenylboronic acid **98a** (97.94 mg, 0.80 mmol, 1.2 eq.) in dry THF (0.6 mL). The tube was evacuated three times and back filled with nitrogen. In another oven-dried Schlenk tube under nitrogen was added 2, 4-dichloropyridine **102** (72 μl, 0.67 mmol, 1 eq.) and then dry THF (1.0 mL). The solution was transferred dropwise into the first Schlenk tube, by cannula transfer. Thoroughly-degassed tetrabutylammonium hydroxide (1.0 M, 1.6 mL) was added and the reaction mixture stirred at 60 °C in an oil bath for 5 h, until no reaction progress was observed by TLC. The reaction mixture was diluted with DCM, filtered through celite plug and the filtrate washed with saturated aq. NaHCO<sub>3</sub> (3 x 10 mL). The aqueous layer was back extracted with DCM (5 mL). The organic layers were combined

and dried over anhydrous  $\text{Na}_2\text{SO}_4$  and concentrated in vacuo to yield a dark pink semisolid compound.  $^1\text{H}$  NMR spectrum of the crude material showed the presence of only the C2 arylated product **103a** 69% yield. The crude product was purified by flash chromatography ( $\text{SiO}_2$ , 4:1, hexane/EtOAc) to afford the sole product, **103a** as yellow viscous oil (115 mg).

Lab book reference number: EYD-1-42-3

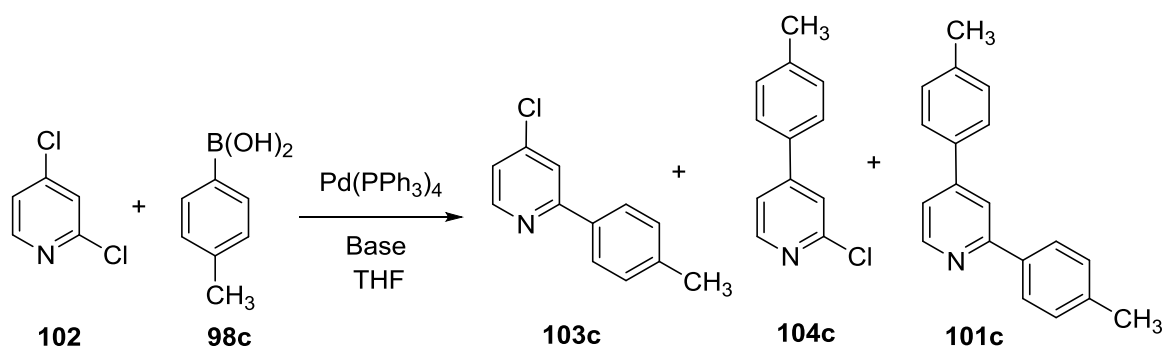
**Exemplar SMCC reaction using  $\text{Pd}(\text{PPh}_3)_4$  as the catalyst, employing 2,4-dichloropyridine and *p*-methoxyphenylboronic acid **98b** as substrates**



To an oven-dried Schlenk tube was added  $\text{Pd}(\text{PPh}_3)_4$  (115.4 mg, 0.10 mmol, 5 mol %), *p*-methoxyphenylboronic acid **98b** (365.6 mg, 2.4 mmol, 1.2 eq.), in dry THF (2 mL). The tube was evacuated three times and back filled with nitrogen. In another oven-dried Schlenk tube under nitrogen was added 2,4-dichloropyridine **102** (215  $\mu\text{l}$ , 2 mmol, 1 eq.) and then dry THF (3 mL). The solution was transferred dropwise into the first Schlenk tube, by cannula transfer. Thoroughly-degassed aqueous tetrabutylammonium hydroxide solution (1.0 M, 5 mL) was added and the reaction mixture stirred at 60 °C in an oil bath for 4 h. The crude products of various reactions, were combined and purified by flash column chromatography ( $\text{SiO}_2$ , 4:1, hexane/EtOAc) to afford two products, the C2 arylated product **103b** (265 mg) as off white oil and the C4 arylated product **104b** (841.8 mg) as an off-white oil, which solidified on standing.

Lab reference book number: EYD-1-40-2

**Exemplar SMCC reaction using Pd(PPh<sub>3</sub>)<sub>4</sub> as the catalyst, employing 2,4-dichloropyridine and *p*-methylphenylboronic acid **98c** as substrates**



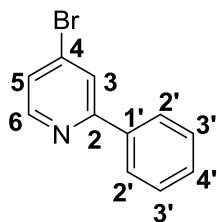
**Scheme 44** Screening of Pd(PPh<sub>3</sub>)<sub>4</sub> in the presence of 4-tolylboronic acid **98c** and 2,4-dichloropyridine **102**.

To an oven-dried Schlenk tube was added Pd(PPh<sub>3</sub>)<sub>4</sub> (23. mg, 0.02 mmol, 1 mol%) and 4-tolylboronic acid **98c** (326.3 mg, 2.4 mmol, 1.2 eq.) in dry THF (3 mL). The tube was evacuated three times and back filled with nitrogen. In another oven-dried Schlenk tube under nitrogen was 2,4-dichloropyridine **102** (210  $\mu$ l, 2 mmol, 1 eq.) diluted in dry THF (2 mL). The solution was transferred dropwise into the first Schlenk tube, by cannula transfer. Thoroughly-degassed aqueous tetrabutylammonium hydroxide solution (1.0 M, 5 mL) was added and the reaction mixture stirred at 70 °C in an oil bath (using a thermocouple to maintain steady temperature at 67.5 °C) for 4 h. The <sup>1</sup>H NMR spectrum of the crude material showed the presence of only **103c** the C2 arylated product in a 61% conversion. The crude product was purified by flash column chromatography to afford the product a light yellow solid **103c** (108 mg, 43%).

*Lab reference number: EYD-2-142-2*

### 3.3.1 Exemplar characterisation data for SMCC products

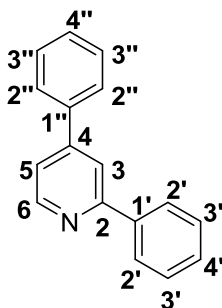
#### 4-Bromo-2-phenylpyridine (99a)<sup>87</sup>



$R_f$  0.46 (85:15, hexane/EtOAc);  $^1\text{H NMR}$  (400 MHz,  $\text{CDCl}_3$ ,  $\delta$ ): 8.49 (d,  $J = 5.3$  Hz, 1H, Ar-H<sup>6</sup>), 8.00 – 7.93 (m, 2H, Ar-H<sup>2'</sup>), 7.88 (d,  $J = 1.8$  Hz, 1H, Ar-H<sup>3</sup>), 7.51 – 7.39 (m, 3H, Ar-H<sup>3'</sup> and H<sup>4'</sup>), 7.37 (dd,  $J = 5.2, 1.8$  Hz, 1H, Ar-H<sup>5</sup>);  $^{13}\text{C NMR}$  (101 MHz,  $\text{CDCl}_3$ ,  $\delta$ ): 159.2 (C), 150.7 (CH), 138.3 (C), 133.8 (C), 130 (CH), 129.2 (2CH), 127.3 (2CH), 125.6 (CH), 124.2 (CH); ATR-IR neat 3041 (w, br), 1563 (s), 1460 (s), 1442 (m), 1377 (m), 772 (s);  $m/z$  (ESI+) 233.9911 [(M+H)<sup>+</sup>,  $^{79}\text{Br}$ ], Calcd for  $\text{C}_{11}\text{H}_9^{79}\text{BrN}$ , 233.9913 found 233.9911.

Lab reference book number: EYD-1-34-4

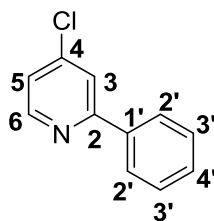
#### 2,4-Diphenylpyridine (101a)<sup>87</sup>



M.P 72.0-73.7 °C (lit.<sup>87</sup> 67-68°C, hexane/ $\text{CH}_2\text{Cl}_2$ ):  $R_f$  0.25 ( $\text{SiO}_2$ , 90:10, pet ether /diethyl ether);  $^1\text{H NMR}$  (400 MHz,  $\text{CDCl}_3$ ,  $\delta$ ): 8.75 (d,  $J = 5.1$ , 1H, Ar-H<sup>6</sup>), 8.06 (d,  $J = 8$ , 2H, Ar-H), 7.94 (s, 1H, Ar-H), 7.70 (d,  $J = 8$ , 2H, Ar-H), 7.56 – 7.41 (m, 7H, Ar-H);  $^{13}\text{C NMR}$  (101 MHz,  $\text{CDCl}_3$ ,  $\delta$ ): 158.2 (C), 150.2 (CH), 149.4 (C), 139.6 (C), 138.7 (C), 129.3 (CH), 128.9 (CH), 128.8 (CH), 127.2 (CH), 120.4 (CH), 118.9 (CH); IR (solid-state ATR,  $\text{cm}^{-1}$ ): 3024 (w, br), 1592 (m), 1539 (m), 1468 (m), 1388 (m), 757 (s), 689 (s). ESI Calcd for  $\text{C}_{17}\text{H}_{14}\text{N}$  232.1135 found 232.1121.

Lab reference book number: EYD-1-25-3

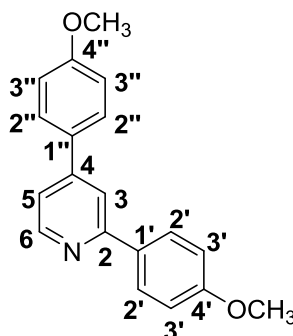
#### 4-Chloro-2-phenylpyridine (103a)<sup>87</sup>



<sup>1</sup>H NMR (400 MHz, CDCl<sub>3</sub>, δ): 8.55 (dd, *J* = 5.3, 0.6 Hz, 1H, Ar-H<sup>6</sup>), 7.99 – 7.92 (m, 2H Ar-H<sup>2'</sup>), 7.70 (dd, *J* = 2.0, 0.6 Hz, 1H, Ar-H<sup>3</sup>), 7.48 – 7.41 (m, 3H, Ar-H<sup>3'</sup> and H<sup>4'</sup>), 7.19 (ddd, *J* = 6.4, 5.3, 1.8 Hz, 2H, Ar-H<sup>5</sup>); (101 MHz, CDCl<sub>3</sub>, δ): 158.9 (C), 150.5 (CH), 144.7 (C), 129.6 (C), 128.9 (CH), 126.98 (2CH), 124.4 (2CH), 122.9 (CH), 122.3 (CH); IR (neat, cm<sup>-1</sup>) 3032 (w, br) 2918 (w), 1476 (m), 1428 (m), 1091 (w), 725 (s), 692 (s); *m/z* (ESI+) 190.0415 [(M+H)<sup>+</sup>, <sup>35</sup>Cl], Calcd for C<sub>11</sub>H<sub>9</sub><sup>35</sup>ClN, 190.0418 found 190.04156.

Lab reference book number: EYD-1-40-2

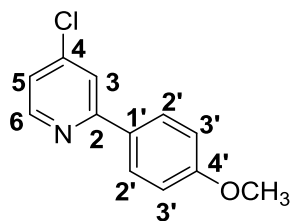
#### 2,4-Bis(*p*-methoxyphenyl)pyridine (101b)<sup>87</sup>



M.P 161.7-163.7 °C (lit<sup>87</sup> 158 °C, hexane/CH<sub>2</sub>Cl<sub>2</sub>): *R*<sub>f</sub> 0.25 (SiO<sub>2</sub>, 85:15, hexane/EtOAc), <sup>1</sup>H NMR (400 MHz, CDCl<sub>3</sub>, δ): 8.66 (d, *J* = 5.2 Hz, 1H, Ar-H<sup>6</sup>), 8.05 – 7.96 (m, 2H, Ar-H<sup>2'</sup>), 7.83 (dt, *J* = 1.6, 0.7 Hz, 1H, Ar-H<sup>3</sup>), 7.69 – 7.63 (m, 2H, Ar-H<sup>2''</sup>), 7.36 (ddd, *J* = 5.2, 1.7, 0.6 Hz, 1H, Ar-H<sup>5</sup>), 7.07 – 6.97 (m, 4H, Ar-H<sup>3'</sup> and 3''), 3.88 (s, 6H, 2xOMe); <sup>13</sup>C NMR (101 MHz, CDCl<sub>3</sub>, δ): 160.9 (2C), 158.1 (C), 150.4 (CH), 149.1 (C), 132.7 (C), 131.4 (C), 128.7 (CH), 119.6 (CH), 117.9 (CH), 114.9 (CH), 114.6 (CH), 100.4 (CH), 55.9 (2CH<sub>3</sub>); IR (solid-state ATR, cm<sup>-1</sup>): 2916 (w, br), 1911 (w, br), 1581 (w, br), 1508 (w), 1042 (m), 811 (s). ESI Calcd for C<sub>19</sub>H<sub>18</sub>NO<sub>2</sub> 292.1321 found 292.1332.

Lab book reference number: EYD-1-24-5

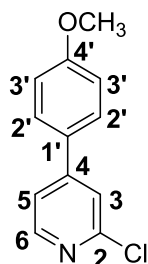
#### 4-Chloro-2-(*p*-methoxyphenyl)pyridine(103b)<sup>88</sup>



$R_f$  0.648 (SiO<sub>2</sub>, 4:1, hexane/EtOAc); <sup>1</sup>H NMR (400 MHz, CDCl<sub>3</sub>,  $\delta$ ): 8.51 (d,  $J$  = 5.3 Hz, 1H, Ar-H<sup>6</sup>), 7.95-7.88 (m, 2H, Ar-H<sup>2'</sup>), 7.63 (dd,  $J$  = 1.8, 0.7 Hz, 1H, Ar-H<sup>3</sup>), 7.14 (dd,  $J$  = 5.3, 1.9 Hz, 1H, Ar-H<sup>5</sup>), 7.00-6.93 (m, 2H, Ar-H<sup>3'</sup>), 3.83 (s, 3H, OMe); <sup>13</sup>C-NMR (101 MHz, CDCl<sub>3</sub>,  $\delta$ ): 160.7 (C), 158.3 (C), 150.8 (CH), 144.3 (C), 130.4 (C), 128.0 (2CH), 121.3 (CH), 119.7 (CH), 113.9 (2CH), 55.1 (CH<sub>3</sub>); IR (solid-state ATR, cm<sup>-1</sup>): 3003 (w, br), 2836 (w), 1607 (m), 1572 (s), 1246 (s), 1174 (s), 1028 (m), 817 (s);  $m/z$  (ESI+) 220.0516 [(M+H)<sup>+</sup>, <sup>35</sup>Cl], Calcd for C<sub>12</sub>H<sub>11</sub><sup>35</sup>ClNO, 220.0524 found 220.0516.

Lab book reference number: EYD-1-42-1

#### 2-Chloro-4-(*p*-methoxyphenyl)pyridine (104b)<sup>87</sup>

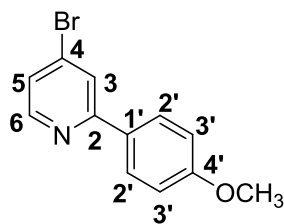


M.P 29.6-31.3°C (lit.<sup>87</sup> MP 53-54 °C):  $R_f$  0.35 (SiO<sub>2</sub>, 4:1, hexane/EtOAc); <sup>1</sup>H NMR (400 MHz, CDCl<sub>3</sub>,  $\delta$ ): 8.43 (d,  $J$  = 5.3 Hz, 1H, Ar-H<sup>6</sup>), 7.90-7.79 (m, 2H, Ar-H<sup>3</sup>), 7.54 (t,  $J$  = 1.7, Hz, 1H, Ar-H<sup>2'</sup>), 7.04 (dt,  $J$  = 5.3, 1.7 Hz, 1H, Ar-H<sup>5</sup>), 6.93-6.82 (m, 2H, Ar-H<sup>3'</sup>), 3.72 (d,  $J$  = 1.7 Hz, 3H, OMe); <sup>13</sup>C NMR (101 MHz, CDCl<sub>3</sub>): 160.7 (C), 158.3 (C), 150.1 (CH), 144.3 (C), 130.3 (C), 128.1 (2CH), 121.3 (CH), 119.6 (2CH), 113.9 (CH), 55.0 (CH<sub>3</sub>); IR (solid-state ATR, cm<sup>-1</sup>): 2958 (w, w), 2838 (w), 1605 (m), 1571 (m), 1246 (m), 1175 (m), 1027 (m), 813 (s);  $m/z$  (ESI+) 220.0521 [(M+H)<sup>+</sup>, <sup>35</sup>Cl], Calcd for C<sub>12</sub>H<sub>11</sub><sup>35</sup>ClNO, 220.0524 found 220.0521.

Lab book reference number: EYD-1-42-3



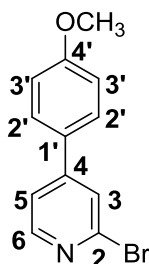
#### 4-Bromo-2-(*p*-methoxyphenyl)pyridine (99b)<sup>87</sup>



$R_f$  0.4 (SiO<sub>2</sub>, 4:1, hexane/EtOAc); <sup>1</sup>H NMR (400 MHz, CDCl<sub>3</sub>,  $\delta$ ): 8.45 (d,  $J$  = 5.3 Hz, 1H, Ar-H<sup>6</sup>), 7.99-7.89 (m, 2H, Ar-H<sup>2'</sup>), 7.87-7.80 (m, 1H, Ar-H<sup>3</sup>), 7.33 (dd,  $J$  = 5.3, 1.8 Hz, 1H, Ar-H<sup>5</sup>), 7.04-6.94 (m, 2H, Ar-H<sup>3'</sup>), 3.87 (s, 3H, OMe): <sup>13</sup>C NMR (101 MHz, CDCl<sub>3</sub>,  $\delta$ ): 160.8 (C), 158.4 (C), 150.0 (CH), 133.2 (C), 130.4 (C), 128.2 (2CH), 122.9 (CH), 114.0 (2CH), 55.2 (CH<sub>3</sub>): IR (solid-state ATR, cm<sup>-1</sup>): 3018 (w, br), 2835 (w), 1582 (m), 1181 (m), 1019 (m), 812;  $m/z$  (ESI+) 264.0029 [(M+H)<sup>+</sup>, <sup>79</sup>Br], Calcd for C<sub>12</sub>H<sub>11</sub><sup>79</sup>BrNO, 264.0019 found 264.0029.

Lab book reference number: EYD-2-118-2

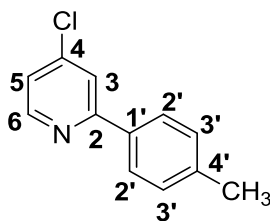
#### 2-Bromo-4-(*p*-methoxyphenyl)pyridine (100b)<sup>87</sup>



M.P 59.5-60.8 °C (lit.<sup>87</sup> MP 57 °C, hexane/CH<sub>2</sub>Cl<sub>2</sub>):  $R_f$  0.28 (SiO<sub>2</sub>, 4:1, hexane/EtOAc); <sup>1</sup>H NMR (400 MHz, CDCl<sub>3</sub>,  $\delta$ ): 8.34 (d,  $J$  = 5.3 Hz, 1H, Ar-H<sup>6</sup>), 7.65 (dt,  $J$  = 1.6, 0.7 Hz, 1H, Ar-H<sup>3</sup>), 7.59-7.51 (M, 2H, Ar-H<sup>2'</sup>), 7.40 (dt,  $J$  = 5.3, 1.3 Hz, 1H, Ar-H<sup>5</sup>), 7.03-6.95 (M, 2H, Ar-H<sup>3'</sup>), 3.86 (s, 3H, OMe): <sup>13</sup>C NMR (101 MHz, CDCl<sub>3</sub>): 160.8 (C), 150.5 (C), 150.1 (CH), 142.7 (C), 128.6 (C), 128.1 (2CH), 124.9 (CH), 120.0 (2CH), 114.5 (CH), 55.2 (CH<sub>3</sub>): IR (solid-state ATR, cm<sup>-1</sup>): 3019 (w, br), 2833 (w), 1891 (w), 1585 (s), 1515 (s), 1247 (s), 814 (s);  $m/z$  (ESI+) 264.0025 [(M+H)<sup>+</sup>, <sup>79</sup>Br], Calcd for C<sub>12</sub>H<sub>11</sub><sup>79</sup>BrNO, 264.0019 found 264.0025.

Lab reference number: EYD-2-118-3

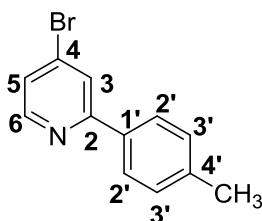
#### 4-Chloro-2-(4-methylphenyl)pyridine (103c)<sup>88</sup>



MP 43-45°C;  $R_f$  0.54 (SiO<sub>2</sub>, 4:1, hexane/EtOAc); <sup>1</sup>H NMR (400 MHz, CDCl<sub>3</sub>, δ): 8.54 (d,  $J$  = 5.3 Hz, 1H, Ar-H<sup>6</sup>), 7.88 – 7.83 (m, 2H, Ar-H<sup>2'</sup>), 7.69 (d,  $J$  = 1.9 Hz, H, 1Ar-H<sup>3</sup>), 7.26 (s, 2H, Ar-H<sup>5</sup>), 7.19 (dd,  $J$  = 5.3, 1.9 Hz, 1H, Ar-H<sup>3'</sup>), 2.40 (s, 3H, Me); <sup>13</sup>C NMR (101 MHz, CDCl<sub>3</sub>, δ): 158.8 (C), 150.2 (C), 144.4 (CH), 139.5 (C), 135.1 (C), 129.4 (2CH), 126.6 (CH), 124.3 (CH), 122.8 (2CH) 21.1 (CH<sub>3</sub>); IR (solid-state ATR, cm<sup>-1</sup>): 3026 (w, br), 2914 (w), 1547 (s), 1453 (m), 1366 (m), 811 (s) 767 (s);  $m/z$  (ESI+) 204.0573 [(M+H)<sup>+</sup>, <sup>35</sup>Cl], Calcd for C<sub>12</sub>H<sub>11</sub><sup>35</sup>ClN, 204.0575 found 204.0573.

Lab reference number: EYD-2-142-2

#### 4-Bromo-2-(*p*-methylphenyl)pyridine (99c)<sup>87</sup>



MP 57-59°C (lit.<sup>87</sup> 61 °C);  $R_f$  0.32 (SiO<sub>2</sub>, 92: 8, hexane/EtOAc); <sup>1</sup>H NMR (400 MHz, CDCl<sub>3</sub>, δ): 8.48 (d,  $J$  = 5.3 Hz, 1H, Ar-H<sup>6</sup>), 7.90 – 7.84 (m, 3H, Ar-H<sup>3</sup> and 2H<sup>3'</sup>), 7.36 (dd,  $J$  = 5.3, 1.8 Hz, 1H, Ar-H<sup>5</sup>), 7.31 – 7.26 (m, 2H, Ar-H<sup>2'</sup>), 2.41 (s, 3H, Me); NMR (101 MHz, CDCl<sub>3</sub>, δ): 159.0 (C), 150.4 (CH), 139.9 (C), 135.4 (C), 133.5 (C), 129.7 (CH), 127.0 (CH), 125.0 (CH), 123.7 (CH), 21.4 (CH<sub>3</sub>); IR (solid-state ATR, cm<sup>-1</sup>): 2912 (w, br), 1609 (w), 1569 (s), 1542 (w), 1374 (w), 807 (s), 680 (m);  $m/z$  (ESI+) 248.0068 [(M+H)<sup>+</sup>, <sup>79</sup>Br], Calcd for C<sub>12</sub>H<sub>11</sub><sup>79</sup>BrN, 248.0069 found 248.0068.

Lab reference book number: EYD-1-22-4

## Appendix (representative NMR spectra)

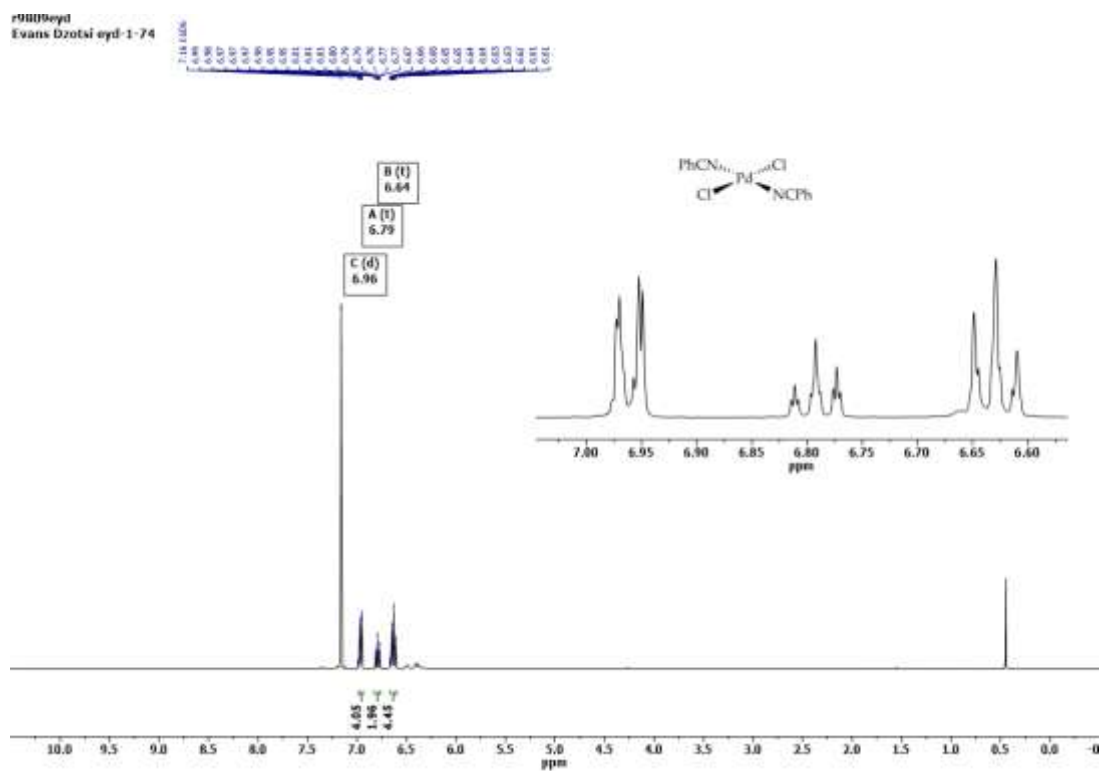


Figure 1A  $^1\text{H}$  NMR spectrum of **84** (400 MHz,  $\text{C}_6\text{D}_6$ ).

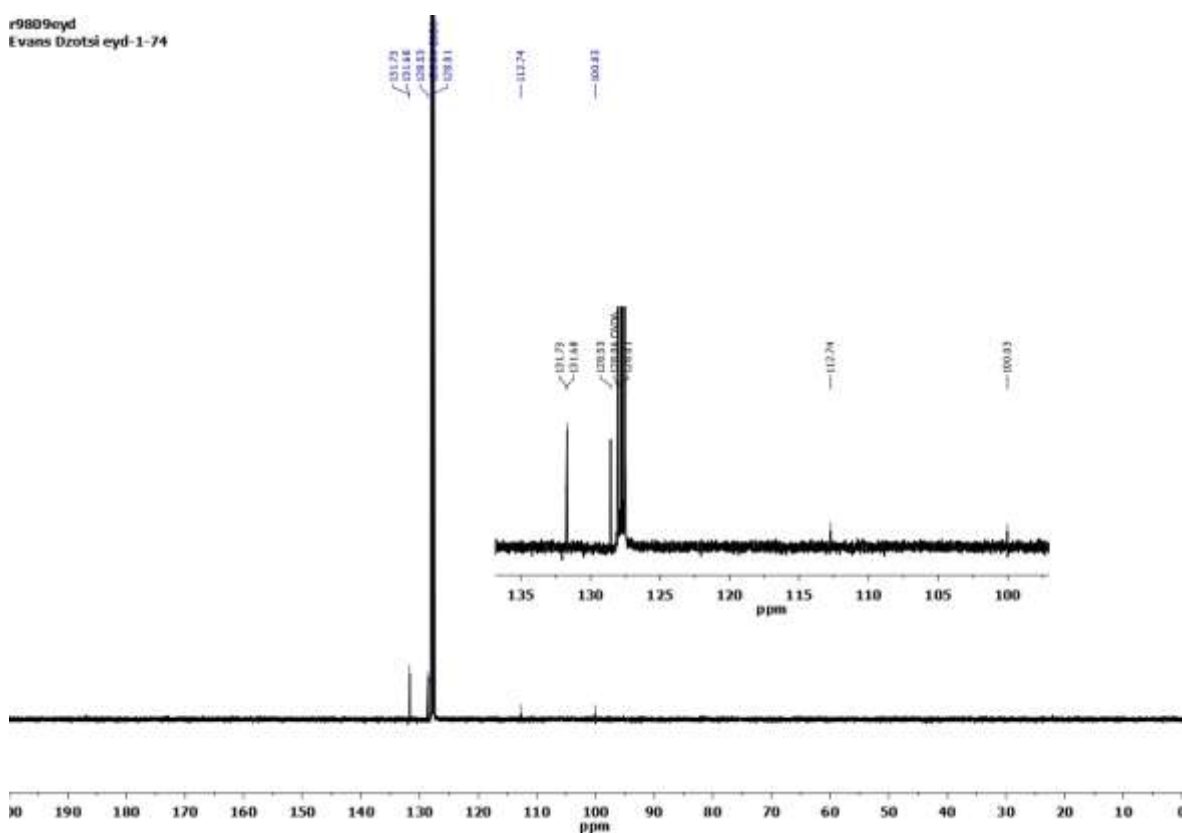


Figure 2A  $^{13}\text{C}$  NMR spectrum of **84** (101 MHz,  $\text{C}_6\text{D}_6$ ).

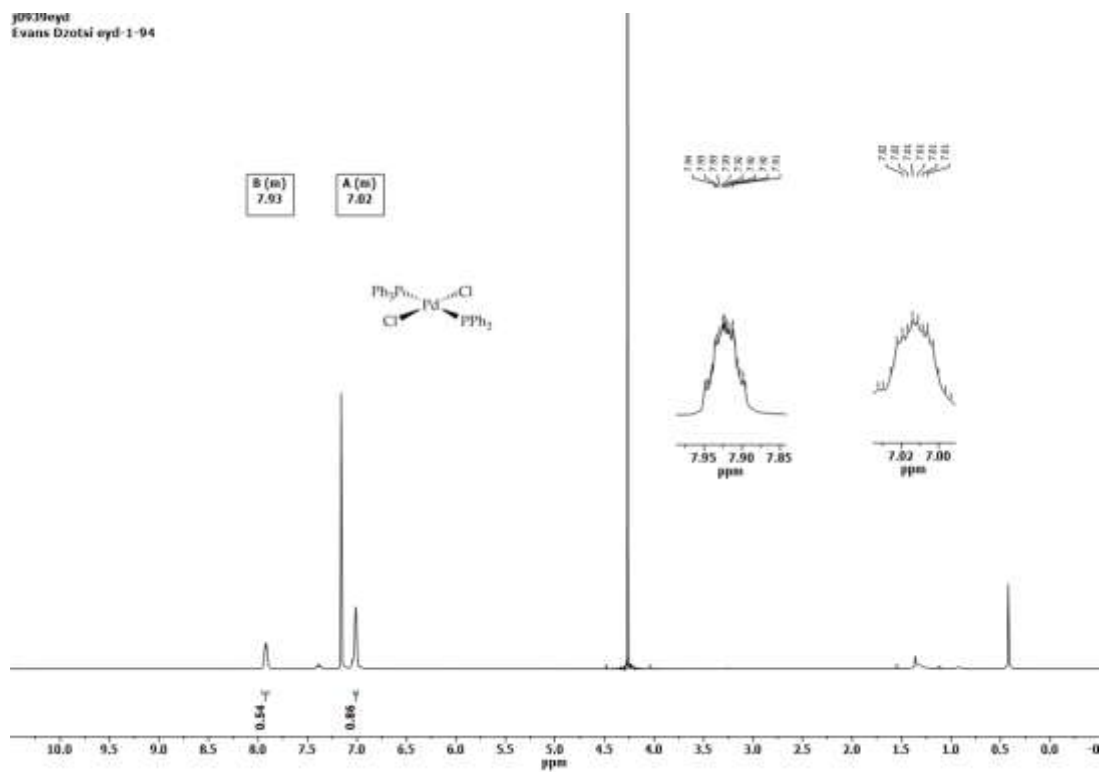


Figure 3A  $^1\text{H}$  NMR spectrum of **86** (400 MHz,  $\text{C}_6\text{D}_6$ ).

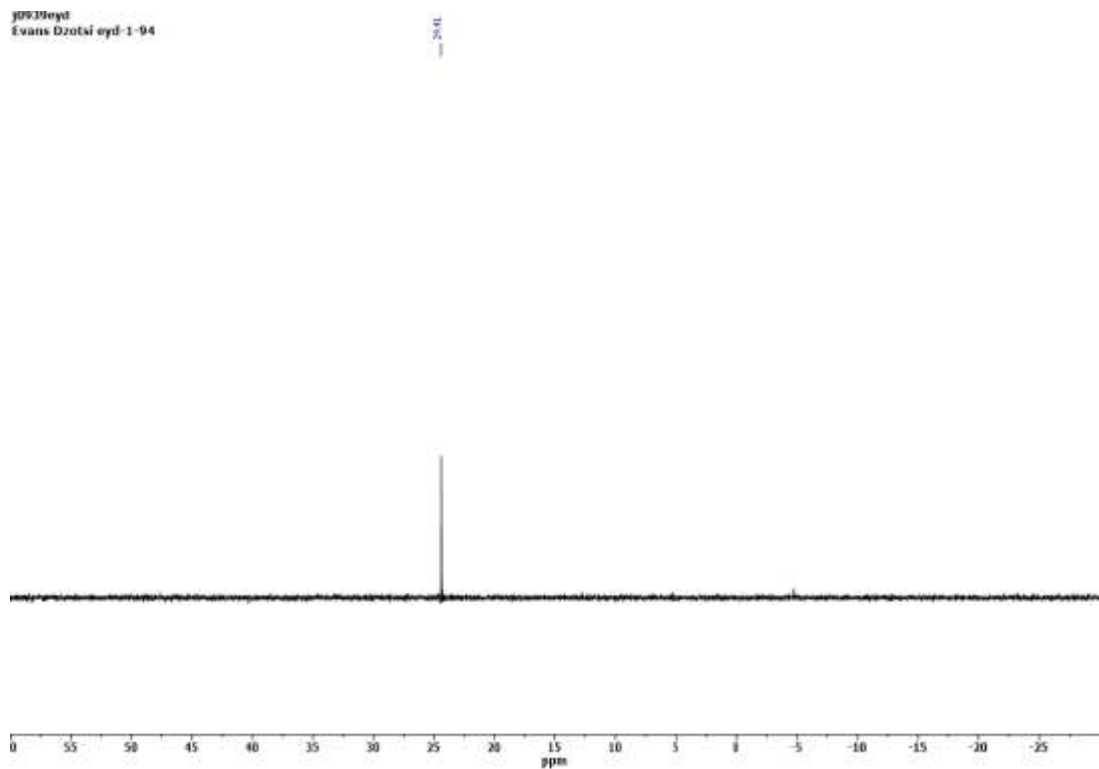


Figure 4A  $^{31}\text{P}$  NMR spectrum of **86** (162 MHz,  $\text{C}_6\text{D}_6$ ).



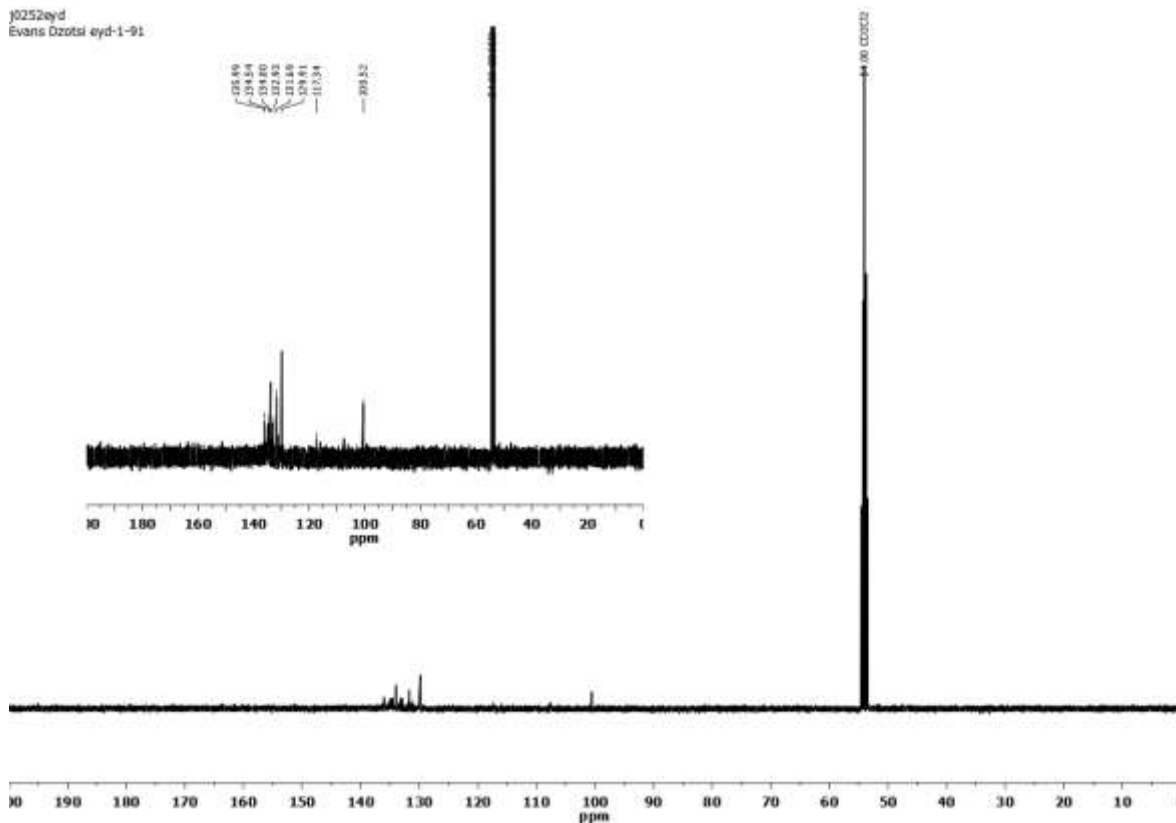


Figure 7A  $^{13}\text{C}$  NMR spectrum of **88** (101 MHz,  $\text{C}_6\text{D}_6$ ).

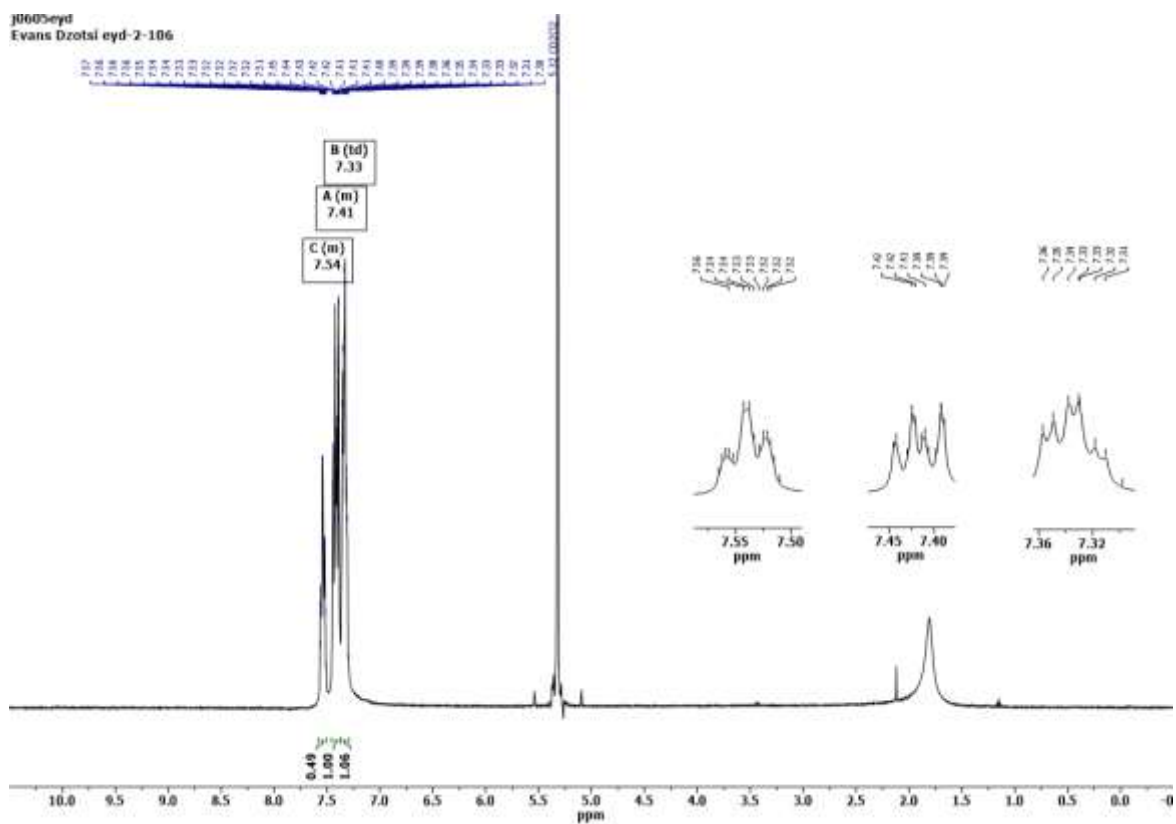


Figure 8A  $^1\text{H}$  NMR spectrum of **89** (400 MHz,  $\text{CD}_2\text{Cl}_2$ ).

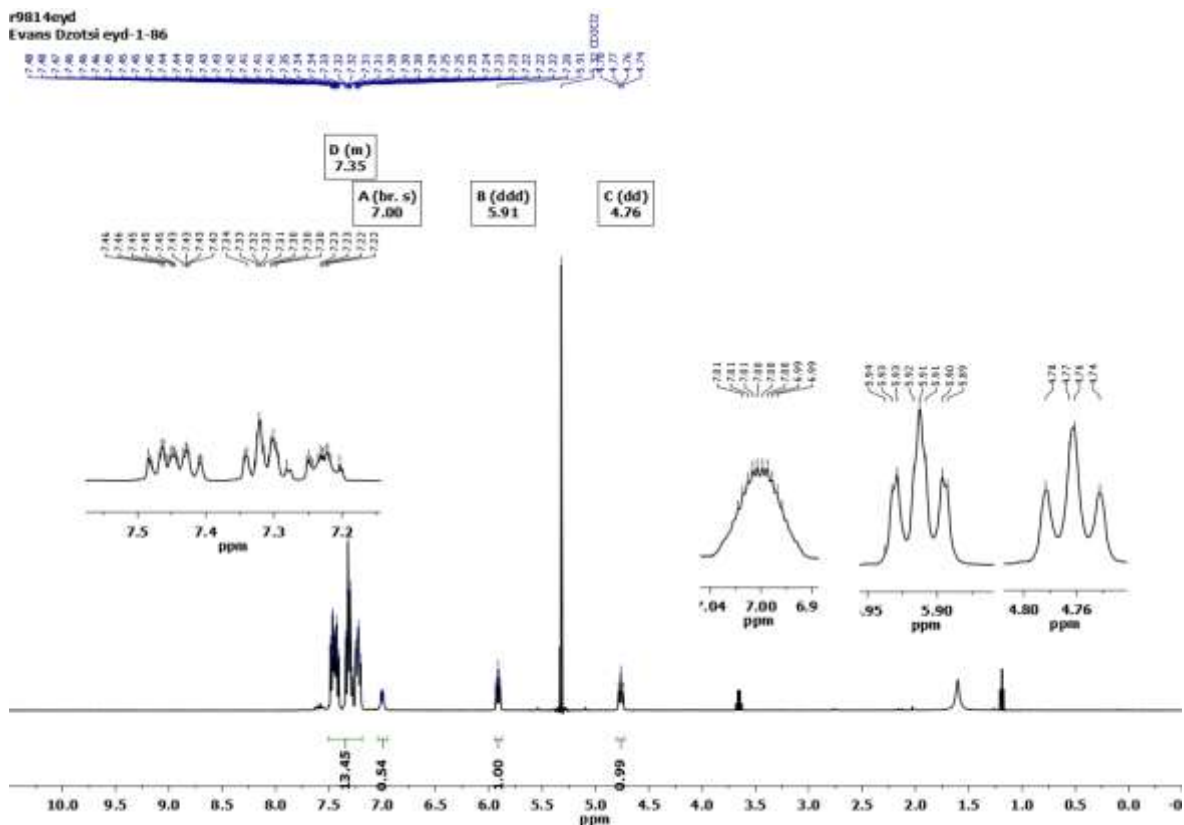


Figure 9A <sup>1</sup>H NMR spectrum of **90** (400 MHz, CD<sub>2</sub>Cl<sub>2</sub>)

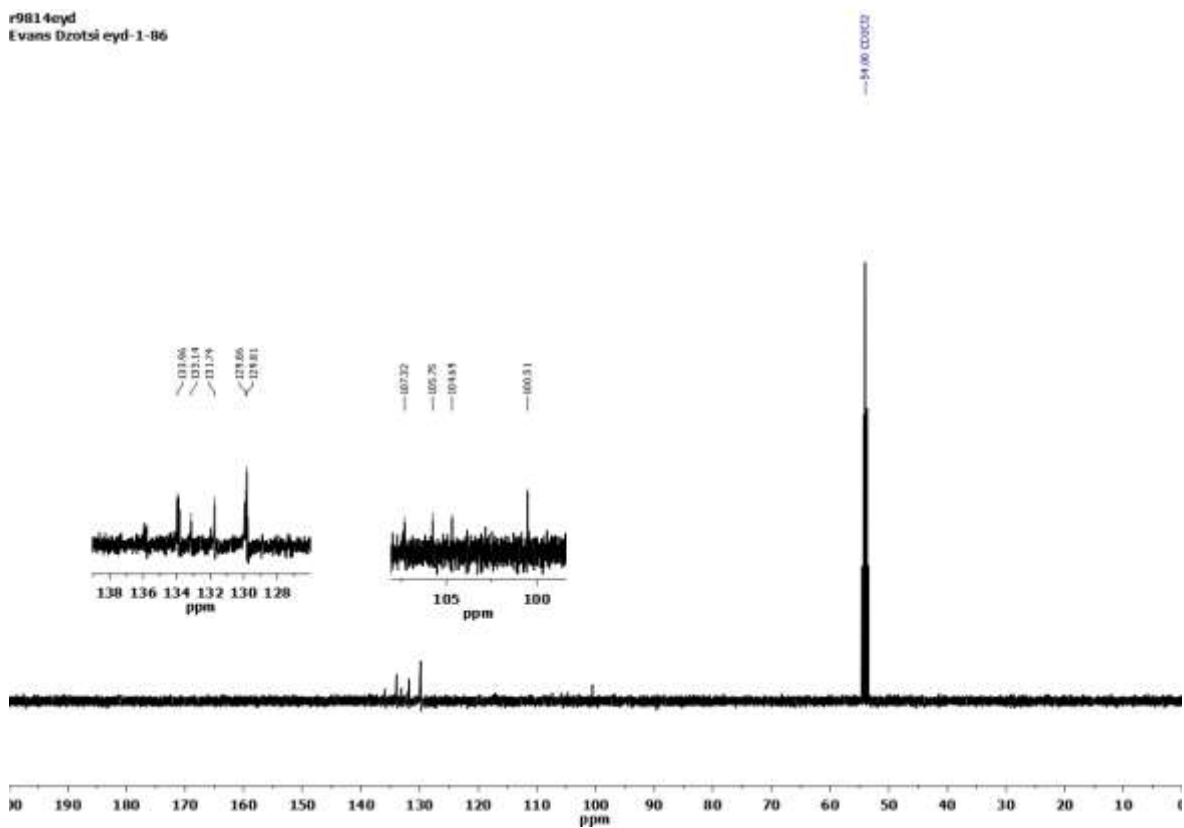


Figure 10A <sup>13</sup>C NMR spectrum of **90** (101 MHz, CD<sub>2</sub>Cl<sub>2</sub>)

rb0119eyd  
Evans Dzotsi eyd-1-34-4

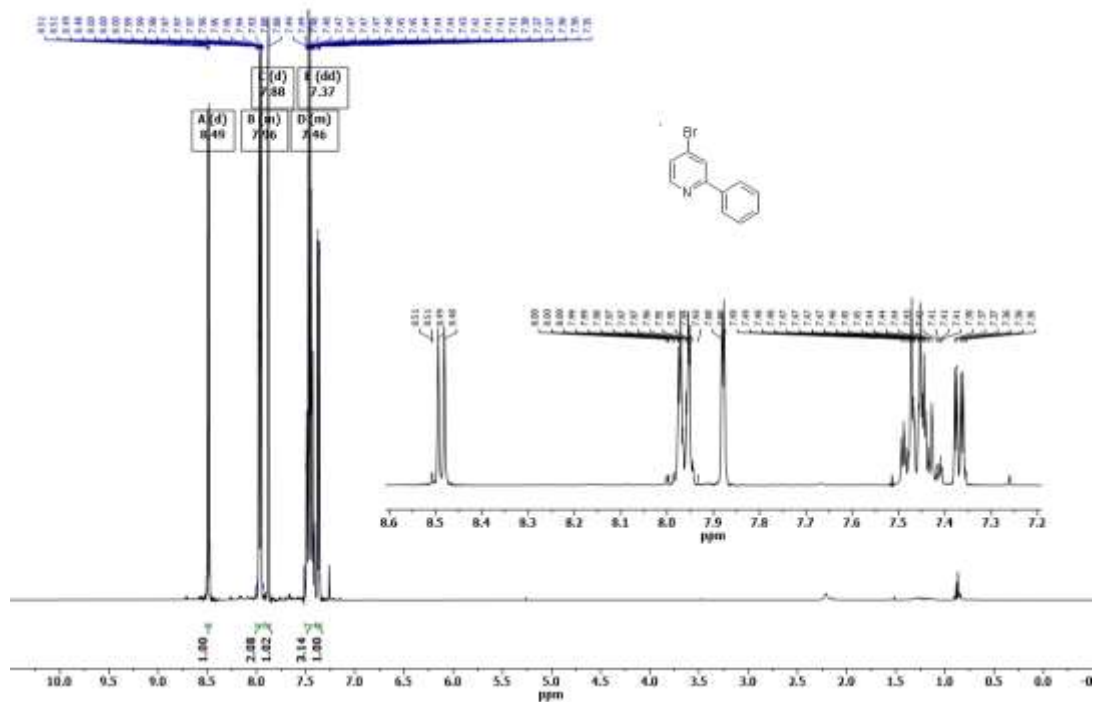


Figure 11A  $^1\text{H}$  NMR spectrum of 99a (400 MHz,  $\text{CDCl}_3$ ).

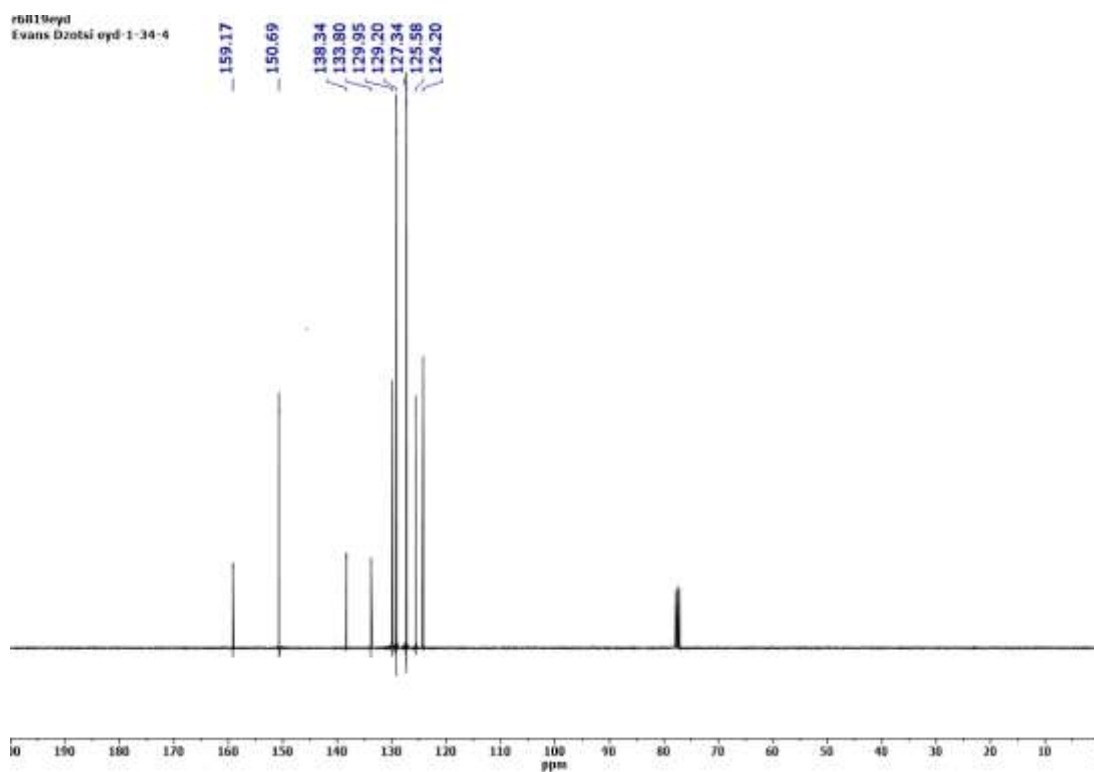


Figure 12A  $^{13}\text{C}$  NMR spectrum of 99a (101 MHz,  $\text{CDCl}_3$ ).



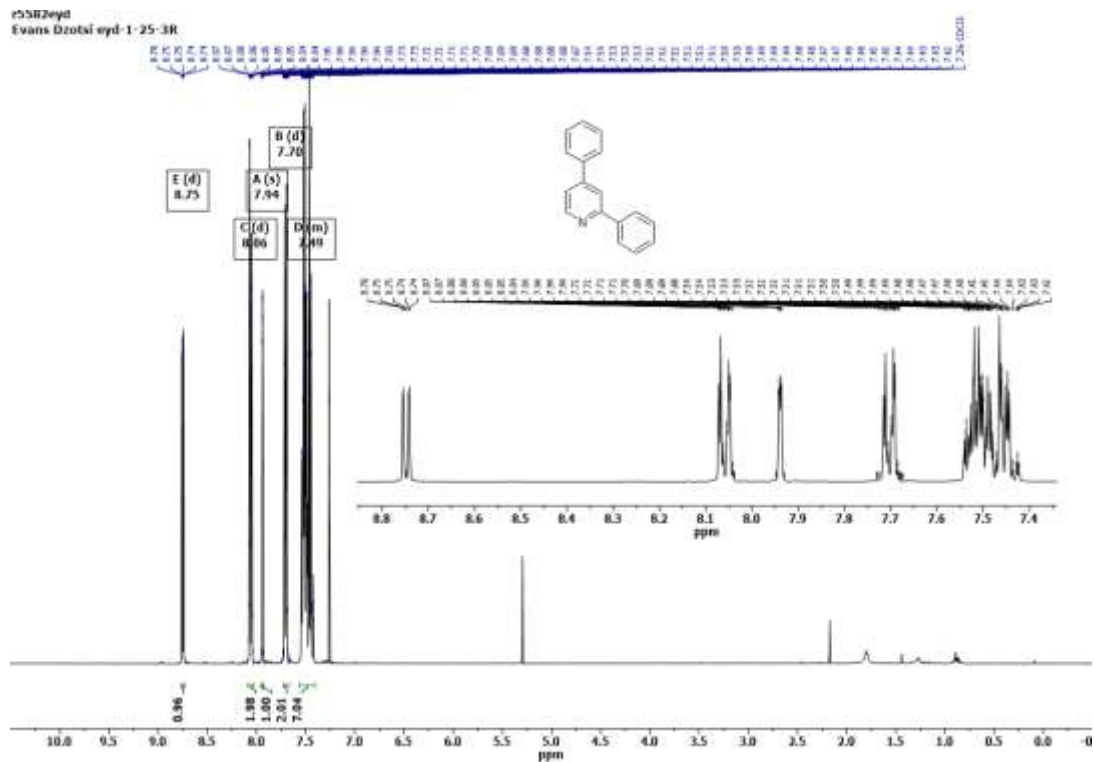


Figure 13A  $^1\text{H}$  NMR spectrum of 101a (400 MHz,  $\text{CDCl}_3$ ).

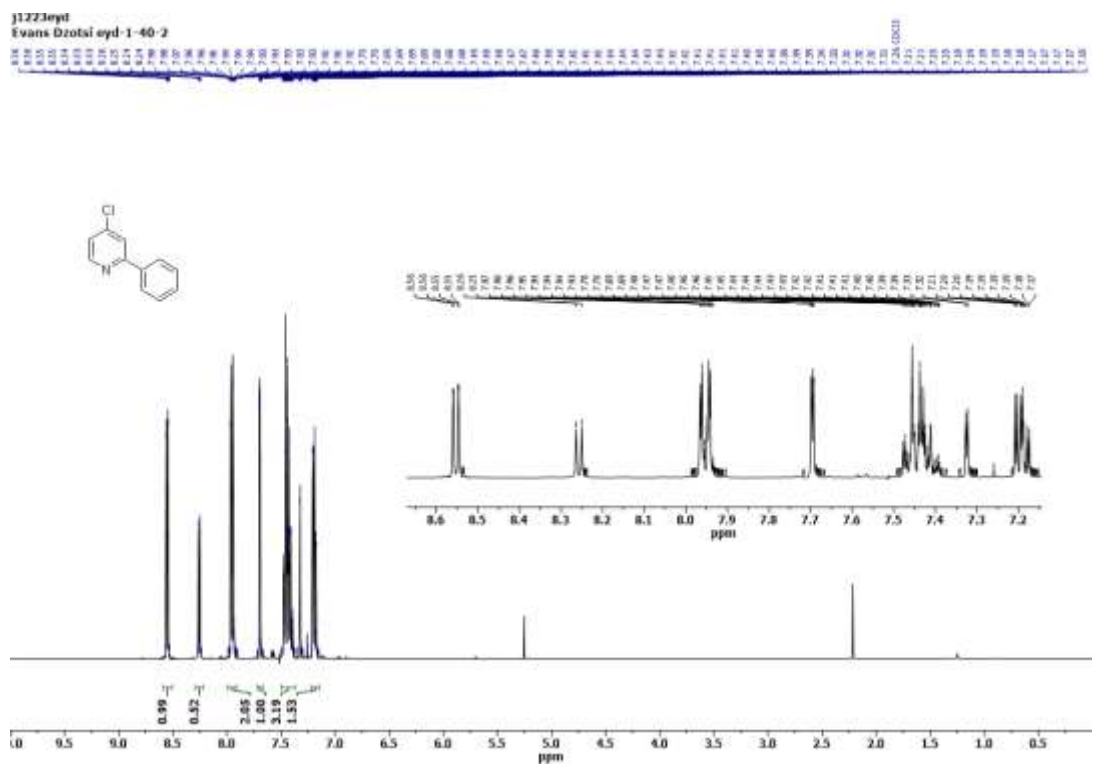


Figure 14A  $^1\text{H}$  NMR spectrum of 103a (400 MHz,  $\text{CDCl}_3$ ).



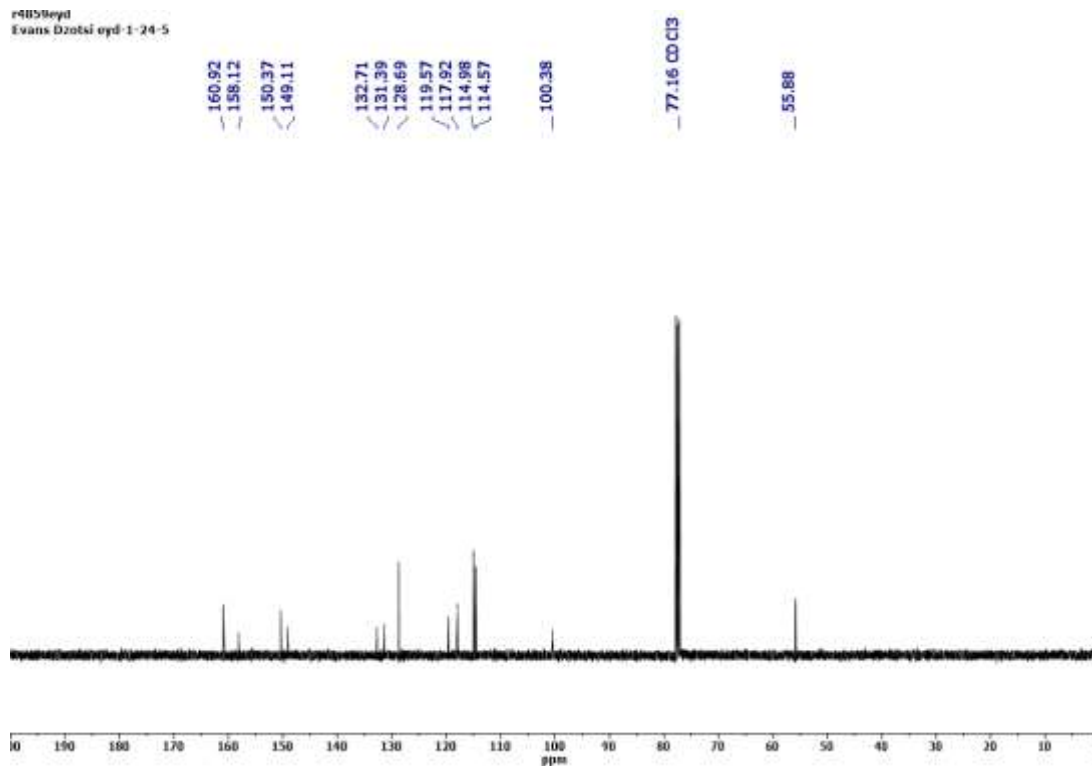


Figure 17A <sup>13</sup>C NMR spectrum of **101b** (101 MHz, CDCl<sub>3</sub>).

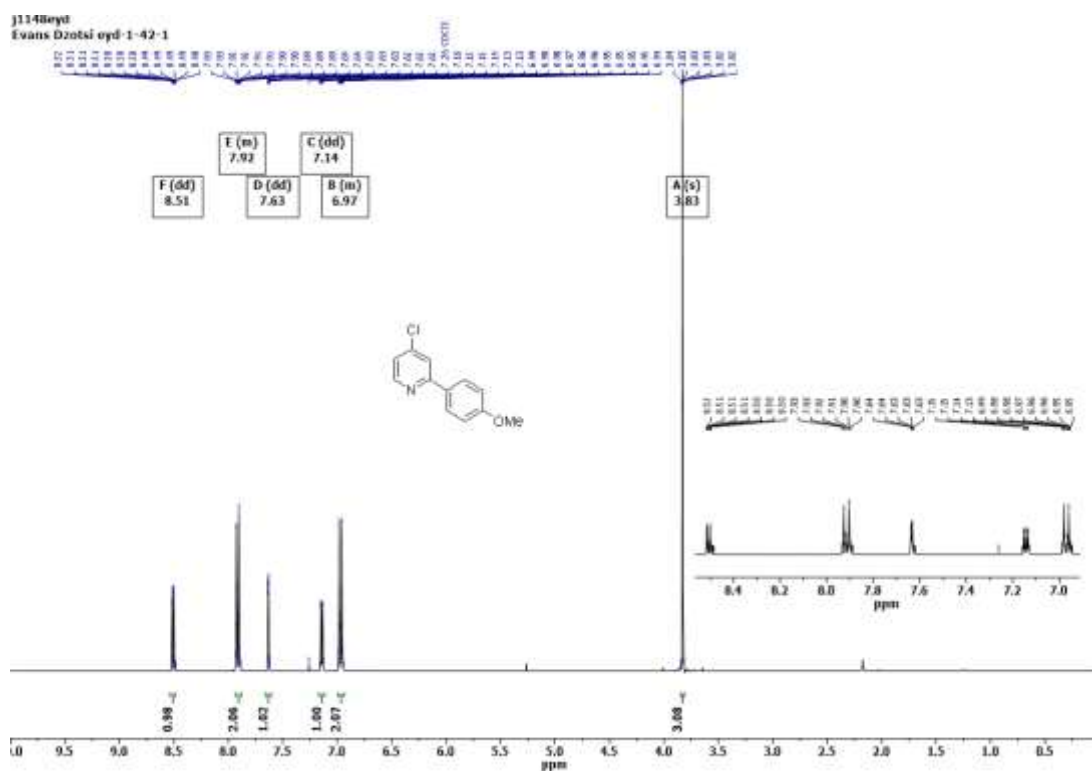


Figure 18A <sup>1</sup>H NMR spectrum of **103b** (400 MHz, CDCl<sub>3</sub>).

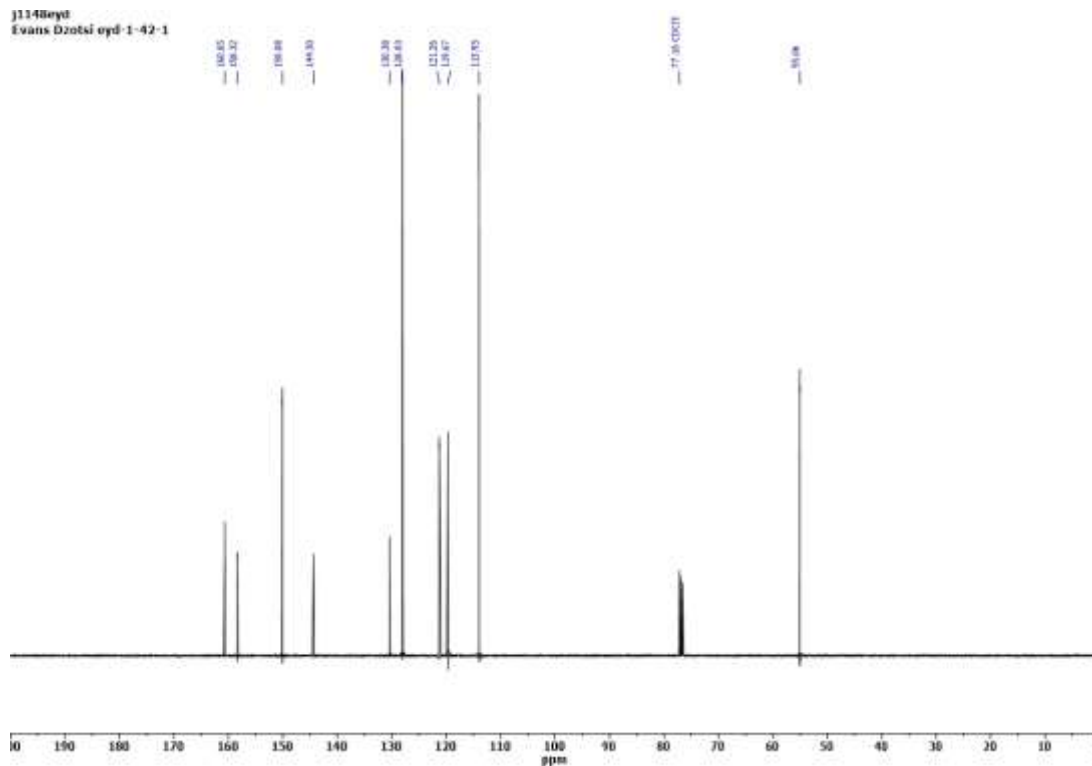


Figure 19A  $^{13}\text{C}$  NMR spectrum of **103b** (101 MHz,  $\text{CDCl}_3$ ).

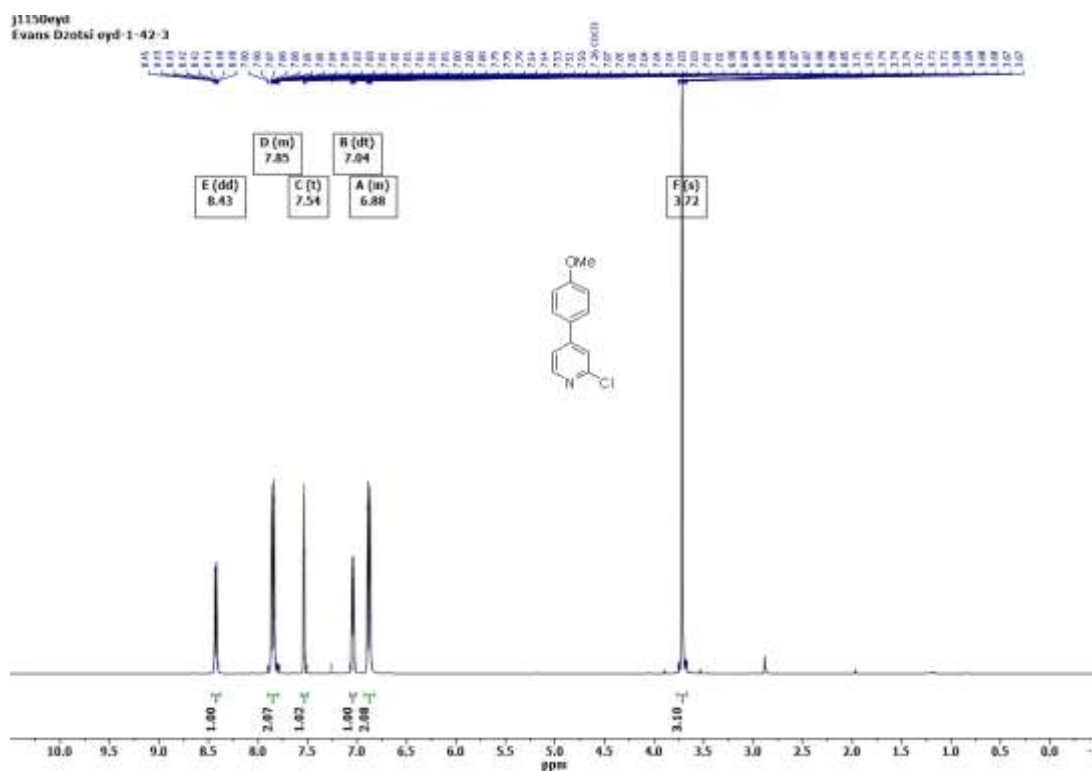


Figure 20A  $^1\text{H}$  NMR spectrum of **104b** (400 MHz,  $\text{CDCl}_3$ ).

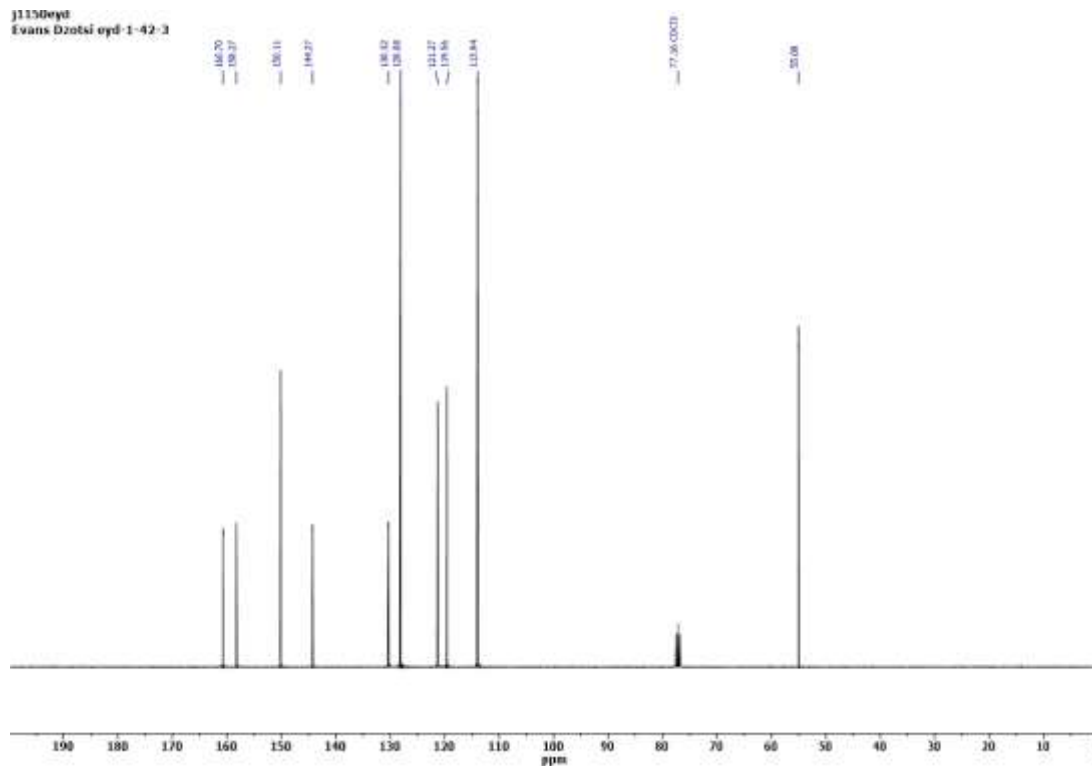


Figure 21A  $^{13}\text{C}$  NMR spectrum of **104b** (101 MHz,  $\text{CDCl}_3$ ).

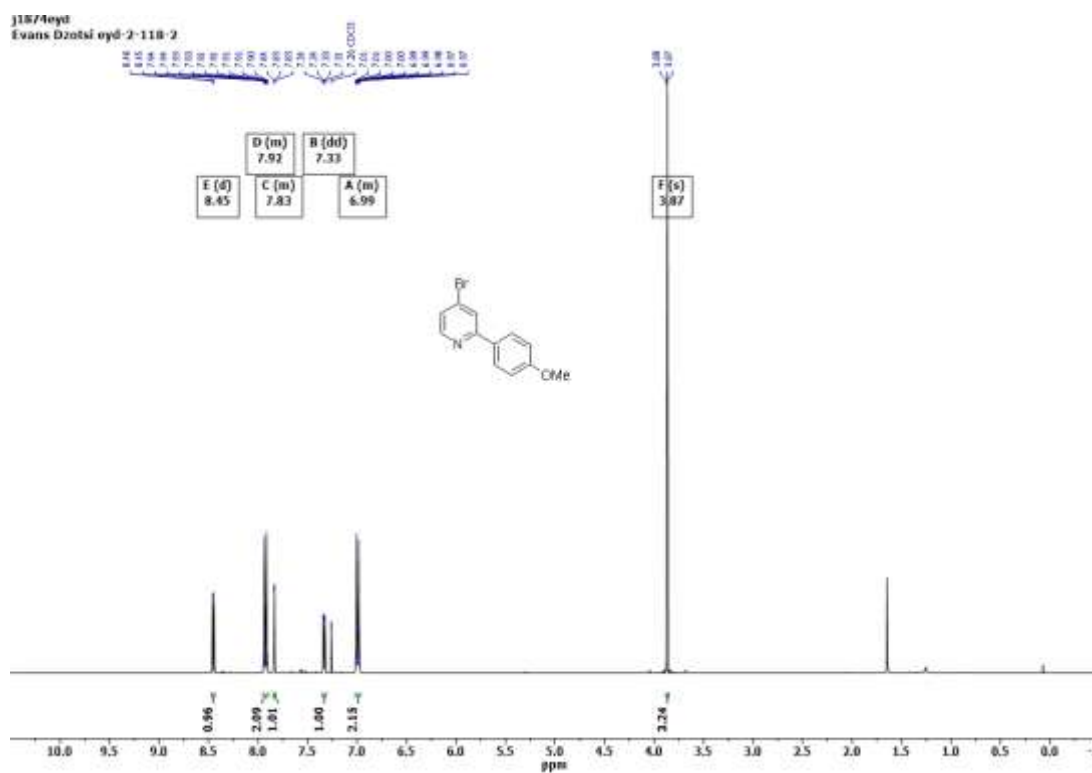


Figure 22A  $^1\text{H}$  NMR spectrum of **99b** (400 MHz,  $\text{CDCl}_3$ ).

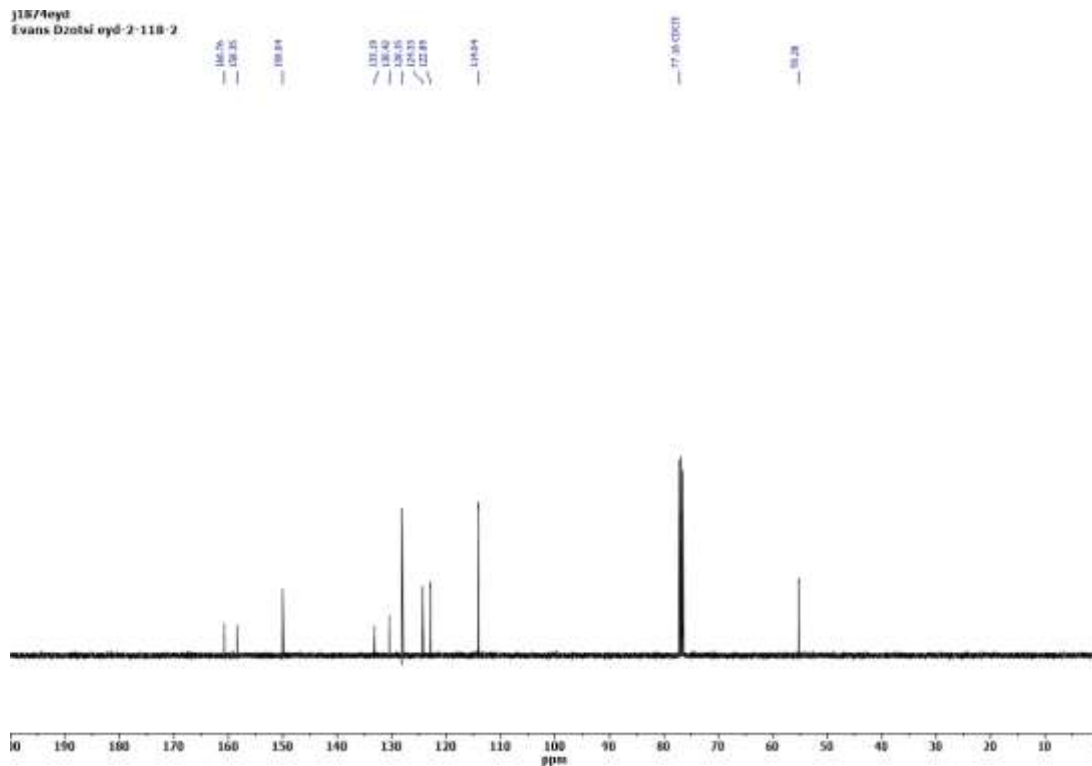


Figure 23A <sup>13</sup>C NMR spectrum of **99b** (101 MHz, CDCl<sub>3</sub>).

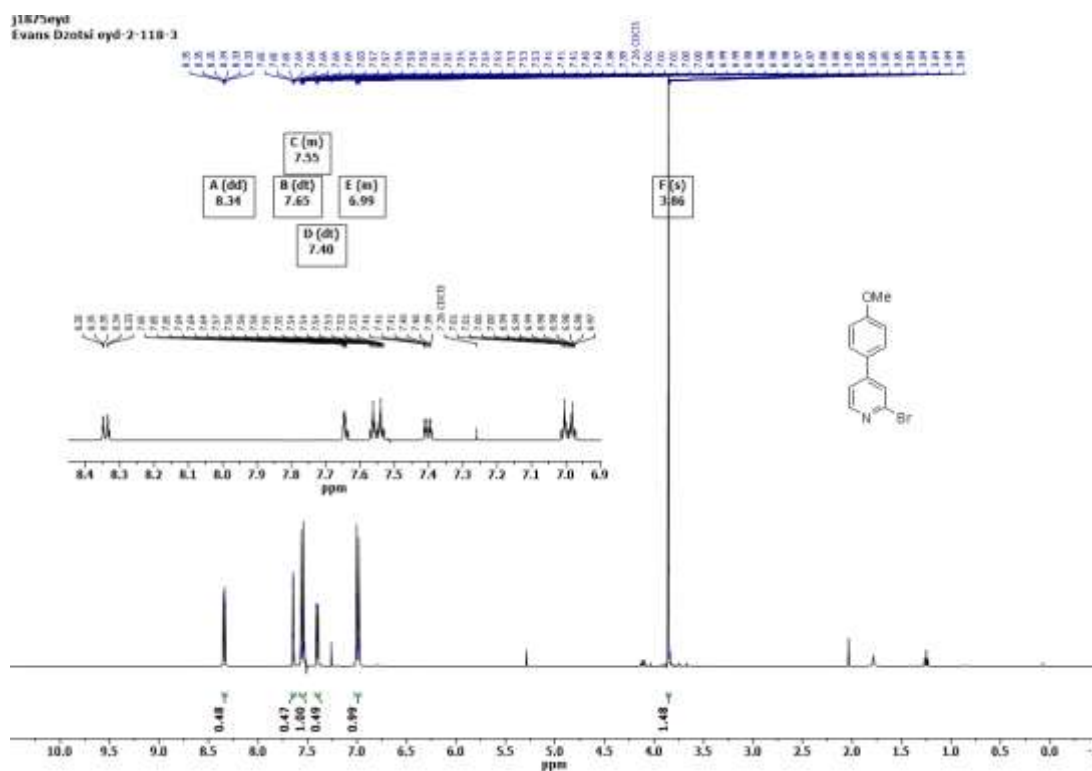


Figure 24A <sup>1</sup>H NMR spectrum of **100b** (400 MHz, CDCl<sub>3</sub>).



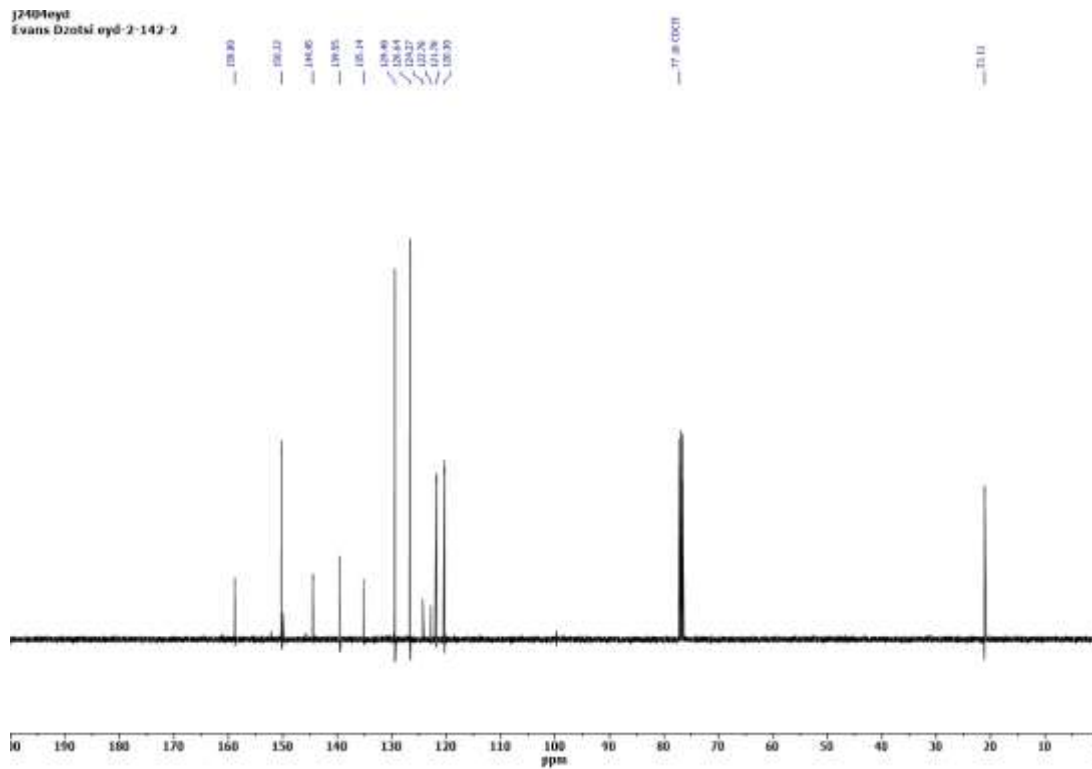


Figure 27A <sup>13</sup>C NMR spectrum of **103c** (101 MHz, CDCl<sub>3</sub>).

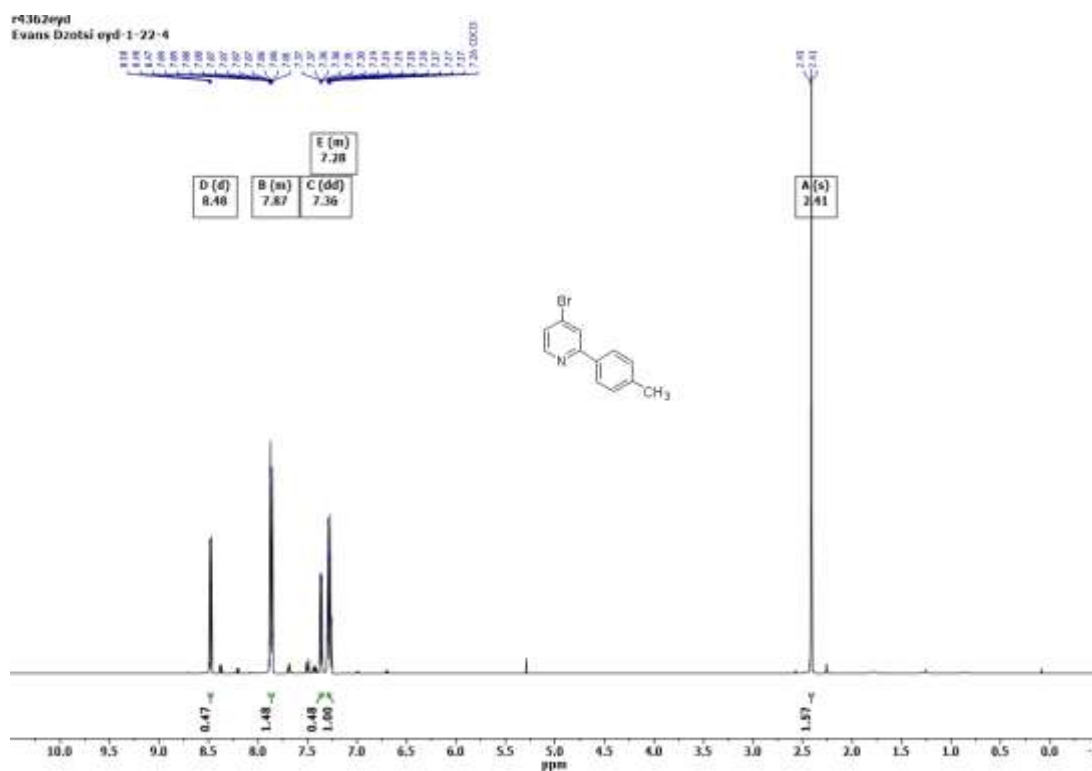
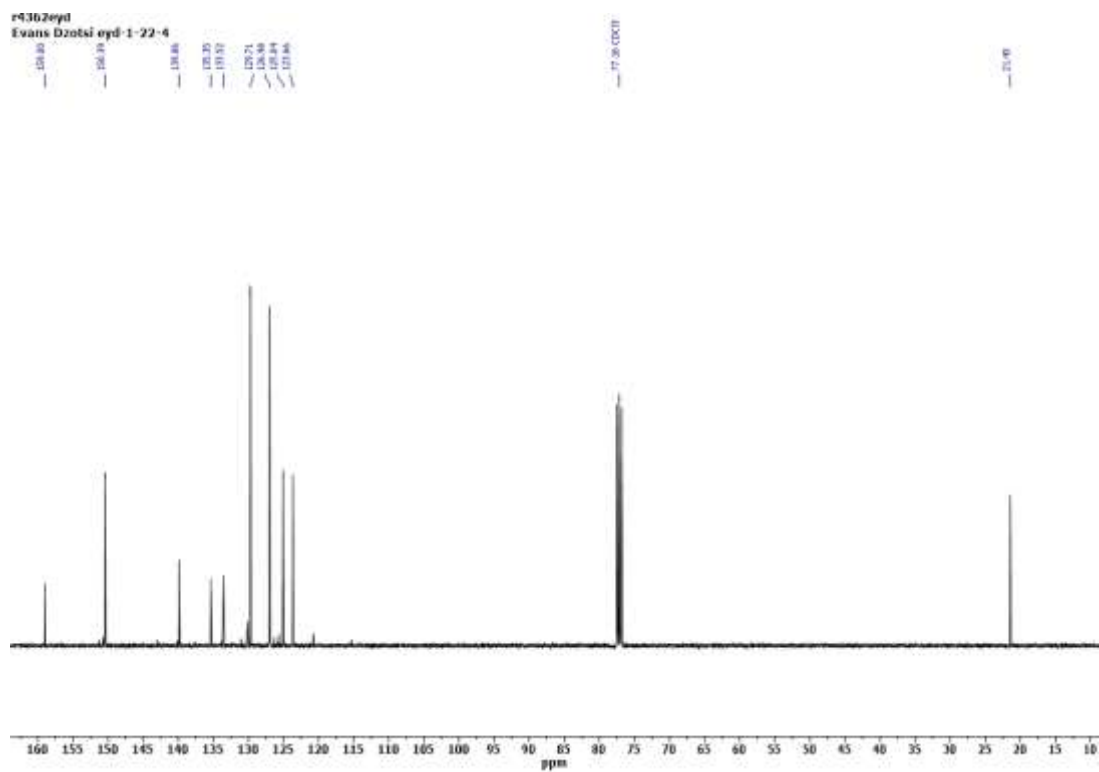
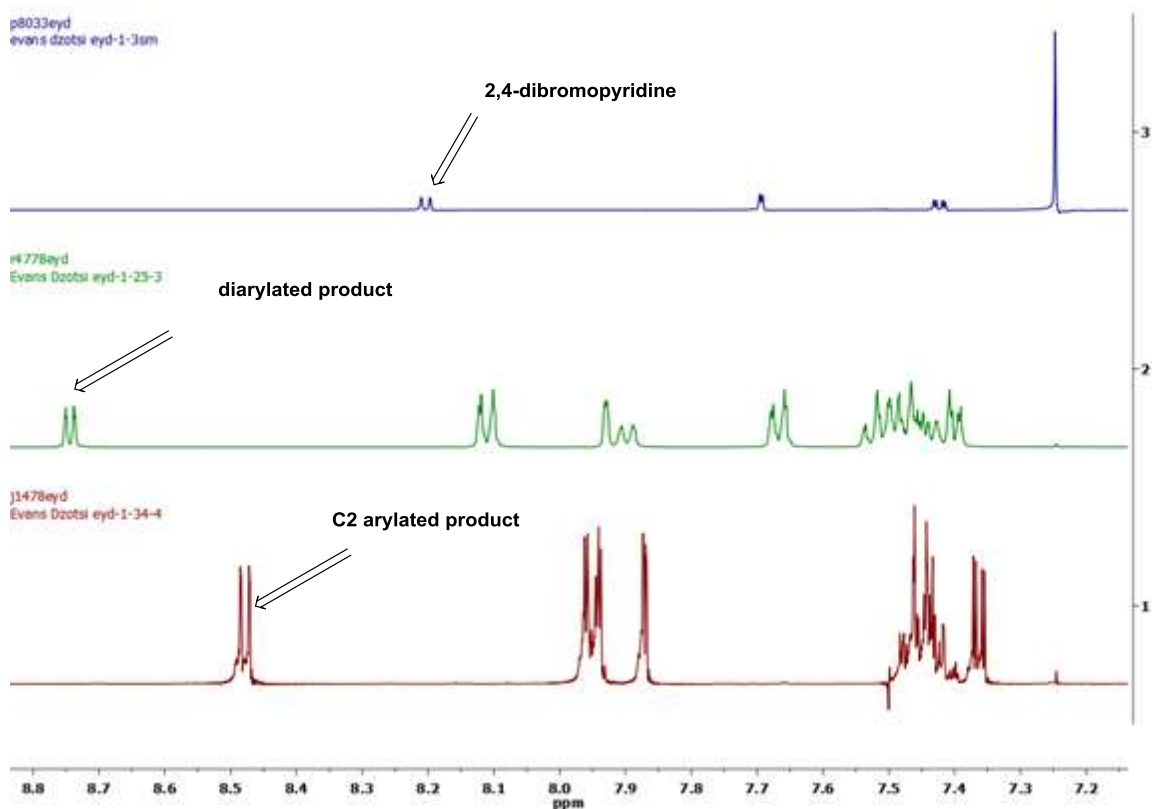


Figure 28A <sup>1</sup>H NMR spectrum of **99c** (400 MHz, CDCl<sub>3</sub>).





**Figure 29A**  $^{13}\text{C}$  NMR spectrum of **99c** (101 MHz,  $\text{CDCl}_3$ ).



**Figure 29A** Exemplar stacked  $^1\text{H}$  NMR spectra showing key differences (between 6.6 and 8.6 ppm) for 2,4-dibromopyridine **97** and the three arylated products derived from phenyl boronic acid **98a** (400 MHz,  $\text{CDCl}_3$ ).

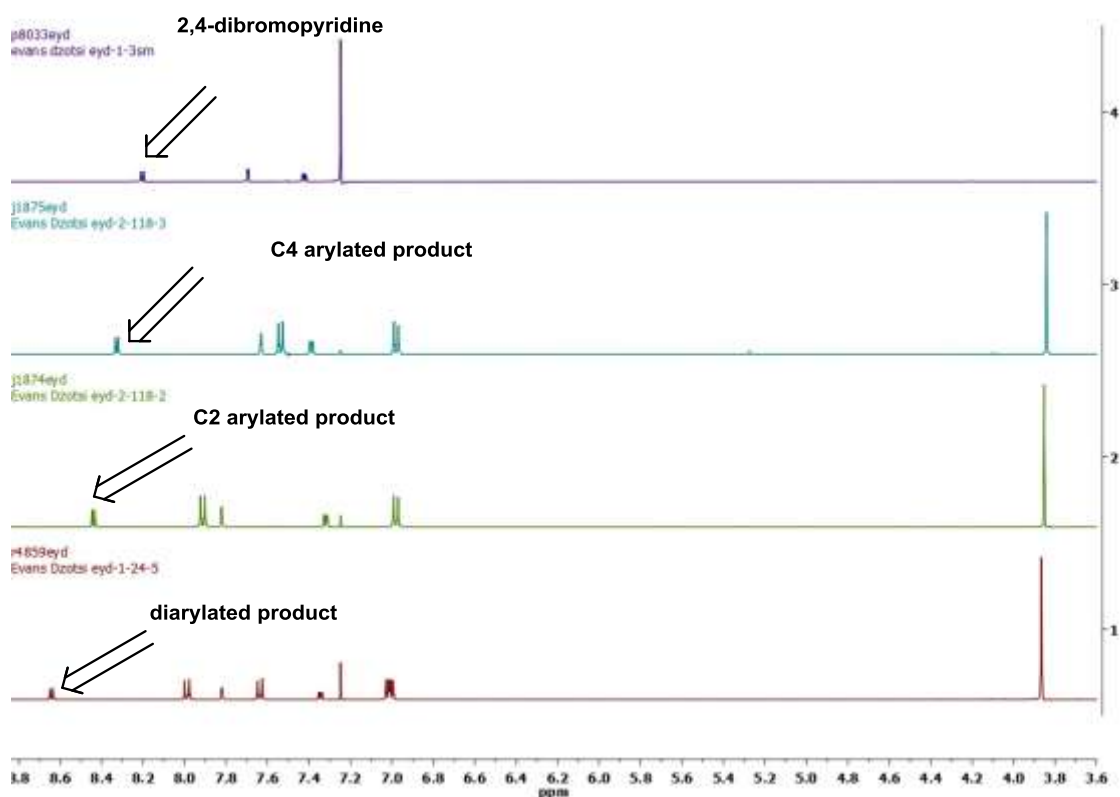


**Figure 30A** Exemplar stacked  $^1\text{H}$  NMR spectra showing key differences (between 3.6 and 8.8 ppm) for 2,4-dibromopyridine **97** and the three arylated products derived from p-methoxyphenyl boronic acid **98b** (400 MHz,  $\text{CDCl}_3$ ).

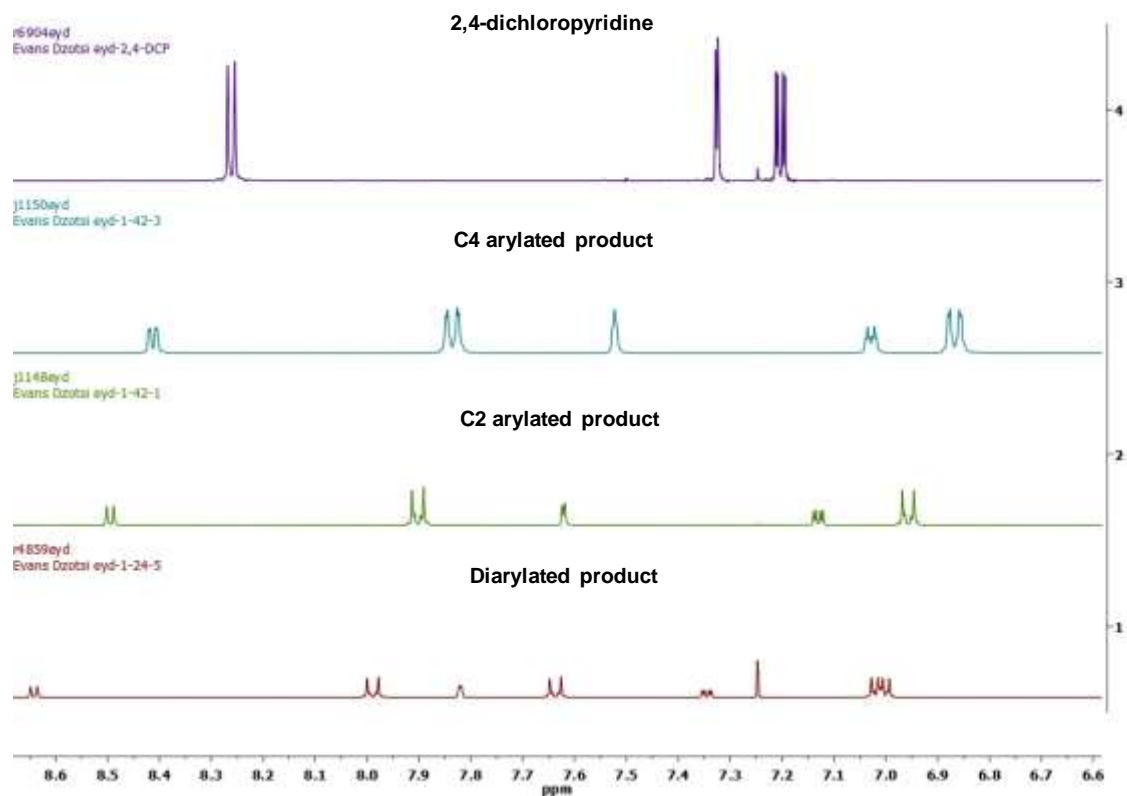


**Figure 31A** Exemplar stacked <sup>1</sup>H NMR spectra showing key differences (between 6.6 and 8.6 ppm) for 2,4-dichloropyridine **102** and the three arylated products derived from p-methoxyphenyl boronic acid **98b** (400 MHz, CDCl<sub>3</sub>).

## Abbreviations

ATR	attenuated total reflectance
Ar	arene
C	celcius
Ea	activation energy
ESI	electron spray ionisation
ETG	ethylene glycol
P	product
IR	infrared
h	hour
Lit	literature
LIFDI	liquid injection field desorption-ionization
o-	ortho
p-	para
Ph	phenyl
PdNPs	Pd nanoparticles
MS	mass spectrometry
MHz	megahertz ( $10^{6s^{-1}}$ )
NMR	nuclear magnetic resonance
PVP	(poly)vinylpyrrolidinone
BINAP	2,2'-bis(diphenylphosphino)-1,1'-binaphthyl
RT	room temperature

TEM	transmission electron microscopy
THF	tetrahydrofuran
TLC	thin layer chromatography
UV	ultraviolet

## Reference

- 1 Ananikova, V. P.; Egorova, K. S. *Angew. Chem. Int. Ed.* **2016**, *55*, 2-15.
- 2 Reay, A. J.; Fairlamb, I. J. S. *Chem. Commun.* **2015**, *51*, 16289-16307.
- 3 Sommer, K. Yu, W.; Richardson, J. M.; Weck, M.; Jones C. W.; *Adv. Synth. Catal.* **2005**, *347*, 161-171.
- 4 Anastasa, P. T.; Kirchhoff, M. M.; Williamson, T. C. *App. Catal.* **2001**, *221*, 3-13.
- 5 Ward, T. R.; Chatterjee, A. *Catal. Lett.* **2016**, *146*, 820-840.
- 6 Pagliaro, M.; Ciriminna, R.; Cara, P. D.; Pandarus, V.; Beland, F. *ChamCatChem* **2012**, *4*, 432-445.
- 7 Nicolaou, K. C.; Bulger, P. G.; Sarlah, D. *Angew. Chem. Int. Ed.* **2005**, *44*, 4442-4489.
- 8 Wang, Z-X.; Tao, J-L.; Zhu, F. *Org. Lett.* **2015**, *17*, 4976-4929.
- 9 Kapdi, A. R.; Prajapati, D. *RSC Adv.* **2014**, *4*, 41245-41259.
- 10 Snieckus. V.; Colacot, T. J.; Kitching, M. O.; Seechurn Johansson, C. C. C. *Angew. Chem. Int. Ed.* **2012**, *51*, 5062-5085.
- 11 Magano, J.; Dunetz, J. *Chem. Rev.* **2011**, *111*, 2177-2250.
- 12 Furuya, T.; Kamlet, A. S.; Ritter, T. *Nature* **2011**, *473*, 470-477.
- 13 Knochel, P.; Greiner, R.; Hammann, M. J.; Haas, D. *ACS, Catal.* **2016**, *6*, 1540-1552.
- 14 Zhao, D.; Li, Z.; Shan, F.; Jiang, L. *Molecules* **2012**, *17*, 12121-12139.
- 15 Frost, C. G.; Plucinski, P.; Reynolds, W. R. *Catal. Sci. Technol.* **2014**, *4*, 948-954.
- 16 Buchwald, S, L.; Martinelli, J, R.; Walker, S, D.; Barder, T, E. *J. Am. Chem. Soc.* **2005**, *127*, 4685-4696.
- 17 Khusnutdinov, R. I.; Bayguzina, A. R.; Dzhemilev, U. M. *Russ. J. Org. Chem.* **2012**, *48*, 309-348.
- 18 Buchwald, S, L.; Martin, R. *Acc. Chem. Res.* **2008**, *41*, 1461-1473.
- 19 Colacot, T. J. *Platinum Metals Rev.* **2012**, *56*, 110-116.
- 20 Carey, J, S.; Laffan D.; Thomson, C.; Williams M, T. *Org. Biomol. Chem*, **2006**, *4*, 2337-2347.
- 21 Milstein, D.; Stille, J. K. J. *Am. Chem. Soc.* **1978**, *100*, 3636-3638.
- 22 Milstein, D.; Stille, J. K. J. *Am. Chem. Soc.* **1979**, *101*, 4992-4998.

- 23 Stille, J. K. *Angew. Chem. Int. Ed.* **1986**, *25*, 508-524.
- 24 Miyaura, N.; Suzuki, A. *J. Chem. Soc., Chem. Commun.* **1979**, 866-867.
- 25 Suzuki, A.; Yanagi, T.; Miyaura, N. *Synth. Commun.* **1981**, *11*, 513-519.
- 26 Sonogashira, K.; Tohda, Y.; Hagihara, N. *Tetrahedron Lett.* **1975**, *16*, 4467-4470.
- 27 Tamao, K.; Sumitani, K.; Kumada, M. *J. Am. Chem. Soc.* **1972**, *94*, 4374-4376.
- 28 Corriu, R. J. P.; Masse, J. P. *J. Chem. Soc., Chem. Commun.* **1972**, 144a.
- 29 Hiyama, T.; Obayashi, M.; Mori, I.; Nozaki, H. *J. Org. Chem.* **1983**, *48*, 912-914.
- 30 Negishi, E.; King, A.O.; Okukado, N. *J. Org. Chem.* **1977**, *42*, 1821-1823.
- 31 de Vries, A. H. M.; Mulders, J. M. C. A.; Mommers, J. H. M.; Henderickx, H. J. W.; de Vries, J. G. *Org. Lett.* **2003**, *5*, 3285-3288.
- 32 Hartwig, J. F.; Carrow, B. P. *J. Am. Chem. Soc.* **2011**, *133*, 2116-2119.
- 33 Lloyd-Jones, G. C.; Lennox, A. J. *J. Chem. Soc. Rev.* **2014**, *43*, 412-443.
- 34 Ellis, P. J.; Fairlamb, I. J. S.; Hackett, S. F. J.; Wilson, K.; Lee, A. F. *Angew. Chem. Int. Ed.* **2010**, *49*, 1820-1824.
- 35 Jutand, A.; Amatore, C.; Le Duc, G. *Chem. Eur. J.* **2012**, *18*, 6616-6625.
- 36 Anderson, C. E.; Kirsch, S. F.; Overman, L. E.; Richards, C. J.; Watson, M. P. *Org. Synth.* **2007**, *84*, 148.
- 37 Bajwa, S. E.; Storr, T. E.; Hatcher, L. E.; Williams, T. J.; Baumann, C. G.; Whitwood, A. C.; Allan, D. R.; Teat, S. J.; Raithby, P. R.; Fairlamb, I. J. S. *Chem. Sci.* **2012**, *3*, 1656-1661.
- 38 (a) Carole, W. A.; Bradley, J.; Sarwar, M.; Colacot, T. *J. Org. Lett.* **2015**, *17*, 5472-5475.  
(b) Fairlamb, I. J. S. *Angew. Chem. Int. Ed.* **2015**, *54*, 10415-10427.
- 39 Fang, P. P.; Jutand, A.; Tian, Z.-Q.; Amatore, C. *Angew. Chem. Int. Ed.* **2011**, *50*, 12184-12188.
- 40 Lloyd-Jones, G. C.; Lennox, A. J. *J. Angew. Chem. Int. Ed.* **2013**, *52*, 7362-7370.
- 41 Sun, H.; Li, X.; Tu, C.; Guo, X.; Zhou, J. *J. Org. Chem.* **2009**, *74*, 697-702.
- 42 Bernard, C. *Platinum Met. Rev.* **2008**, *52*, 38-45.
- 43 Buchwald, S. L.; Yang, B. H.; Singer, R. A.; Wolfe, J. P. *J. Am. Chem. Soc.* **1999**, *121*, 9550-9561.
- 44 Bedford, R. B.; Betham, M.; Coles, S. J.; Frost, R. M.; Hursthouse, M. B. *Tetrahedron*, **2005**, *61*, 9663-9669.
- 45 Kotha, S.; Lahiri, K.; Kashinath, D. *Tetrahedron* **2002**, *58*, 9633-9695.

- 46 Nolan, S. P.; Scott, N. M.; Stevens, E. D.; Mei, J.; Navarro, O.; Marion, N. *J. Am. Chem. Soc.* **2006**, *128*, 4101-4111.
- 47 Guo, Q-X; Liu, L; Fu, Y; Zhanng, Z-P; Li, J; Cui, X. *J. Org. Chem.* **2007**, *72*, 9342-9345.
- 48 Eppinger, J.; Herdtweck, E.; Reiner, T.; Faul, S. H.; Jantke, D.; Marziale, N. A. *Green Chem.* **2011**, *13*, 169-177.
- 49 Zhang, S.; Cao, J.; Lin, Y.; Li, S. *J. Org. Chem.* **2007**, *72*, 4067-4072.
- 50 Galardon, E.; Ramdeehul, S.; Brown, J. M.; Cowley, A.; Hii, K. K.; Jutand, A. *Angew. Chem, Int. Ed.* **2002**, *41*, 1760-1763.
- 51 Zhang, C.; Huang, J.; Trudell, M. L.; Nolan, S. P. *J. Org. Chem.* **1999**, *64*, 3804-3805.
- 52 Tao, B.; Boykin, D. W. *J. Org. Chem.* **2004**, *69*, 4330-4335.
- 53 Liebscher, J.; Yin, L.; *Chem. Rev.* **2007**, *107*, 133-173.
- 54 Chand, D. K.; Mandali, P. K. *Catal. Comm.* **2013**, *31*, 16-20.
- 55 Siddiqui, M. R. H.; Tahir, M. N.; Tremel, W.; Alkathlan, H. Z.; Al-Warthan, A.; Adil, S. F.; Kuniyil, M.; Khan, M.; Khan M. *Dalton Trans.* **2014**, *43*, 9026-9036.
- 56 El-Sayed, M. A.; Boone, E.; Li, Y. *Langmuir* **2002**, *18*, 4921-4925.
- 57 Perez-Lorenzo, M. *J. Phys. Chem. Lett.* **2012**, *3*, 167-174.
- 58 Zhou, X-F.; Zhao, Y-Q.; Xu, H-J. *J. Org. Chem.* **2011**, *76*, 8036-8041.
- 59 Finke, R. G.; Widegren, J. A.; *J. Mol. Catal. A*, **2003**, *198*, 317-341.
- 60 Klingelhöfer, S.; Heitz, W.; Greiner, A.; Oestreich, S.; Förster, S.; Antonietti, M.; *J. Am. Chem. Soc.* **1997**, *119*, 10116-10120.
- 61 Zhou, Q-L.; Wang, L-X.; Xie, J-H.; Wang, A-E. *Tetrahedron* **2005**, *61*, 259-266.
- 62 Basato, M.; Zecca, M.; Biffis, A. *J. Mol. Cat. Chem. A* **2001**, *173*, 249-274.
- 63 Tu, A.; Yang, Z.; Marder, T. B.; Li, Q.; Zhang, H.; Wu, B.; Yu, G.; Zhang, H.; Wang, H.; Deng, Y.; Liu, J. *Org. Lett.* **2008**, *13*, 2661-2664.
- 64 Bach, T.; Stock, C.; Schroter, S. *Tetrahedron* **2005**, *61*, 2245-2267.
- 65 Buchwald, S. L.; Milne, J. E. *J. Am. Chem. Soc.* **2004**, *126*, 13028-13032.
- 66 Yin, J.; Patel, S.J.; Luzung, R. M. *J. Org. Chem.* **2010**, *75*, 8330-8332.
- 67 Tu, T; Sun, Z, Xu, M; Dong, N; Liu, Z. *J. Org. Chem.* **2013**, *78*, 7436-7444.
- 68 Buchwald, S. L.; Cheong, P, H-Y.; Mustard, T. J. L.; Yang, Y. *Angew. Chem. Int. Ed.* **2013**, *52*, 14098-14102.
- 69 McGlacken, G. P.; Schmidt, A. F.; Cano, R. *Chem. Sci.* **2015**, *6*, 5338-5346. (b) Tang, D. T. D.; Collins, K. D.; Ernst, J. B.; Glorius, F. *Angew. Chem. Int. Ed.* **2014**, *53*, 1809-1813.



- 70 Ackermann, L.; Vicente, R.; Kapdi, A. R. *Angew. Chem. Int. Ed.* **2009**, *48*, 9792-9826.
- 71 Xi, W.; Shi, L. *Chem. Soc. Rev.*, **2012**, *41*, 7687-7697.
- 72 Walsh, P. J.; Tomson, N. C.; Gao, F.; Trongsiwat, N.; Bellomo, A.; Sha, S-C.; Zhang, J. *J. Am. Chem. Soc.* **2016**, *138*, 4260-4266.
- 73 Larrosa, I.; Hernandez, F. J.; Islam, S.; Colletto, C. *J. Am. Chem. Soc.* **2016**, *138*, 1677-1683.
- 74 Bellina, F.; Caucheruccio, S.; Rossi, R. *Eur. J. Org. Chem.* **2006**, *2006*, 1379-1382.
- 75 Emmert, M. H.; Cook, A. K.; Xie, Y. J.; Sanford, M. S. *Angew. Chem. Int. Ed.* **2011**, *50*, 9409-9412.
- 76 Kubota, A.; Emmert, M. H.; Sanford, M. S. *Org. Lett.* **2012**, *14*, 1760-1763.(b)  
Sanford, M. S.; Neufeldt, S. R. *Acc. of Chem. Res.* **2012**, *6*, 936-946.
- 77 Tang, D.-T. D.; Collins, K. D.; Glorius, F. *J. Am. Chem. Soc.* **2013**, *135*, 7450-7453.
- 78 Lane, B. S.; Brown, M. A.; Sames, D. *J. Am. Chem. Soc.* **2005**, *127*, 8050-8057.
- 79 Kannan, S.; James, A. J.; Sharp, P. R. *J. Am. Chem. Soc.* **1998**, *120*, 215-216.
- 80 Szlyk, E.; Barwiolek, M. *Thermochimica Acta* **2009**, *495*, 85-89.
- 81 Brumbaugh, J. S.; Sen, A. *J. Am. Chem. Soc.* **1988**, *110*, 803.
- 82 Bushnell, G. W.; Hunter, R. G.; McFarland, J. J.; Dixon, K. R. *Can. J. Chem.* **1972**, *50*, 3694-3699.
- 83 Lee, A. F.; Ellis, P. J.; Fairlamb, I. J. S.; Wilson, K. *Dalton Trans.* **2010**, *39*, 10473-10482.
- 84 Son, S. U.; Jang, Y.; Park, J.; Na, H. B.; Park, H. M.; Yun, H. J.; Lee, J.; Hyeon, T. *J. Am. Chem. Soc.* **2004**, *126*, 5026-5027.
- 85 Reay, A. J. PhD thesis, University of York, 2016.
- 86 Hurst, E. C. PhD thesis, University of York, 2009.
- 87 Cid, M. M.; Alonso-Gomez, J-L.; Sicre, C. *Tetrahedron* **2006**, *62*, 11063-11072. (b) Cid, M. M.; Maseras, F.; Braga, A. A. C.; Sicre, C. *Tetrahedron* **2008**, *64*, 7437-7443.
- 88 Singh, P. P.; Vishwakarma, R. A.; Aithagani, S. K, Yadav, M.; Singh, V. P. *J. Org. Chem.* **2013**, *78*, 2639-2648.